Top Curr Chem (2013) 340: 209–276
DOI: 10.1007/128_2013_438

Published online: 11 May 2013

Differentiation of Enantiomers by Capillary Electrophoresis

Gerhard K. E. Scriba

Abstract Capillary electrophoresis (CE) has matured to one of the major liquid phase enantiodifferentiation techniques since the first report in 1985. This can be primarily attributed to the flexibility as well as the various modes available including electrokinetic chromatography (EKC), micellar electrokinetic chromatography (MEKC), and microemulsion electrokinetic chromatography (MEEKC). In contrast to chromatographic techniques, the chiral selector is mobile in the background electrolyte. Furthermore, a large variety of chiral selectors are available that can be easily combined in the same separation system. In addition, the migration order of the enantiomers can be adjusted by a number of approaches. In CE enantiodifferentiations the separation principle is comparable to chromatography while the principle of the movement of the analytes in the capillary is based on electrophoretic phenomena. The present chapter will focus on mechanistic aspects of CE enantioseparations including enantiomer migration order and the current understanding of selector–selectand structures. Selected examples of the basic enantioseparation modes EKC, MEKC, and MEEKC will be discussed.

Keywords Capillary electrophoresis · Chiral selector · Electrokinetic chromatography · Enantiodifferentiation · Enantiomer migration order · Micellar electrokinetic chromatography · Microemulsion electrokinetic chromatography · Mobility model · Selector–selectand complex

Contents

G.K.E. Scriba (✉)
Department of Pharmaceutical/Medicinal Chemistry, Friedrich Schiller University Jena, Philosophenweg 14, 07743 Jena, Germany
e-mail: gerhard.scriba@uni-jena.de

Abbreviations

CD	Cyclodextrin
Dns	Dansyl
EKC	Electrokinetic chromatography
EOF	Electroosmotic flow
id	Inner diameter
MEKC	Micellar electrokinetic chromatography
MEEKC	Microemulsion electrokinetic chromatography
(+)-18C6H4	(+)-(18-Crown-6)-2,3,11,12-tetracarboxylic acid

"*What can more resemble my hand or my ear, and be more equal in all points, than its image in a mirror? And yet, I cannot put such a hand as is seen in the mirror in the place of its original*." As stated by Immanuel Kant in 1783 in his discourse on metaphysics [1], a chiral object and its mirror image, although looking alike, are nevertheless incongruent. This epistemological analysis of a philosopher is also true in nature with regard to the interaction of chiral compounds with chiral biological targets which makes the differentiation of enantiomers a fundamental natural phenomenon. Chiral molecules play important parts in many aspects of life sciences, medical sciences, synthetic chemistry, food chemistry, as well as many other fields. Consequently, analytical techniques capable of differentiating stereoisomers, specifically enantiomers, are required. Chromatographic and electromigration techniques are currently most often applied due to the fact that these techniques separate not only enantiomers but also diastereomers and other chemically related compounds. For analytical enantioseparations, high-performance liquid chromatography (HPLC) and capillary electrophoresis (CE) are most often employed for non-volatile analytes while gas chromatography (GC) is preferably applied in the case of volatile analytes.

In capillary electrophoretic separation techniques analyses are performed in narrow bore capillaries exploiting the electrophoretic mobilities of charged molecules upon

the application of high electric field strength. Typically, the chiral selector is added to the background electrolyte in contrast to chromatography where the selector is bound to the stationary phase in most cases. Thus, in CE the chiral selector represents a so-called pseudostationary phase that may possess its own electrophoretic mobility. Combined with the different modes of CE including electrokinetic chromatography (EKC), micellar electrokinetic chromatography (MEKC), and, more recently, microemulsion electrokinetic chromatography (MEEKC), a multitude of separation scenarios can be realized contributing to the high flexibility of CE. Finally, the small quantities of samples, chemicals, and (if any) organic solvents render CE as an environmentally friendly and cost-effective technique.

This chapter discusses the current understanding of CE enantioseparations and will highlight examples in EKC, MEKC, and MEEKC. Capillary electrochromatography (CEC), which is considered a hybrid technique combining the separation principles of CE and HPLC, will not be considered here.

1 Historical Development of CE Enantioseparations

The first publication of an (achiral) CE analysis is often considered to be the paper by Jorgenson and Lukacs analyzing dansyl (Dns)-amino acids and other analytes in 75 μm inner diameter (id) fused-silica capillaries which was published in 1981 [2]. Approximately 4 years later the first CE enantioseparation was reported by Gassmann et al. who separated Dns-amino acids in the presence of a copper (II)–histidine complex as chiral selector [3]. It took until the late 1980s until further enantioseparations by CE were reported, including the paper by Cohen et al. using copper(II)–*N*,*N*-didecyl-L-alanine as chiral selector in a SDS micellar system in 1987 [4], or cyclodextrins (CDs) as chiral selectors in separations employing capillary isotachophoresis reported by Smolkova-Keulemansova and coworkers in 1988/1889 [5–7] and in capillary gel electrophoresis as demonstrated by Guttman et al. in 1988 [8]. The use of CDs in EKC was systematically addressed by Fanali in 1989 [9]. In this year several groups also reported the use of chiral micelles for analytical enantioseparations in MEKC. Terabe's group employed bile salt micelles for enantioseparations of Dns-amino acids [10, 11] while Dobashi et al. demonstrated the feasibility of *N*-dodecanoyl-L-valine as chiral surfactant for the separation of the enantiomers of amino acid derivatives [12, 13]. Since then many groups have focused on CE enantioseparations developing many chiral selectors and numerous applications so that CE can be considered a mature and reliable technique for analytical enantioseparations. This is also reflected in many review articles including recent publications [14–22] as well as monographs [23, 24]. Furthermore, special issues dedicated to enantioseparations by CE are regularly published by journals such as Journal of Chromatography A, Electrophoresis, Journal of Separation Science, Journal of Pharmaceutical and Biomedical Analysis, and others.

2 Fundamentals of CE Enantioseparations

CE can be regarded as an automated version of conventional (planar) electrophoresis. Separations are carried out in capillaries with an inner diameter (id) of 20–100 μm so that dissipation of Joule heat is very effective, allowing the application of high voltages up to 30 kV. The small diameters make CE a miniaturized technique requiring only small amounts of chemicals, solvents, and samples. The capillaries are manufactured from fused silica so that detection modes such as UV- or laser-induced fluorescence detection are typically carried out by on-column detection but hyphenation to a mass spectrometer is nowadays also routine. Therefore, staining techniques as in conventional electrophoresis are not required. The output of commercial instruments resembles a conventional chromatogram and can be integrated for quantitative analyses. While gel electrophoresis can only be applied to large molecules, CE allows the separation of small molecules including stereoisomers as well as the analysis of large molecules such as proteins or DNA and even whole cells.

In electrophoresis the mobility of an analyte is determined by the electrophoretic mobility of a particle, μ_{ep}, as a function of charge, q, and size of the analyte represented by the radius, r, for a spherical particle according to

$$\mu_{ep} = \frac{q}{6\pi\eta r}, \tag{1}$$

where η is the viscosity of the background electrolyte. In the case of acidic or basic analytes, the charge is a function of the pH of the electrolyte solution. In addition, the charged surface of the capillary results in the electroosmotic flow (EOF) as a general mass flow. The EOF creates a plug-like flow profile as compared to the parabolic flow profile of pressure driven chromatographic techniques rendering CE a high resolution technique. The mobility of the EOF is described by

$$\mu_{EOF} = \frac{\varepsilon\zeta}{4\pi\eta}, \tag{2}$$

where ε is the permittivity of the electrolyte solution and ζ is the zeta-potential resulting from the negatively charged capillary surface due to pH-dependent dissociation of the silanol groups.

The effective mobility of a solute is the sum of both electrophoretic forces, μ_{ep} and μ_{EOF}, according to

$$\mu_{eff} = \mu_{ep} + \mu_{EOF}. \tag{3}$$

As in chromatography, CE enantioseparations can be divided into indirect and direct methods. In the indirect approach the analyte enantiomers are derivatized with an enantiopure reagent to form a pair of diastereomers via covalent bonds. The diastereomers can be subsequently separated, in principle, under achiral conditions.

Direct methods refer to the separation of enantiomers in a chiral environment. This requires the presence of a chiral selector that is added to the background electrolyte. The separation is based on the formation of transient diastereomeric complexes in a thermodynamic equilibrium. This is identical with the situation in chromatographic techniques so that the stereospecific recognition of the analyte enantiomers by a chiral selector represents a chromatographic phenomenon [25]. The fact that the selector is mobile in CE compared to chromatography (a so-called "pseudo-stationary phase") is not a fundamental difference between the techniques. For this reason, enantioseparations by CE are also referred to as EKC. The transport of the analyte and/or the analyte–selector complex to the detector is achieved by electrokinetic phenomena. Thus, enantioseparations in CE contain a chromatographic and an electrophoretic component.

Many mathematical models have been proposed to describe the influence of the main parameters of a CE separation such as the concentration of the chiral selector, pH, EOF, nature of the background electrolyte co-ion and organic solvent additives. Most models assume a 1:1 complexation between the enantiomers and the chiral complexation agent although equations describing multiple complexation equilibria have been developed [26–28]. The analyte as well as the chiral selector may be neutral, anionic, cationic, or zwitterionic. In addition to buffer additives (other than the chiral selector) and the nature of the capillary wall (coated or uncoated), which may both affect the EOF, the charge of the solute and the chiral selector determine the mechanism and direction of the migration in CE. Therefore, the nature of the chiral additive contributes not only to the separation selectivity but also, in the case of charged selectors, to the migration direction and magnitude.

The theoretical models may be divided into "mobility difference models" where a separation is expressed as the difference between the effective mobilities of the enantiomers and "selectivity models" that use the separation selectivity α expressed as the ratio between either the effective mobilities of the enantiomers or the complexation constants as a measure of the separation. Only a few models required for the basic understanding of the separation mechanism will be briefly discussed. Further models have been summarized, for example, in [15, 20, 29, 30].

The development of the initial mobility difference model is attributed to Wren and Rowe [31] although the principal equation was derived earlier by Stepanova and Stepanov [32]. Assuming 1:1 complexation, the formation of transient diastereomeric complexes of the enantiomers R and S with a chiral selector, C, is characterized by the complexation constants K_R and K_S:

$$R + C \rightarrow RC \quad K_R = \frac{[RC]}{[R][C]}, \tag{4}$$

$$S + C \rightarrow SC \quad K_S = \frac{[SC]}{[S][C]}.$$

Generally, the effective mobility of an analyte, μ_{eff}, i.e., the apparent mobility corrected for the mobility of the EOF, is the sum of the electrophoretic mobilities of all different species in which the analyte may exist weighted by the mole fraction φ of the respective species

$$\mu_{\text{eff}} = \sum_n \varphi^n \cdot \mu^n, \tag{5}$$

where n is the number of the species present under the experimental conditions. Assuming that for a given chiral separation the enantiomers exist only in a complexed and non-complexed form, (5) becomes for the R-enantiomer

$$\mu^R_{\text{eff}} = f \cdot \mu_f + (1 - f)\mu^R_{\text{cplx}}, \tag{6}$$

where μ_{f} is the mobility of the free enantiomer, μ^R_{eff} is the mobility of the analyte–selector complex, and f is the fraction of the non-complexed species. Considering the complexation constant, K, and the concentration of the selector, $[C]$, the effective mobility of the R-enantiomer may be expressed as

$$\mu^R_{\text{eff}} = \frac{\mu_f + \mu^R_{\text{cplx}} K_R[C]}{1 + K_R[C]}. \tag{7}$$

Thus, the effective mobility of an analyte, μ_{eff}, interacting with a chiral selector is a function of the mobility of the free analyte, μ_{f}, the (limiting) mobility of the analyte–selector complex, μ_{cplx}, the complexation constant, K, (also referred to as binding constant or distribution constant), and the concentration of the chiral selector [31].

An enantioseparation is observed when the effective mobilities of the enantiomers differ, i.e.,

$$\Delta\mu = \mu^R_{\text{eff}} - \mu^S_{\text{eff}} = \frac{\mu_f + \mu^R_{\text{cplx}} K_R[C]}{1 + K_R[C]} - \frac{\mu_f + \mu^S_{\text{cplx}} K_S[C]}{1 + K_S[C]}. \tag{8}$$

The chromatographic enantioselective mechanism (also referred to as the thermodynamic mechanism) is the result of different affinities of the enantiomers towards the chiral selector reflected in differences in the complexation constants, i.e., $K_R \neq K_S$. The electrophoretic enantioselective mechanism is due to differences in the limiting mobilities of the enantiomer–selector complexes, i.e., $\mu^R_{\text{eff}} \neq \mu^S_{\text{eff}}$, caused, for example, by differences in the hydrodynamic radii of the complexes due to a "better fit" of one of the enantiomers. Both mechanisms can contribute simultaneously but the chromatographic mechanism is typically the predominant mechanism because the hydrodynamic radii of the two enantiomer–selector complexes do not differ

significantly and the effective charges of the two complexes are identical. In the case of equal complex mobilities ($\mu^R_{\text{cplx}} = \mu^S_{\text{cplx}} = \mu_{\text{cplx}}$) (8) may be rewritten as [25]

$$\Delta\mu = \frac{[C](\mu_f - \mu_{\text{cplx}})(K_R - K_S)}{1 + [C](K_R + K_S) + K_R K_S [C]^2}. \tag{9}$$

However, it has been clearly shown, that enantioseparations in CE are possible, even in the case of equal complexation constants, i.e., by the electrophoretic enantioselective mechanism based solely on mobility differences of the transient diastereomeric complexes [33]. In the case of equal complexation constants ($K_R = K_S = K$) (8) can be transformed to [25]

$$\Delta\mu = \frac{K[C]\,(\mu^R_{\text{cplx}} - \mu^S_{\text{cplx}})}{1 + K[C]}. \tag{10}$$

This separation mechanism is not possible in the case of immobilized selectors such as in chromatography. Examples for CE enantioseparations with essentially equal binding constants of the enantiomers based on different limiting mobilities of the complexes have been described [33–35].

Although frequently applied to investigating migration phenomena, the model of Wren and Rowe has the disadvantage that it does not account for the protonation equilibrium of the analyte in its free and complexed form. The latter may lead to different charge densities of the complexes at a given pH of the background electrolyte based on a complexation-induced pK_a shift resulting in different limiting mobilities of the diastereomeric selector–enantiomer complexes [36]. Analyte protonation equilibrium was included by Vigh and coworkers in a series of papers [37–39]. For example, for a weakly acidic compound the effective mobility, μ_{eff}, of an enantiomer can be expressed as [37]

$$\mu^R_{\text{eff}} = \frac{\mu^0_- + \mu^0_{\text{RCD}^-} K_{\text{RCD}^-}[C]}{1 + K_{\text{RCD}^-}[C] + \frac{[\text{H}_3\text{O}^+]}{K_a}(1 + K_{\text{HRCD}}[C])}, \tag{11}$$

where μ^0_- is the mobility of the fully deprotonated free analyte, $\mu^0_{\text{RCD}^-}$ is the mobility of the complex between the fully deprotonated species and the chiral selector, K_a is the dissociation constant of the analyte, K_{RCD^-} and K_{HRCD} are the complexation constants of the dissociated and non-dissociated species, $[\text{H}_3\text{O}^+]$ is the hydronium ion concentration of the buffer, and $[C]$ is the concentration of the chiral selector. Assuming identical dissociation constants of the analyte enantiomers the following selectivity model is obtained to characterize the enantioseparation:

$$\alpha = \frac{\mu^R_{\text{eff}}}{\mu^S_{\text{eff}}} = \frac{1 + \frac{\mu^0_{\text{RCD}^-}}{\mu^0_-} K_{\text{RCD}^-}[C]}{1 + \frac{\mu^0_{\text{SCD}^-}}{\mu^0_-} K_{\text{SCD}^-}[C]} \cdot \frac{1 + K_{\text{SCD}^-}[C] + \frac{[\text{H}_3\text{O}^+]}{K_a}(1 + K_{\text{HSCD}}[C])}{1 + K_{\text{RCD}^-}[C] + \frac{[\text{H}_3\text{O}^+]}{K_a}(1 + K_{\text{HRCD}}[C])}. \tag{12}$$

Subsequently, the so-called "chiral charged resolving agent migration model" (CHARM) for the permanently charged chiral selectors was developed including the mobility of the chiral selector [40]. The effective mobility of the *R* enantiomer is given by

$$\mu_{\text{eff}}^{R} = \frac{\mu_f + \mu_{\text{RCD}} K_{\text{RCD}}[\text{CD}] + K[\text{H}_3\text{O}^+](\mu_{\text{HR}} + \mu_{\text{HRCD}} K_{\text{HRCD}}[\text{CD}])}{1 + K_{\text{RCD}}[\text{CD}] + K[\text{H}_3\text{O}^+](1 + K_{\text{HRCD}}[\text{CD}])}. \tag{13}$$

Again the selectivity ratio of the effective mobilities of the enantiomers was applied to characterize an enantioseparation. Depending on the dissociation behavior of the analytes, the model was subdivided into forms for non-electrolytes, strong electrolytes, and weak electrolytes. The migration order of the enantiomers depends on the K and μ values. The model was eventually extended, introducing a binding selectivity term, a size selectivity term representing the mobility ratio of the transient diastereomeric complexes, and parameter for the effect of the complexation on the analyte mobility [41].

Dubsky et al. have developed a theoretical model based on the model by Wren and Rowe to rationalize the often observed superior enantioselectivity of randomly substituted chiral selectors compared to single isomer selectors [42, 43]. The randomly substituted CD was treated as a mixture of a (large) number of defined chiral selectors with different substitution patterns. In this system the effective mobility can be described by an equation formally identical to the equation used for a single selector system, i.e.,

$$\mu_i^{\text{eff}} = \frac{\mu_f + \mu_i^{\text{over}} K_i^{\text{over}} c_{\text{cs}}^{\text{tot}}}{1 + K_i^{\text{over}} c_{\text{cs}}^{\text{tot}}}, \tag{14}$$

where μ_{f} is the mobility of the free analyte, $c_{\text{cs}}^{\text{tot}}$ is the total concentration of the mixture of chiral selectors, i.e., the CDs with different substitution patterns. K_i^{over}, and μ_i^{over} are the overall (apparent) complexation constants and the overall (apparent) limiting mobilities of the complexes, respectively. K_i^{over} is defined by

$$K_i^{\text{over}} = \sum_q \chi^q K_i^q, \tag{15}$$

where χ^q is the molar fraction of the qth CD substitution isomer in the mixture and K_i^q the individual apparent complexation constants of the analyte with the q$^{\text{th}}$ CD isomer. Thus, the overall complexation constant of a multiple isomer CD system is the weighted sum of all individual constants with the mol fractions of the individual CDs as the weights. μ_i^{over} is described by

$$\mu_i^{\text{over}} = \frac{\sum_q \chi^q K_i^q \mu_i^q}{K_i^{\text{over}}}. \tag{16}$$

Equation 16 illustrates that the overall limiting mobility of an enantiomer interacting with a mixture of selector isomers is no longer an independent physicochemical (electrophoretic) property but depends on the distribution of the enantiomer between chiral and achiral environments represented by the complexation constant, K_i^{over}. Thus, μ_i^{over} becomes an apparent parameter influenced by the chromatographic as well as electrophoretic mechanisms so that the overall limiting mobilities of two enantiomers, μ_1^{over} and μ_2^{over}, may substantially differ even in the case of equal individual mobilities for every q^{th} CD in the isomer mixture, i.e., $\mu_1^q = \mu_2^q$. Therefore, even if enantiomers are separated solely on the chromatographic basis using one or another single isomer CD of the mixture an additional electrophoretic separation mechanism may appear if the two CDs are combined. This is even more likely when a mixture of many individual CD isomers is used as is the case in randomly substituted CDs. The theory has been experimentally proven for the enantioseparation of lorazepam using heptakis(6-*O*-sulfo)-β-CD as a single isomer selector and randomly sulfated β-CD as a mixture of multiple isomers [43]. The difference between the effective mobilities of the enantiomers as shown in Fig. 1 increases with increasing concentrations of randomly sulfated β-CD while remaining almost constant in the case of the single isomer CD. The enantioselectivity of the selectors expressed as the ratio of the binding constants, K_i^{over}, is similar for both selectors (1.29 vs 1.32 for the single isomer CD and the multiple isomer CD, respectively) despite the fact that heptakis (6-*O*-sulfo)-β-CD forms stronger complexes compared to randomly sulfated β-CD. However, there is a large difference between the apparent limiting mobilities, μ_i^{over}, for the enantiomers in the case of the multiple isomer CE while the values are practically identical in the case of heptakis(6-*O*-sulfo)-β-CD (Fig. 1). Thus, the enantioseparation with the single isomer CD is largely governed by the (thermodynamic) enantioselectivity of the selector, the electrophoretic enantioselective mechanism (complex mobility) significantly affecting the (increased) enantioseparation observed for the multiple isomer selector represented by randomly sulfated β-CD.

As described in this section, significant differences exist between enantioseparations in pressure-driven chromatographic systems and systems based on electrophoretic phenomena, although the general enantioselective recognition mechanism (i.e., the complexation of the analyte enantiomers by a chiral selector) is the same in both techniques. One striking example is the above-mentioned fact that enantioseparations are possible even if there is no stereoselective recognition of the enantiomers by the selector which can be attributed to the fact that the diastereomeric selector–selectand complexes are mobile and may differ in their respective mobilities.

3 Enantiomer Migration Order

3.1 Techniques for Enantiomer Migration Order Reversal

One of the most striking features of CE is the fact that the enantiomer migration order may be adjusted relatively easily by variation of the experimental conditions.

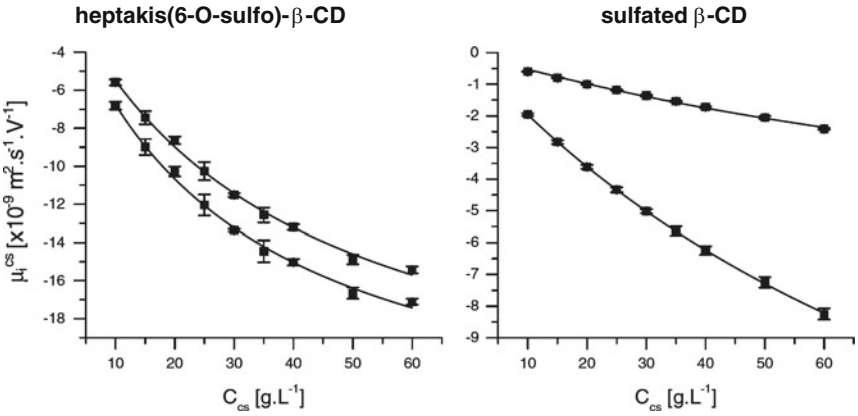

	1st enantiomer [x 10^{-3} L/g]	2nd enantiomer [x 10^{-9} $m^2V^{-1}s^{-1}$]
K_i^{over}	28.1 ± 1.8	36.1 ± 2.3
$\mu_i^{cs(over)}$	– 25.0 ± 0.8	– 25.5 ± 0.7

	1st enantiomer [x 10^{-3} L/g]	2nd enantiomer [x 10^{-9} $m^2V^{-1}s^{-1}$]
K_i^{over}	7.1 ± 1.1	9.4 ± 0.2
$\mu_i^{cs(over)}$	– 7.9 ± 0.9	– 22.8 ± 0.3

Fig. 1 Effective mobility of the enantiomers of lorazepam using heptakis(6-*O*-sulfo)-β-CD (*left*) and randomly sulfated β-CD (*right*) as chiral selectors in a 50 mM tris-tricine buffer, pH 8.11, using an applied voltage of 15 kV. The complexation constants and complex mobilities obtained from curve fitting according to (11) are also presented. (Reproduced with permission of Wiley from [42] © 2010)

For the determination of the enantiomeric excess (ee) the minor enantiomer has to be determined in the presence of a large amount of the other enantiomer. Based on the requirements by the regulatory authorities the excess of one enantiomer may be 1,000-fold. As peak tailing and peak fronting can be observed in CE it may be feasible to determine the minor enantiomer in front of a tailing peak of the main component or after a large fronting peak. Most chiral selectors used in CE are available only in one stereoisomeric form so that reversal of the enantiomer migration order often cannot be achieved by switching to the other enantiomer of the selector. Therefore, other phenomena must be exploited in such cases.

Considering the mobility difference models mentioned above, reversal of the enantiomer migration order is observed when the algebraic sign of the difference of the effective mobilities of enantiomers 1 and 2, $\Delta\mu = \mu_{eff1} - \mu_{eff2}$, or the terms $(K_1 - K_2)$ or $(\mu_f - \mu_{cplx})$ is reversed [44]. In a selectivity model [e.g., (12)], opposite migration order is observed when $\alpha = \mu_{eff1}/\mu_{eff2} > 0$ or < 0. Because the chromatographic principle reflected in the complexation of the solutes as well as the electrophoretic principles affect the effective mobilities of the enantiomers, the following mechanisms can affect the enantiomer migration order [44, 45]:

1. The strength of the complexation of the enantiomers by the selector.
2. The direction and magnitude of the EOF.
3. The direction and magnitude of the mobility of the free analyte.

4. The direction and magnitude of the mobility of the chiral selector.
5. The direction and magnitude of the mobility of the diastereomeric selector–enantiomer complexes.

Combinations may apply. Various scenarios are also possible due to the fact that detection in CE can be performed at the cathodic end (normal polarity of the applied voltage) as well as the anodic end of the capillary (reversed polarity of the applied voltage) so that cathodic as well as anodic mobility can be exploited. Different techniques have been utilized in order to reverse the migration order of enantiomers based on the general phenomena listed above. They are schematically summarized in Fig. 2 considering certain combinations of experimental conditions. However, other combinations than the depicted ones may also apply leading to comparable effects so that the current discussion of mechanisms leading to opposite enantiomer migration order cannot be comprehensive.

The first mechanism is the most obvious. Two chiral selectors possess opposite complexation selectivity toward the enantiomers of an analyte, i.e., enantiomer 1 is bound more strongly than enantiomer 2 by one selector but more weakly than enantiomer 2 by the other selector. If the overall migration direction is not altered by the exchange of the selector this will result in opposite enantiomer migration order. In the case of a positively charged analyte that is detected at the cathode the more weakly complexed analyte migrates first (Fig. 2a). In contrast, analyzing a negatively charged solute with an electrophoretic mobility towards the anode that is carried to the detector at the cathodic end of the capillary (Fig. 2b), the more strongly complexed stereoisomer will migrate first because the more weakly complexed enantiomer possesses a relatively higher mobility towards the anode. Examples of opposite chiral recognition include separations applying the enantiomers of a selector such as in the case of the synthetic polymeric micelles possessing either L- or D-valine as head group [46], in a ligand exchange system when switching the chiral chelator D-penicillamine to L-penicillamine [47], chiral surfactants based on β-L-glucose or β-D-glucose [48], or using the enantiomers of a chiral crown ether as selector [49]. Different complexation selectivities have also been observed for CDs as a group of chiral selectors available in only one configuration. In this case different complexes were formed depending on the size of the CD cavity, the CD derivative, the substitution pattern, or the position of the substituents (see also discussion on complex structures below) as summarized in [44, 45]. Recent examples include [50–57]. Opposite enantiomer migration order of analytes has also been found in the presence of CD derivatives with identical substituents but different substitution patterns [58, 59]. Furthermore, opposite stereoselective recognition of enantiomers by CDs has been observed depending on the charge of the analyte. Thus, one enantiomer is preferentially complexed in the charged form while the other enantiomer is complexed more strongly when the analyte is uncharged. This behavior has been reported for amphoteric compounds such as amino acid derivatives [36] or small peptides [35, 60, 61] (see also Sect. 3.2). Interestingly, the stereoselective recognition can also be affected by the nature of the background electrolyte. Thus, opposite migration order has been

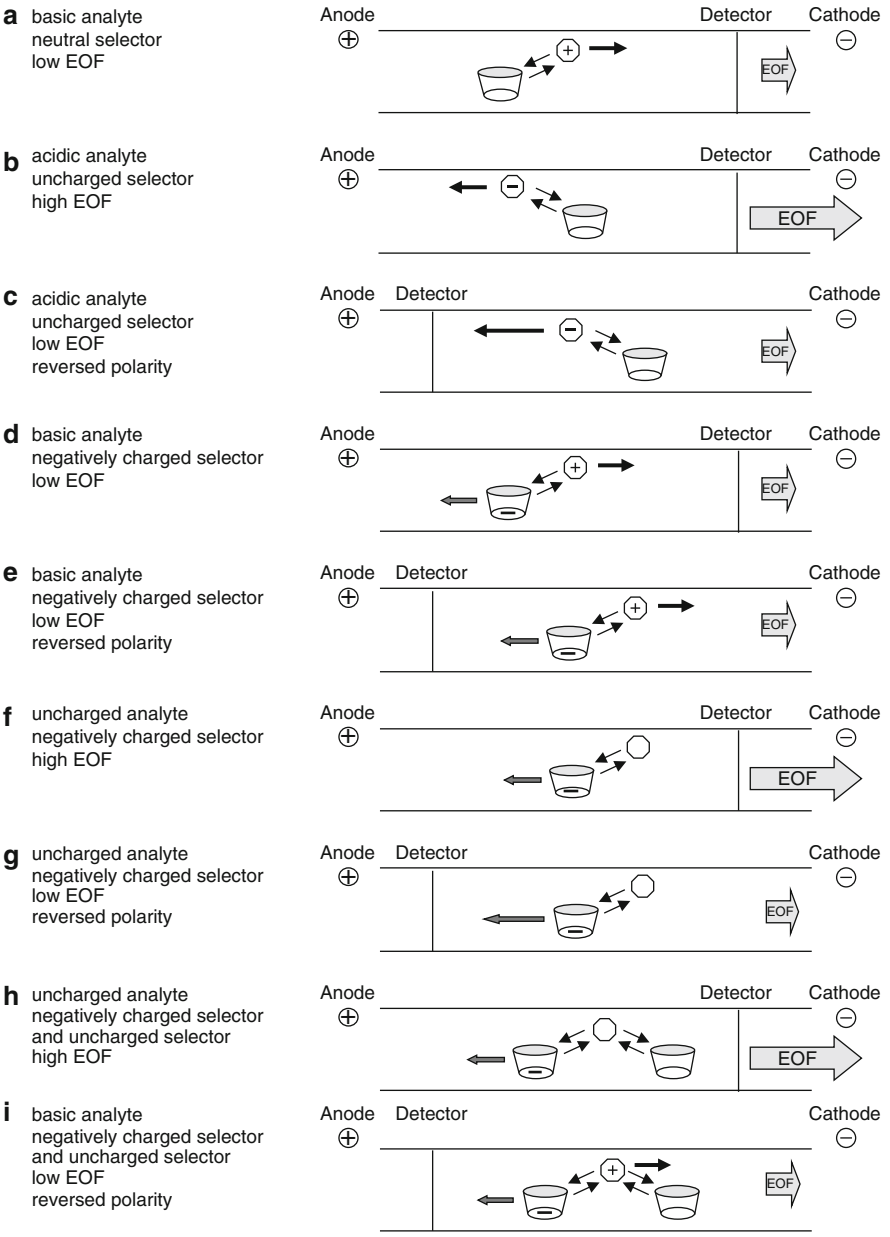

Fig. 2 Schematic representation of migration modes in capillary electrophoresis enantioseparations. The octagon represents the analyte with a possible charge indicated where appropriate. The *basket* represents the chiral selector. A charged selector is indicated by the additional *minus sign*. The *arrows* represent the electrophoretic mobility of analyte and selector, respectively. The net mobility in the different scenarios is always directed towards the detector

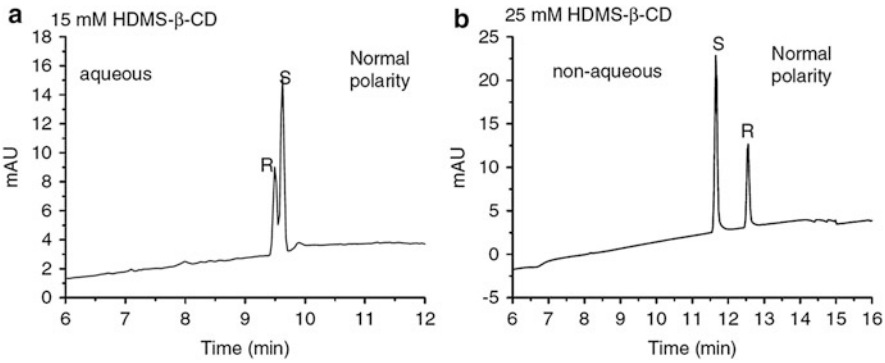

Fig. 3 Enantioseparation of propranolol using heptakis(2,3-di-*O*-methyl-6-*O*-sulfo)-β-CD as chiral selector in (**a**) 100 mM phosphoric acid adjusted to pH 3 by the addition of triethanolamine and (**b**) 10 mM ammonium formate/0.75 M formic acid in methanol. Other experimental conditions: 40/48.5 cm, 50 μm id fused-silica capillary, 15°C, 25 kV, UV detection at 230 nm. (Reproduced with permission of Wiley from [62] © 2010)

observed for propranolol using sulfated cyclodextrins as selectors in aqueous and non-aqueous electrolyte solutions [62–64] as shown for propranolol in the presence of heptakis(2,3-di-*O*-methyl-6-*O*-sulfo)-β-CD (Fig. 3) as a consequence of different complexes between analyte and the CD in an aqueous buffer and a methanolic electrolyte (see also Sect. 4.1). Finally, reversal of the migration order in case of different selector structures has been found in other modes such as MEKC using sugar-based surfactants [48] (Fig. 4) or in ligand-exchange CE using different chelating agents [65, 66].

The EOF is a non-stereoselective force affecting all components of a given separation system in the same way. Many methods are available to increase, decrease, eliminate, or reverse the direction of the EOF by modification of the capillary wall. Elimination or reversal of the EOF can result in opposite migration order under otherwise identical experimental conditions. The enantioselectivity of the chiral selector towards the analyte remains unchanged under both experimental set-ups. For example, opposite migration order of the enantiomers of an anionic compound using an uncharged selector can be observed comparing the situation at a low velocity of the EOF (Fig. 2c) to the situation at a high EOF (Fig. 2b). This has been illustrated for 1,1′-binaphthyl-2,2′-diyl hydrogen phosphate using β-CD as chiral selector in a fused-silica capillary (Fig. 5) [67]. At a low pH the EOF is essentially suppressed so that the negatively charged analytes migrate towards the anode applying reversed polarity of the voltage. Consequently, the more weakly complexed (*R*)-(−)-enantiomer is detected first due to a higher overall mobility. Increasing the pH of the background electrolyte to pH 6.5 results in a significant increase in the EOF so that the analytes are now detected at the cathode (normal polarity of the voltage). Because the more strongly bound (*S*)-(+)-enantiomer displayed an overall lower mobility towards the anode it is now detected first at the cathodic end of the capillary. Opposite migration order can also be observed when comparing bare fused-silica capillaries with a cathodic EOF with capillaries

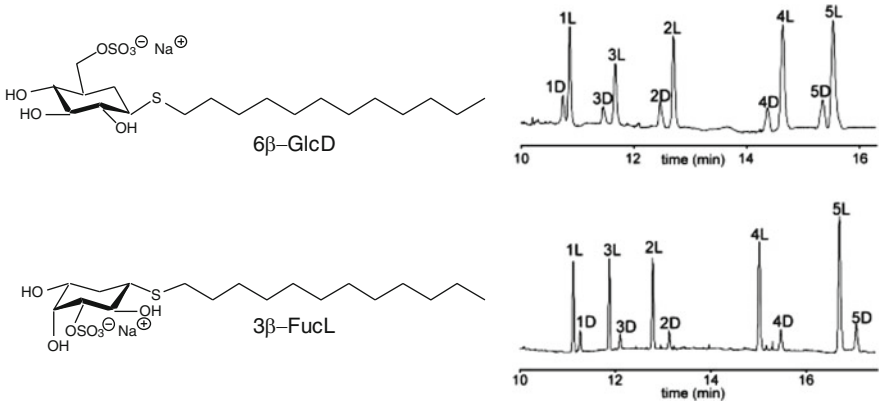

Fig. 4 Enantioseparation of Dns-amino acids (D/L ration 1:3) in MEKC using (*top*) sodium *n*-dodecyl 1-thio-β-D-glucopyranoside 6-hydrogen sulfate (6β-GlcD) and (*bottom*) sodium *n*-dodecyl 1-thio-β-L-fucopyranoside 3-hydrogen sulfate (3β-FucL) as chiral selector. Experimental conditions: 56/64.5 cm, 50 µm id fused-silica capillary, 50 mM phosphate buffer, pH 6.5, containing 30 mM of the surfactant, 25°C, 20 kV, UV detection at 215 nm. Peak assignment: (*1*) Dns-Val, (*2*) Dns-Leu, (*3*) Dns-Met, (*4*) Dns-Phe, (*5*) Dns-Trp. (Reproduced with permission of Wiley from [48] © 2008)

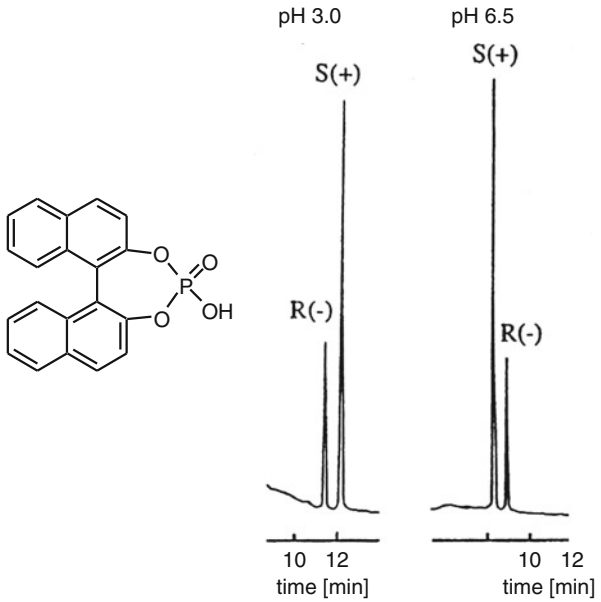

Fig. 5 Enantioseparation of 1,1′-binaphthyl-2,2′-diyl hydrogen phosphate (*S*/*R* ratio 2:1) using 2.5 mg/mL β-CD as chiral selector in 50 mM phosphate buffer (**a**) pH 3.0 and negative polarity of the applied voltage (−400 V/cm), and (**b**) pH 6.5 and normal polarity of the applied voltage (+400 V/cm). Experimental conditions: 50/60 cm, 50 µm id fused-silica capillary, 20°C, UV detection at 210 nm. (Reproduced with permission of Elsevier from [67] © 1996)

coated with positively charged compounds, resulting in an anodic EOF. Examples can be found in [68–70].

Analyte mobility may also be exploited for a reversal of the enantiomer migration order if the analyte can be analyzed as anionic and cationic species. In a fused-silica capillary the direction of the EOF and the mobility of a cationic analyte are both towards the cathode while they are in the opposite direction in the case of an anionic analyte. If the stereoselective recognition of the selector towards the analyte enantiomers remains unchanged whether the cation or the anion is complexed, reversal of the migration order will result. Thus, at a given pH of the background electrolyte the more strongly complexed enantiomer migrates second when analyzing the cationic form due to a lower effective mobility (Fig. 2a). In contrast, when analyzed as anionic species at a higher pH the more weakly complexed enantiomer exhibits a higher mobility towards the anode so that the more strongly complexed analyte is carried faster to the cathode by the EOF (Fig. 2b) resulting in opposite migration order compared to the analysis of the cationic form of the analyte. Examples can be found in [36, 71, 72].

Exploiting the mobility of the chiral selector for a reversal of the enantiomer migration order can be performed in two ways, using either permanently charged chiral selectors or selectors that can exist in either a charged or an uncharged form depending on the pH of the background electrolyte and exhibit identical chiral recognition towards the analyte enantiomers independent of the charge of the selector. A general advantage of charged selectors is the fact that uncharged analytes may also be separated. The situation of a permanently charged selector will be discussed first. For example, using a negatively charged complexation agent (possessing an electrophoretic anodic mobility) for the enantioseparation of a cationic compound, the more weakly complexed enantiomer will be detected first at the cathodic end of the capillary at a low selector concentration (Fig. 2d). At a high concentration the carrier ability of the charged selector can be exploited detecting the analyte at the anode. Thus, upon reversal of the polarity of the applied voltage the more strongly complexed analyte will be transported faster to the detector at the anodic end of the capillary resulting in a reversal of the enantiomer migration order (Fig. 2e). The same scenario would result with the combination of an uncharged analyte and a negatively charged selector. At low selector concentrations the more weakly complexed enantiomer is detected first at the cathode if a sufficiently high EOF exists (Fig. 2f), while under reversed polarity of the applied voltage exploiting the carrier ability of the selector the more strongly bound enantiomer will be detected first at the anodic end of the capillary (Fig. 2g). An example is the simultaneous separation of isomers and enantiomers of the dipeptide α/β-Asp-PheOMe in a pH 5.25 background electrolyte in the presence of carboxymethyl-β-CD (Fig. 6) [73]. At pH 5.25 the peptides are essentially uncharged while the CD is negatively charged. In addition, the inner wall of the capillary was coated with polyacrylamide in order to eliminate the EOF when using the CD as a carrier. Thus, at the low CD concentration the migration order is obtained as shown in Fig. 6a. The migration order of each enantiomeric pair is opposite at high concentrations of carboxymethyl-β-CD under reversed polarity of

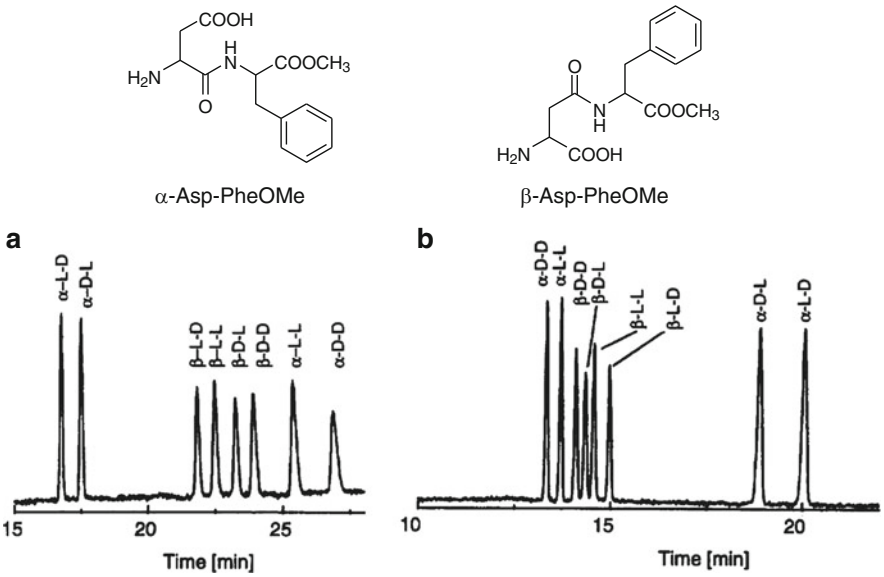

Fig. 6 Separation of enantiomers of the α/β-isomers of Asp-PheOMe under (**a**) normal polarity of the applied voltage (detection at the cathode) and (**b**) exploiting the carrier ability of the selector under reversed polarity of the applied voltage (detection at the anode). Experimental conditions: (**a**) 40/47 cm, 50 μm id fused-silica capillary, 50 mM sodium phosphate buffer, pH 5.25, 15 mg/mL carboxymethyl-β-CD, +20 kV, 20°C, UV detection at 215 nm and (**b**) 40/47 cm, 50 μm id polyacrylamide-coated capillary, 50 mM sodium phosphate buffer, pH 5.25, 60 mg/mL carboxymethyl-β-CD, −20 kV, 20°C, UV detection at 215 nm. (Reproduced with permission of Elsevier from [73] © 1998)

the applied voltage (Fig. 6b). Other examples can be found in [74–78] including the use of positively charged selectors [79, 80]. In the case of selectors possessing functional groups such as carboxylic acids or amines which are charged as a function of the pH of the background electrolyte, the selectors may be used as either neutral complexation agent without a self-mobility or as a charged compound with an electrophoretic self-mobility. If the chiral recognition towards the enantiomers does not change with the charge of the chiral selector, opposite migration order will be observed when detecting the enantiomers at the anode (reversed polarity of the voltage) as compared to the detection at the cathode (normal polarity of the voltage). The combinations are schematically illustrated for a positively charged analyte in Fig. 2a (uncharged form of the selector) and Fig. 2e (charged form of the selector). Examples of enantioseparations based on this principle or migration order reversal have been described in [81, 82].

Another technique applies a combination of chiral selectors. In this mode the selectors have to possess opposite chiral recognition towards the analyte enantiomers [83] or different mobilities in case the chiral recognition is the same but occurs with a different magnitude [84]. In the first case the migration order is a function of the CD used at a higher concentration in the binary mixture. This

mechanism is essentially the same as using the individual selector alone as discussed above as first option of a reversal of the enantiomer migration order. In the second scenario typically a charged and an uncharged selector are combined. The migration order of the enantiomers in the absence of the uncharged selector results from the analyte complexation by the charged complexation agent depending on whether the analyte itself is charged or uncharged and whether detection is subsequently carried out at the anodic or the cathodic end of the capillary. For example, when using a negatively charged selector for the separation of a neutral analyte detecting at the cathode, the more weakly complexed enantiomer will migrate first because it is carried to the detector by the EOF while the analyte–selector complex migrates towards the anode (Fig. 2f). Adding an uncharged selector with the same chiral recognition but stronger analyte complexation compared to the charged selector competition between the selectors for the analyte enantiomers results in a lower overall binding of the more strongly complexed enantiomer by the negatively charged selector. As a consequence, the complex between the neutral selector and the more strongly bound enantiomer is carried to the detector at the cathode by the EOF faster than the more weakly bound enantiomer (Fig. 2h) and reversal of the enantiomer migration order results. This has been shown for the separation of the enantiomers (*R*,*R*)- and (*S*,*S*)-hydroxybenzoin (the compound also exists as a mesoform) (Fig. 7) [85]. In a fused-silica capillary using a phosphate buffer, pH 9.0, as background electrolyte, the (*S*,*S*)-configured enantiomer migrates before the (*R*,*R*)-enantiomer in the presence of sulfated β-CD as chiral selector. Upon addition of increasing amounts of neutral β-CD co-migration is first observed followed by enantioseparation with reversed migration order, i.e., (*R*,*R*)-hydroxybenzoin before (*S*,*S*)-hydroxybenzoin. Interestingly the migration order of the enantiomers of the related substances benzoin or benzoin methyl ether is not affected by the addition of β-CD (Fig. 7). Another example of enantiomer migration order reversal of a neutral analyte as a function of a binary selector system is reported in [84]. A similar observation has also been made for protonated analytes in combination with negatively charged sulfated β-CD under reversed polarity of the applied voltage and detection at the anodic end of the capillary [86, 87] as schematically illustrated in Fig. 2i. In this set-up the more strongly complexed enantiomer is detected first when only working with the negatively charged selector. Adding an uncharged selector, with the same chiral recognition but stronger analyte complexation compared to the charged selector competition between the selectors for the analyte enantiomers, results in a lower overall binding of the more strongly complexed enantiomer by the negatively charged selector. As a consequence, the more weakly bound enantiomer is less retarded by the uncharged selector increasing its binding by the charged selector so that it now reaches the detector at the anode first. The combination of a CD with a polymeric chiral surfactant can also result in the reversal of the migration order of enantiomers [88].

It has also been shown that achiral additives in a system containing a chiral selector can affect the enantiomer migration order. Thus, it has been observed that addition of an achiral surfactant above the critical micelle concentration reversed the

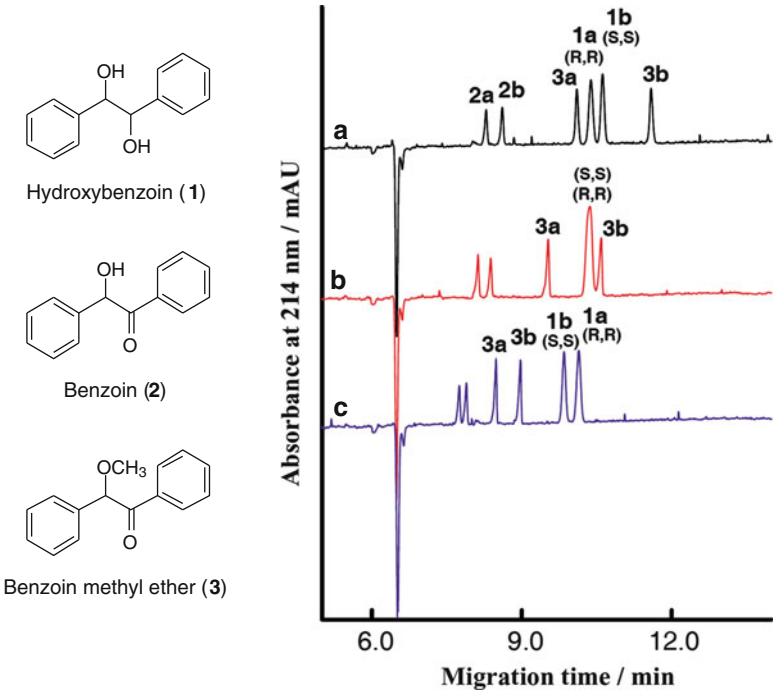

Fig. 7 Enantiomer migration order of benzoin derivatives in the presence of 3.5% (w/v) sulfated β-CD as a function of the addition of β-CD: (*A*) no addition, (*B*) 0.3 mM β-CD, and (*C*) 0.9 mM β-CD. Experimental conditions: 50/57 cm, 50 μm id fused-silica capillary, 50 mM borate buffer, pH 9.0, 25°C, 20 kV, UV detection at 214 nm. Peak assignment: (*1*) hydroxybenzoin, (*2*) benzoin, (*3*) benzoin methyl ether. (Reproduced with permission of Elsevier from [85] © 2004)

migration order of the enantiomers of amino acids in chiral ligand exchange [89] or in the presence of vancomycin as chiral selector [90]. The effects may be explained by a change of the electrophoretic mobility of the selector upon interaction with the micelles or by a preferred partitioning of the more weakly complexed enantiomer into the micelles which will migrate with the micelles in the opposite direction compared to the situation in the absence of the micelles. Furthermore, the same effect has been observed in an MEKC system containing γ-CD upon addition of 2-propanol [91]. A switch of the enantioselectivity of the complexation in the presence of organic solvents may be considered as the underlying mechanism.

Finally, complex mobility may be the reason for a reversal of the enantiomer migration order. This mechanism applies when the phenomenon is observed as a function of the concentration of the chiral selector or the pH of the background electrolyte. Of course, the mobility of the selector–selectand complex is also exploited in several cases above, especially in the case of charged chiral selectors in combination with the application of opposite polarity of the applied voltage. However, the present case refers to the situation when reversal of the migration order is observed without altering the polarity of the voltage but just upon increasing the selector

concentration. Moreover, the phenomenon has also been observed for uncharged selectors. In the present scenario the reversal is due to an increasing influence of the enantiomer–selector complex mobilities compared to the mobility of the free analyte. As can be concluded from (8), the enantiomer migration order will not depend on the concentration of a chiral selector if both, the enantioselective affinity and the limiting mobilities of the diastereomeric complexes act in the same direction. Thus, assuming a protonated analyte and a neutral selector, the (*S*)-enantiomer will be detected before the (*R*)-enantiomer independent of the selector concentration if $K_R > K_S$ and $\mu^R_{\mathrm{cplx}} < \mu^S_{\mathrm{cplx}}$ and, in addition, the EOF does not affect the migration order. However, if $\mu^R_{\mathrm{cplx}} > \mu^S_{\mathrm{cplx}}$ and $K_R > K_S$, the enantiomer migration order may be either $S > R$ or $R > S$ depending on the magnitude of the differences of the binding constants and the mobilities of the complexes. Generally speaking, at low selector concentration a relatively low molar fraction of the analyte is complexed. Consequently, the migration order of the enantiomers is determined by their magnitude of complexation by the selector so that the more strongly complexed enantiomer migrates second because it is retarded relative to the more weakly bound enantiomer. At high selector concentrations both enantiomers are bound to a significant extent so that the migration order is determined by the mobilities of the transient diastereomeric complexes. In many cases the diastereomeric complexes possess equal mobilities so that deterioration of the enantioseparation is observed at high selector concentrations. However, in the case where the mobilities of the transient diastereomeric differ and the complex of the more strongly bound enantiomer has the higher mobility, reversal of the migration order will be observed. The mechanism was described first by Schmitt and Engelhardt in 1993 for Dns-Phe as analyte and hydroxypropyl-β-CD as selector [92]. Recent publications on this topic include [34, 93–97]. A recent example is illustrated in Fig. 8 for the separation of the enantiomers of ketoconazole in a phosphate buffer, pH 3.0, using hydroxypropyl-β-CD as chiral selector [34]. Upon increasing the CD concentration, co-migration of the peaks and subsequent reversed enantiomer migration order were observed. The behavior could be rationalized based on the apparent complexation constants, K, and the limiting mobilities of the analyte–CD complexes, μ_{cplx}, also compiled in Fig. 8. Ketoconazole is a weak base so that the compound is protonated at pH 3 and migrates towards the cathode. At low CD concentrations the more weakly complexed (2*R*,4*S*)-enantiomer migrates first. However, the tighter complex between hydroxypropyl-β-CD and the (2*S*,4*R*)-enantiomer possesses the higher electrophoretic mobility of $3.85 \pm 0.08 \times 10^{-9}\ \mathrm{m^2\ V^{-1}\ s^{-1}}$ compared to the complex of the (2*R*,4*S*)-enantiomer ($3.65 \pm 0.09 \times 10^{-9}\ \mathrm{m^2\ V^{-1}\ s^{-1}}$). Thus, when increasing the CD concentration the molar fraction of complexed analyte also increases so that the mobilities of the complexes become more and more dominant. In the present case complex mobility and stereoselectivity of the CD counteract each other. As a consequence, co-migration of the enantiomers results at first and, subsequently, an enantioseparation but with opposite migration order of the enantiomers as compared to low selector concentrations. At high CD concentrations the complex mobilities determine the migration order of the enantiomers so that the (2*S*,4*R*)-enantiomer is now detected first.

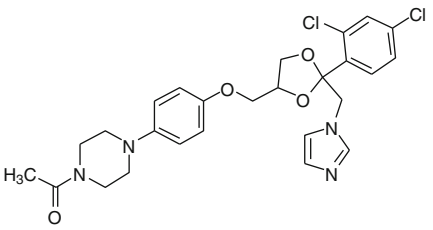

Enantiomer	K [M^{-1}]	μ_{cplx} [$m^2V^{-1}s^{-1}$ x 10^{-9}]
2R,4S	427 ± 11	3.65 ± 0.09
2S,4R	456 ± 9	3.85 ± 0.08

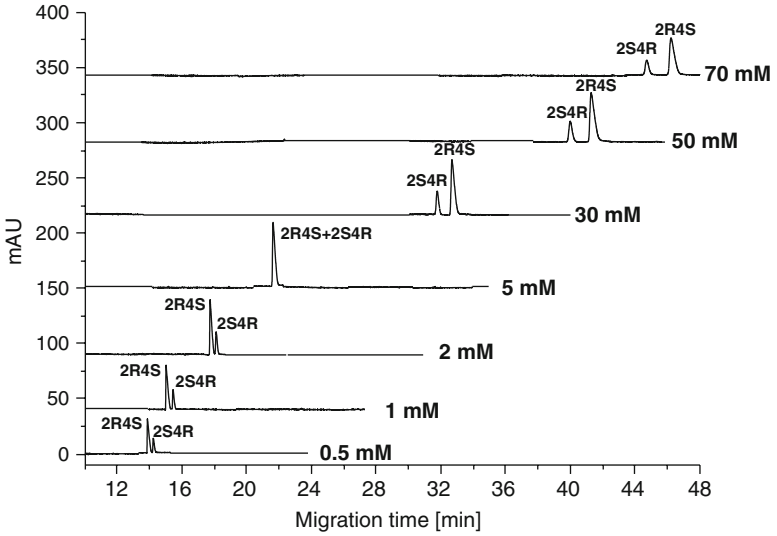

Fig. 8 Migration order of the enantiomers of ketoconazole as a function of the concentration of hydroxypropyl-β-CD as chiral selector as well as complexation constants and mobilities of the analyte–CD complexes. Experimental conditions: 56/64.5 cm, 50 μm id fused-silica capillary, 100 mM sodium phosphate buffer, pH 3.0, 15°C, 30 kV, UV detection at 200 nm. (Electropherograms reproduced with permission of Wiley from [34] © 2009)

The higher mobility of the complex of the more strongly bound enantiomer may be explained by an increased charged density resulting from a smaller size of the complex formed between the selector and the more tightly bound enantiomer as compared to the more weakly complexed enantiomer. Another phenomenon translating into a higher charge density of the stronger complex is the complexation-induced pK_a shift. A reversal of the enantiomer migration order was observed when increasing the pH of the background electrolyte in a rather narrow pH range for Dns-amino acids [36, 98] and small peptides [35, 60, 61, 80, 82, 99–101] in the range of pH = pK_a ± 2 using neutral or charged CD derivatives as chiral selectors.

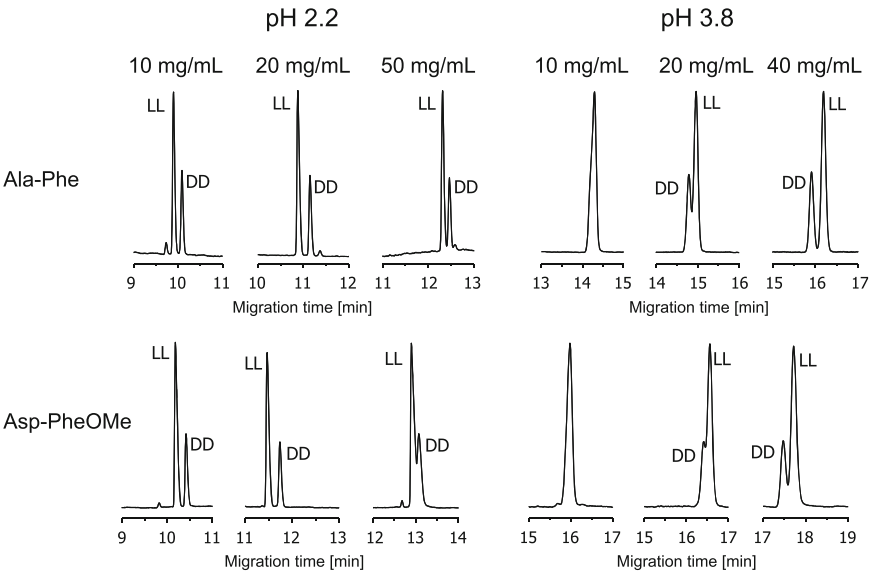

Peptide	$\mu_{H_2A^+}$ [10^{-9} $m^2s^{-1}V^{-1}$]	$\mu_{CD\text{-}H_2A^+}$ [10^{-9} $m^2s^{-1}V^{-1}$]	K_+ [M^{-1}]	K_n [M^{-1}]	pK_a	$pK_{a/cplx}$
L-Ala-L-Phe	17.9 ± 0.1	7.6 ± 0.6	34 ± 4	22 ± 4	3.26 ± 0.01	3.45 ± 0.04
D-Ala-D-Phe	17.9 ± 0.1	7.5 ± 0.5	42 ± 5	23 ± 4	3.26 ± 0.01	3.53 ± 0.04
L-Asp-L-PheOMe	17.0 ± 0.1	8.5 ± 0.3	63 ± 6	78 ± 4	3.16 ± 0.01	3.07 ± 0.02
D-Asp-D-PheOMe	17.0 ± 0.1	8.5 ± 0.3	79 ± 7	81 ± 4	3.16 ± 0.01	3.15 ± 0.02

Fig. 9 pH-dependent reversal of the migration order of the enantiomers of Ala-Phe and Asp-PheOMe using β-CD as chiral selector as well as mobilities, binding constants and pK_a values of the free analytes and the respective complexes. Experimental conditions: 50/57 cm, 50 mm id fused-silica capillary, 50 mM sodium phosphate buffer containing 2 M urea, 20°C, 25 kV, UV detection at 214 nm. (Electropherograms reproduced with permission of Wiley from [102] © 2010)

This phenomenon was attributed to a change of the pK_a value of the analyte upon complexation by the selector. If the pK_a is shifted towards higher values, the complex of the more strongly bound enantiomer has a higher overall charge compared to the complex of the more weakly bound enantiomer. The increasing contribution of the complex mobilities counteracts the enantioselectivity of the chiral selector represented by the complexation constants leading to a reversal of the enantiomer migration order at high concentrations of the selector. A recent example is the analysis of the LL- and DD-stereoisomers of the dipeptides Ala-Phe and Asp-PheOMe using β-CD as chiral selector [102]. At pH 2.2 the LL-enantiomers migrated before the DD-stereoisomers while reversed migration order was observed at pH 3.8 (Fig. 9). Complexation constants of the protonated form, K_+, and the neutral (zwitterionic) species of the peptide enantiomers, K_n, the mobilities of the

free analyte, $\mu_{H_2A^+}$, and the enantiomer–selector complexes, $\mu_{CD-H_2A^+}$, as well as the pK_a values of the complexes p$K_{a/cplx}$ can analyzed in order to rationalize the observed migration behavior. At pH 2,2 (about 1 unit below the pK_a value of the peptides), the peptides are essentially positively charged and the migration behavior is governed by the complexation constants, K_+, i.e., the selectivity of β-CD towards the protonated species. Thus, the LL-enantiomers migrate before the DD-stereoisomers. After an initial improvement of the resolution upon increasing the CD concentration, the separation deteriorated because of the increasing influence of the complex mobilities $\mu_{CD-H_2A^+}$ which are essentially equal. Furthermore, an enantioselective complexation-induced pK_a shift was found, with the higher shift of the more strongly complexed DD-enantiomers. This results in a shift of the equilibrium in favor of the protonated form of the complex at pH values close to the pK_a of the analytes. Consequently, the mobility of the complex becomes greater than the mobility of the free analyte at this specific pH value. Because the complexation constants of the neutral peptide, K_n, are essentially equal the enantiomer migration order is dominated by complex mobility. Thus, the enantiomer displaying the higher complex mobility migrates first. In the present case this applies to the DD-enantiomers, i.e., reversal of the enantiomer migration order is observed. Moreover, the resolution increases at higher CD concentrations because the friction of the complexed analyte is also increased. Similar pH-dependent reversal of the enantiomer migration order was also observed in the case of Dns-amino acids [36, 98] and other small peptides [35, 61, 80, 82, 99].

Enantiomer migration order reversal as a function of the selector concentration has also recently been described in chiral ligand exchange CE with the Cu(II)-D-quinic acid system as selector for the enantioseparation of tartaric acid in a pH 5.0 background electrolyte [103]. Keeping the concentration of Cu(II) constant at 10 mM, reversal of the enantiomer migration order was observed upon increasing the concentration of D-quinic acid from 10 to 120 mM. The same effect was observed when keeping the D-quinic acid concentration constant at 15 mM and increasing the concentration of Cu(II) from 1 to 10 mM. Subsequent spectroscopic studies proved the assumption that D-quinate acts as a bidentate ligand coordinated through the carboxylate oxygen and the C-1 hydroxyl group so that the formation of 1:1, 1:2 and 1:3 Cu(II)–D-quinate complexes is possible depending on the concentration ratio [104]. Furthermore, it was concluded from circular dichroism spectra that the 1:1 Cu(II)–D-quinate complex had a coordination selectivity for D-tartrate while the 1:2 Cu(II)–D-quinate complex displayed selectivity for L-tartrate. Thus, complexes with different stoichiometries and selectivities are formed depending on the Cu(II) D-quinic acid ratio leading to opposite enantiomer migration order. Therefore, this scenario resembles more the first situation discussed in this section where enantiomer migration order reversal is due to different selectors with different stereoselectivities rather than a reversal based on different mobilities of the selector–selectand complexes.

3.2 Theoretical Model of Enantiomer Migration Order Reversal

The dependence of the enantiomer migration order on selector concentration and pH of the background electrolyte appeared especially intriguing and has been the subject for theoretical models in order to rationalize and predict reversal of the enantiomer migration. A mathematical approach developed for a weak base and a neutral chiral selector considered the protonation equilibria of the free base and the analyte–selector complex as well as the complexation equilibria between the protonated and neutral species of the analyte with the selector [105, 106]. The effective mobility of an analyte, μ_{eff}, can be described as

$$\mu_{\text{eff}} = \frac{\mu_{\text{HB}^+} + \mu_{\text{HB}^+\text{C}} \cdot K_+ \cdot [C]}{1 + K_+ \cdot [C]} \cdot \frac{1}{1 + 10^{\text{pH} - \left(\text{p}K_\text{a} + \log \frac{1 + K_+ \cdot [C]}{1 + K_n \cdot [C]}\right)}}, \tag{17}$$

expressing μ_{eff} as a function the selector concentration, $[C]$, the pH of the background electrolyte, the pK_a value of the analyte, the binding constants of the protonated and neutral species, K_+ and K_n, and the mobilities of the protonated free species and the corresponding complex, μ_{HB^+} and $\mu_{\text{HB}^+\text{C}}$, respectively. The separation selectivity, S, is expressed as

$$\begin{aligned} S &= \frac{\mu_{\text{eff1}}}{\mu_{\text{eff2}}} \\ &= \frac{(\mu_{\text{HB}^+} + \mu_{\text{HB}^+\text{CD1}} \cdot K_{+1} \cdot [\text{CD}]) \cdot (10^{\text{p}K_\text{a}} \cdot (1 + K_{+2} \cdot [\text{CD}]) + 10^{\text{pH}} \cdot (1 + K_{n2} \cdot [\text{CD}]))}{(\mu_{\text{HB}^+} + \mu_{\text{HB}^+\text{CD2}} \cdot K_{+2} \cdot [\text{CD}]) \cdot (10^{\text{p}K_\text{a}} \cdot (1 + K_{+1} \cdot [\text{CD}]) + 10^{\text{pH}} \cdot (1 + K_{n1} \cdot [\text{CD}]))}. \end{aligned} \tag{18}$$

According to (18) a separation results from $\mu_{\text{eff1}} \neq \mu_{\text{eff2}}$ which is achieved when the enantiomers differ in the binding constants of the protonated species ($K_{+1} \neq K_{+2}$), the neutral species ($K_{\text{n1}} \neq K_{\text{n2}}$), and/or the mobilities of the two enantiomer–selector complexes ($\mu_{\text{HB}^+\text{C1}} \neq \mu_{\text{HB}^+\text{C2}}$).

Buffer pH and CD concentration are experimental variables. In a typical experiment one of them is set at a constant value so that (17) can be simplified. At a constant CD concentration μ_{eff} transforms to $\mu_{\text{eff/CD}}$:

$$\mu_{\text{eff/CD}} = \frac{\mu_{+/\text{CD}}}{1 + 10^{(\text{pH} - \text{p}K_{\text{a/CD}})}}, \tag{19}$$

where $\mu_{+/\text{CD}}$ is the effective mobility of the fully protonated analyte and p$K_{\text{a/CD}}$ is the pK_a value, both at the fixed CD concentration. $\mu_{+/\text{CD}}$ is described by

$$\mu_{+/\mathrm{CD}} = \frac{\mu_{\mathrm{HB}^+} + \mu_{\mathrm{HB}^+\mathrm{CD}} \cdot K_+ \cdot [\mathrm{CD}]}{1 + K_+ \cdot [\mathrm{CD}]}, \tag{20}$$

and $\mathrm{p}K_{\mathrm{a/CD}}$ by

$$\mathrm{p}K_{\mathrm{a/CD}} = \mathrm{p}K_{\mathrm{a}} + \log \frac{1 + K_+ \cdot [\mathrm{CD}]}{1 + K_n \cdot [\mathrm{CD}]}. \tag{21}$$

In the absence of a selector, μ_{f} is expressed by

$$\mu_f = \frac{\mu_{\mathrm{HB}^+}}{1 + 10^{(\mathrm{pH}-\mathrm{p}K_{\mathrm{a}})}}. \tag{22}$$

At an infinitely high CD concentration the complex mobility can be described by

$$\mu_c = \frac{\mu_{\mathrm{HB}^+\mathrm{CD}}}{1 + 10^{(\mathrm{pH}-\mathrm{p}K_{\mathrm{a/c}})}}, \tag{23}$$

where $\mathrm{p}K_{\mathrm{a/c}}$ is the $\mathrm{p}K_{\mathrm{a}}$ value of the diastereomeric analyte–CD complex and a function of the $\mathrm{p}K_{\mathrm{a}}$ of the free analyte and the complexation constants K_+ and K_n according to

$$\mathrm{p}K_{\mathrm{a/c}} = \mathrm{p}K_{\mathrm{a}} + \log \frac{K_+}{K_n}, \tag{24}$$

where $\mathrm{p}K_{\mathrm{a/c}}$ is the limiting value of $\mathrm{p}K_{\mathrm{a/CD}}$ for $[\mathrm{CD}] \rightarrow \infty$ according to (21) and is referred to as the complexation-induced $\mathrm{p}K_{\mathrm{a}}$ shift. At constant pH (17) can be simplified to (7). K is the apparent complexation constant defined by

$$K = \frac{K_+ + K_n \cdot 10^{(\mathrm{pH}-\mathrm{p}K_{\mathrm{a}})}}{1 + 10^{(\mathrm{pH}-\mathrm{p}K_{\mathrm{a}})}}, \tag{25}$$

where K_+, K_n, μ_{HB^+}, and $\mu_{\mathrm{HB}^+\mathrm{CD}}$ are pH-independent parameters while K, μ_{f}, and μ_{c} are pH-dependent parameters.

A systematic classification of enantiomer migration order as a function of selector concentration [CD] and buffer pH specifically considering the $\mathrm{p}K_{\mathrm{a}}$ of the analyte can be constructed as a 3D plot of the selectivity S possessing four corner points with low/high [CD] and low/high pH (Fig. 10) [105]. In each corner point the selectivity can be described as a function of the complexation equilibria between the charged and electroneutral species of the basic analyte and the selector as well as the mobility of the free analyte and the limiting mobility of the analyte–selector complexes. Depending on the conditions, only one or several of these factors will affect the selectivity. Therefore, at constant pH or selector concentration the selectivity (and with it the enantiomer migration order) parallel to the edges of the surface plot can be concluded. Knowing the selectivity in the corner points one

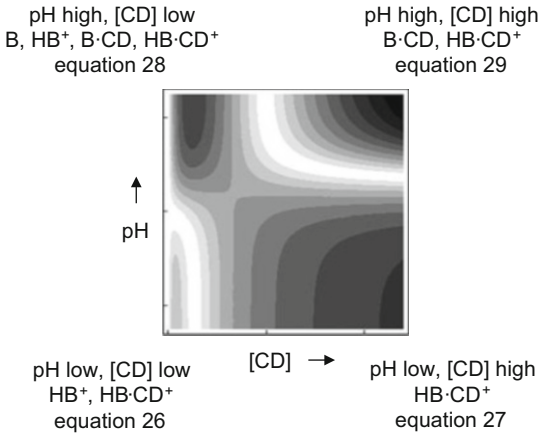

Fig. 10 Schematic representation of a 3D contour plot illustrating the low/high pH and low/high selector concentration conditions at the corner points. (Adapted with permission of Elsevier from [20] © 2011)

can deduce whether a selectivity change, i.e., reversal of the enantiomer migration order, occurs along the plot upon changing either pH or [CD].

In the mathematical treatment "low" and "high" pH with regard to analyte pK_a are defined as pH $\rightarrow -\infty$ and pH $\rightarrow +\infty$, respectively, meaning that the analyte is essentially fully protonated at "low" pH while it is basically completely deprotonated, i.e., neutral, at "high" pH. [CD] is defined between 0 (low) and $+\infty$ (high). At infinite [CD] essentially only the analyte–CD complexes exist. At [CD] = 0 enantioseparation is not possible, so that for mathematical treatment an infinitesimal CD concentration is assumed where selectivity S is derived from the first derivative $\delta S/\delta$[CD] at [CD] = 0. For $\delta S/\delta$[CD] < 0 S becomes < 1, for $\delta S/\delta$[CD] $= 0$ S becomes equal to 1, and for $\delta S/\delta$[CD] > 0 S becomes > 1.

At the vertex 1 with pH $\rightarrow -\infty$ and infinitesimal [CD] (pH low, [CD] low) basically only the non-complexed fully protonated analyte is present so that

$$\frac{\delta S}{\delta[\mathrm{CD}]} = \frac{\mu_{\mathrm{HB}^+} \cdot (-K_{+1} + K_{+2}) + \mu_{\mathrm{HB}^+\mathrm{CD1}} \cdot K_{+1} - \mu_{\mathrm{HB}^+\mathrm{CD2}} \cdot K_{+2}}{\mu_{\mathrm{HB}^+}}. \tag{26}$$

Therefore, complex mobilities and binding constants of the protonated analytes determine selectivity S and enantiomer migration order.

At the corner point 2 at pH $\rightarrow -\infty$ and [CD] $\rightarrow +\infty$ (pH low, [CD] high) essentially only the protonated analyte–CD complex exists, so that S is solely a function of the complex mobilities according to

$$S = \frac{\mu_{\mathrm{HB}^+\mathrm{CD1}}}{\mu_{\mathrm{HB}^+\mathrm{CD2}}}. \tag{27}$$

At the vertex 3 at pH $\rightarrow +\infty$ and infinitesimal [CD] (pH high, [CD] low) the analyte exists mainly in the neutral free form so that

$$\frac{\delta S}{\delta[\mathrm{CD}]} = \frac{\mu_{\mathrm{HB}^+} \cdot (-K_{n1} + K_{n2}) + \mu_{\mathrm{HB}^+\mathrm{CD1}} \cdot K_{+1} - \mu_{\mathrm{HB}^+\mathrm{CD2}} \cdot K_{+2}}{\mu_{\mathrm{HB}^+}}. \tag{28}$$

Here, S depends on the ratio of the affinity constants of the protonated analyte, K_{+1}/K_{+2}, relative to the ratio of binding constants of the neutral species, K_{n1}/K_{n2}, as well as on the dimensions of the affinity constants K_+ relative to K_n.

Finally, at the corner point 4 with pH $\rightarrow +\infty$ and [CD] $\rightarrow +\infty$ (pH high, [CD] high) the neutral, fully complexed species predominates resulting in

$$S = \frac{\mu_{\mathrm{HB}^+\mathrm{CD1}}}{\mu_{\mathrm{HB}^+\mathrm{CD2}}} \cdot \frac{K_{+1} \cdot K_{n2}}{K_{+2} \cdot K_{n1}}. \tag{29}$$

The coexisting protonated and neutral forms of the analytes are essentially complexed so that the selectivity is a function of complex mobilities as well as the binding constants of the protonated and neutral species.

Depending on the complexation constants and the complex mobilities, 15 different scenarios were classified mathematically with regard to the selectivity at the 4 corner points as summarized in Table 1 [106]. The model identifies four basic mechanisms leading to the inversion of the enantiomer migration order of a weak base in the presence of a neutral chiral selector, three in a pH-dependent manner and one as a function of the selector concentration. Further mechanisms for a reversal of the enantiomer migration order such as the use of selectors with opposite stereoselective recognition of the analyte enantiomers are not described by the model and were not considered.

A pH-dependent reversal of the enantiomer migration order is described by parallels between the corner points 1 and 3 (low [CD]) or 2 and 4 (high [CD]) of the selectivity plot (Fig. 10). It may be observed due to (1) inversion of the complex mobilities caused by an enantioselective pK_a shift, (2) inversion of the ratio of the mobilities of the analyte–selector complex and the free analyte due to a significant complexation-induced pK_a shift to a higher value, and (3) opposite chiral recognition of the protonated and the effectively electroneutral forms of the analyte by the chiral selector.

Mechanism 1 refers to the effects between the second and fourth corner points at high selector concentration. Comparing (27) and (29) it is clear that the migration order is affected by the ratio of the complexation constants $K_{+1}K_{n2}/K_{+2}K_{n1}$. Because the ratio K_+/K_n affects the protonation equilibrium of the complex [(24)] this relationship can be expressed as the difference of the pK_a values of the diastereomeric analyte enantiomer–CD complexes by $10^{\mathrm{p}K\mathrm{a/c1}-\mathrm{p}K\mathrm{a/c2}}$. Thus, the higher the ratio K_+/K_n, i.e., the more preferred the protonated form is complexed compared to the neutral species, the higher the resulting pK_a shift. Because only the protonated species contributes to the effective mobilities, the enantiomer with the higher complexation-induced pK_a

Table 1 Systematic classification of the separation selectivity with regard to the enantiomer migration order as derived from (26) to (29) in the area around the four corner points of the selectivity plot as defined by the extremes of pH and [CD][a]

	Selectivity				Enantiomer migration order reversal			
	Low pH		High pH		pH-dependent		[CD]-dependent	
Case	High [CD] (27)	Low [CD] (26)	High [CD] (29)	Low [CD] (28)	High [CD] (27–29)	Low [CD] (26–28)	Low pH (26–27)	High pH (28–29)
I	$S = 1$	$S = 1$	$S < 1$	$S < 1$	–	–	–	–
II		$S < 1$	$S = 1$	$S \leq 1$	–	–	–	–
III				$S > 1$	–	+	–	–
IV			$S < 1$	$S \leq 1$	–	–	–	–
V				$S > 1$	–	+	–	+
VI			$S > 1$	$S \leq 1$	–	–	–	+
VII				$S > 1$	–	+	–	–
VIII	$S < 1$	$S \leq 1$	$S \leq 1$	$S \leq 1$	–	–	–	–
IX				$S > 1$	–	+	–	+
X			$S > 1$	$S \leq 1$	+	–	–	+
XI				$S > 1$	+	+	–	–
XII		$S > 1$	$S \leq 1$	$S \leq 1$	–	+	+	–
XIII				$S > 1$	–	–	+	+
XIV			$S > 1$	$S \leq 1$	+	+	+	+
XV				$S > 1$	+	–	+	–

[a]A pH-dependent and selector-dependent reversal of the enantiomer migration order under the appropriate conditions is indicated by "+". For example, in the case of IX, selectivities at low pH/low [CD] and low pH/high [CD] show the same ratio compared to 1 so that no selector-dependent migration order reversal is observed as indicated by "−" in the (26–27) transition column on the right hand side of the table. In contrast, selectivities at low [CD]/low pH and low [CD]/high pH have opposite ratios which results in a pH-dependent enantiomer migration order reversal indicated by "+" in the (26–28) transition column.
(Adapted with permission of The American Chemical Society from [106] © 2010)

shift exhibits the higher pH-dependent mobility in the pH range close to the pK_a value of the analyte. An enantioselective pK_a shift can also result in a reversal of the enantiomer migration order at low selector concentration. This is observed when the difference between the complexation constants is rather small compared to the complex mobilities. A pH-dependent change in the ratio K_+/K_n is always associated with an enantioselective pK_a shift. Therefore, at low pH the affinity constants may dominate the migration order while at high pH complex mobilities will determine the order so that a reversal may be observed.

In contrast, mechanism 2, i.e., reversal of the enantiomer migration order due to a significant pK_a shift, will only be observed at low selector concentrations. The pK_a shift may be stereoselective but this must not necessarily be the case. The situation is described between the first [(26)] and third corner point [(28)] in the selectivity plot (Fig. 10). In this scenario the complexation constants dominate the enantiomer migration order and the conditions have to be fulfilled by both enantiomers. The ratio of the electrophoretic mobilities of the free species, μ_f, and the complex, μ_c,

can be reversed. At low pH, all species are essentially fully charged so that the pH-dependent mobilities μ_f and μ_c can be approximately described by the pH-independent parameters μ_{HB^+} and μ_{HB^+CD}, with $\mu_{HB^+} > \mu_{HB^+CD}$ due to the larger hydrodynamic radius of the complex. Upon increasing the buffer pH, μ_f and μ_c described by (22) and (23) are also affected by the respective protonation equilibria pK_a and $pK_{a/c}$. At low pH the ratio μ_c/μ_f can be described by μ_{HB^+CD}/μ_{HB^+} while at high pH it is described by $\mu_{HB^+CD}K_+/\mu_{HB^+}K_n$. Subsequently, reversal of the migration order will be observed when K_+/K_n exceeds μ_{HB^+}/μ_{HB^+CD}. At low pH when μ_f is higher compared to μ_c the enantiomer exhibiting the higher complexation constant migrates last while at a sufficiently high pH the more strongly complexed enantiomer migrates first when μ_c exceeds μ_f.

Probably the most obvious mechanism resulting in a pH-dependent reversal of the enantiomer migration order is mechanism 3 which is based on opposite stereoselective recognition of the analyte enantiomers as protonated and neutral species by a selector. This will lead to an inversion of the enantiomer migration order at low selector concentrations. In addition, opposite stereoselective recognition of the charged and uncharged forms will also result in differences in the K_+/K_n ratios of the enantiomers which will translate into enantioselective complexation-induced pK_a shifts (mechanism 1). Therefore a pH-dependent reversal of EMO will most likely also be observed at high selector concentrations as a function of both mechanisms. The pH-dependent reversal of the enantiomer migration order at low selector concentrations in the (27 → 29) transition column can be caused by all three mechanisms in cases VII, IX, XI, and XII, while only mechanism 2 leads to the migration order reversal in cases III, V, and XIV.

Selector concentration-dependent reversal of the enantiomer migration order can be observed at low and high pH, i.e., along the parallels to the corner points 1 and 2 (low pH) or 3 and 4 (high pH) of the selectivity plot (Fig. 10). Typically, the mobility of the free analyte, μ_f, exceeds the mobility of the complex, μ_c, due to its smaller size resulting in a higher charge density. Thus, for $\mu_c < \mu_f$ and $\mu_{c1} < \mu_{c2}$ the migration order is reversed when the affinity constant ratio K_2/K_1 exceeds $(\mu_f - \mu_{c1})/(\mu_f - \mu_{c2})$. Thus, inversion can be observed when the complex of the more strongly bound enantiomer also exhibits the higher complex mobility. The respective enantiomer will migrate last at low selector concentrations when the migration order is determined by the complexation constants but first at high selector concentrations when complex mobilities dominate. This mechanism can occur at high and low pH. At high pH where $\mu_c < \mu_f$ selector concentration-dependent reversal of the enantiomer migration order can also be observed when the more strongly complexed enantiomer possesses the lower complex mobility. In this case the ratio K_1/K_2 exceeds $(\mu_{c2} - \mu_f)/(\mu_{c1} - \mu_f)$.

The mechanism described for $\mu_c < \mu_f$ applies to all cases of selector-dependent reversal of the enantiomer migration order at low pH as indicated in (26) and (27), and the transition column in Table 1, and at high pH in the (28–29) column in cases VI, X, and XIII. The situation described for $\mu_c < \mu_f$ causes reversed migration order at high pH for cases V and XIV. In case IX both mechanisms can apply.

As an example of the pH dependent reversal of the enantiomer migration order illustrating the model, the enantioseparations of the LL- and DD-enantiomers of

Ala-Tyr and Asp-PheOMe using 2,6-dimethyl-β-CD as chiral selector were selected [105]. While Ala-Tyr displayed a pH-dependent inversion of the migration order of the enantiomers, Asp-PheOMe did not (Fig. 11a). At pH 2.2, the LL-enantiomer of Ala-Tyr migrated first with the enantioseparations deteriorating at higher concentrations. At pH 3.0, no separations were observed, while at pH 3.8, selectivity initially increased with increasing CD concentrations, quickly reaching a plateau. At pH 3.8 D-Ala-D-Tyr migrated before L-Ala-L-Tyr. The experimentally determined pH-independent parameters, μ_{HB^+}, μ_{HB^+CD}, K_+, and K_n, as well as pK_a and p$K_{a/c}$, are summarized in Table 2 and were used to calculate the selectivity curves shown in Fig. 11b. At pH 2.2 and 3.0 the curves also predicted a selector concentration-dependent reversal of the migration order that was not experimentally observed, probably due to the low resolution counteracted by diffusion phenomena. The separation behavior of Ala-Tyr could be rationalized based on these data. D-Ala-D-Tyr is complexed more strongly by the CD than the LL-enantiomer over the entire pH range. K_+ values are about ninefold higher than the K_n values, resulting in a pK_a shift of almost one unit (Table 2). Therefore, a reversal of the mobility ratio of the peptide–CD complex and the free analyte results when increasing the buffer pH in the vicinity of the pK_a of the peptide. At low selector concentrations, the more strongly complexed DD-enantiomer migrates more slowly than L-Ala-L-Tyr at pH 2.2 when the protonated form dominates and first when the pH is raised to pH 3.8. The deteriorating effect of increased selector concentrations at pH 2.2 is caused by the increasing influence of μ_{HB^+CD}, which differs only slightly between the enantiomers if at all. At pH 3.0, no separation is observed as the mobilities of the free from and the analyte–CD complexes differ only slightly.

A pH-dependent reversal of the enantiomer migration order was not observed for Asp-PheOMe in the presence of 2,6-dimethyl-β-CD, as can easily be rationalized from the pH-independent complexation constants and mobilities listed in Table 2; the separation selectivity is shown in Fig. 11b. Only a minor non-enantioselective pK_a shift and essentially identical $\mu_{HB^+\times CD}$ values were found for the enantiomers. The migration behavior of the Asp-PheOMe enantiomers can be rationalized using the complexation and mobility data. D-Asp-D-PheOMe is complexed more strongly than the LL-enantiomer in both, the protonated as well as the zwitterionic species. As μ_{HB^+CD} and pK_a values of both enantiomers are identical, the pH-dependent complex mobilities, μ_c, of both enantiomers are essentially equal in the pH range close to the pK_a of the analyte. Moreover, the mobility of the free analyte always exceeds μ_c due to the minor pK_a shift. Thus, the LL-enantiomer always migrates in front of the DD-isomer independent of the buffer pH. Due to the slightly weaker interaction of the zwitterionic form with the CD, the ratio of the mobilities of free and complexed analytes decreases upon increasing the buffer pH, resulting in a deteriorated separation selectivity at higher pH values.

The theoretical model has also been used to analyze the effect of pH on complex formation between β-CD and the migration order of the enantiomers of the dipeptides Ala-Phe, Ala-Tyr, and Asp-PheOMe [102].

Gas and coworkers recently developed the software Simul 5 Complex that allows the simulation of analyte separation by CE including the effects of complexation

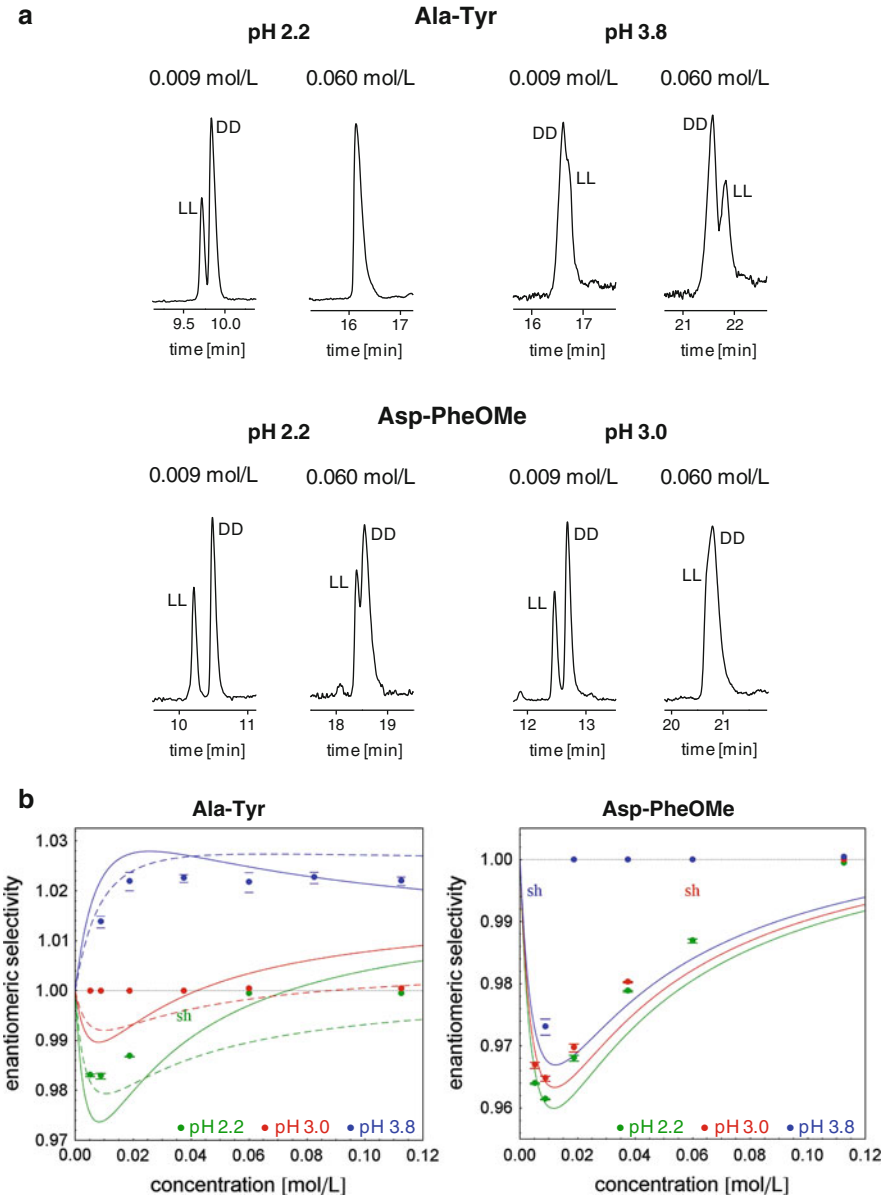

Fig. 11 (**a**) Electropherograms of the separation of the LL- and DD-enantiomers of Ala-Tyr and Asp-PheOMe using 2,6-dimethyl-β-CD as chiral selector. Experimental conditions: 40/50.2 cm, 50 μm id fused-silica capillary, 20°C, 25 kV, UV detection at 214 nm, pH 2.2: 60 mM sodium phosphate buffer, pH 3.0: 40 mM sodium phosphate buffer, pH 3.8: 30 mM sodium aspartate buffer. (**b**) Selectivity plots as a function of the CD concentration at pH 2.2 (*green*), 3.0 (*red*), and 3.8 (*blue*). The *symbols* represent the experimentally determined values, *sh* indicates a shoulder. (Adapted with permission of The American Chemical Society from [105] © 2009)

Table 2 Apparent mobilities and equilibrium constants describing the complexation of the LL- and DD-enantiomers of the Ala-Tyr and Asp-PheOMe by 2,6-dimethyl-β-CD as chiral selector

	Ala-Tyr		Asp-PheOMe	
Parameter	DD	LL	DD	LL
μ_{HB^+} (10^{-9} m^2 s^{-1} V^{-1})	15.88 ± 0.07		15.66 ± 0.08	
$\mu_{HB\cdot CD^+}$ (10^{-9} m^2 s^{-1} V^{-1})	6.68 ± 0.06	6.55 ± 0.06	5.89 ± 0.09	5.84 ± 0.10
K_+ (L/mol)	165 ± 7	139 ± 6	141 ± 6	116 ± 5
K_n (L/mol)	18.5 ± 1.5	15.0 ± 1.5	114 ± 7	94 ± 6
pK_a	3.12 ± 0.01		2.99 ± 0.01	
p$K_{a/c}$	4.07 ± 0.03	4.08 ± 0.03	3.08 ± 0.02	3.08 ± 0.02

Data reproduced with permission of The American Chemical Society from [105] © 2009

equilibria [107–109]. The program is based on separation selectivity analogous to (18) and can handle neutral and charged analytes as well as selectors. It also considers electromigration dispersion caused by the complexation. One of the examples used for the verification of the software was the above-mentioned enantioseparation of the LL- and DD-enantiomers of Ala-Tyr using 2,6-dimethyl-β-CD as chiral selector. The 3D plot of the selectivity as a function of the pH of the background electrolyte and CD concentration as well as the calculated electropherograms at pH 1.91 and 4.51 are shown in Fig. 12 [109]. They are in excellent agreement with the experimental data shown in Fig. 11. At low pH (pH 1.91 in the simulation and pH 2.2 in the experiments described in [105]) the enantiomers can be separated at low CD concentrations and the separation deteriorates when increasing the selector concentration. At high pH (pH 3.8 in the experiments vs pH 4.51 in the simulations) only partial separation of the enantiomers was observed. The simulations revealed electromigration dispersion as one of the main reasons for the poor enantioseparation at these pH values.

The simulation also demonstrated an interesting fact. At pH values higher than the pK_a of the analyte, the effective mobilities of the enantiomers increase with increasing selector concentrations because the complexation constants of the neutral forms are smaller compared to the charged species (Table 2). As the mole fraction of the charged complexed forms increase with increasing selector concentrations, the effective mobilities also increase. Therefore it was concluded that a pH value must exist where the effective mobilities of the enantiomers are independent of the CD concentration. As can be concluded from Fig. 12a, this pH value is between 3 and 4; the exact values were 3.393 for the LL-enantiomer and 3.405 for L-Ala-L-Tyr [109].

4 Chiral Selectors and Selector-Analyte Complex Structures

Many structurally diverse chiral compounds have been investigated as chiral selectors in CE including CDs, macrocyclic glycopeptide antibiotics, proteins, crown ethers, chiral ligand-exchangers, chiral ionic liquids, and chiral surfactants derived from

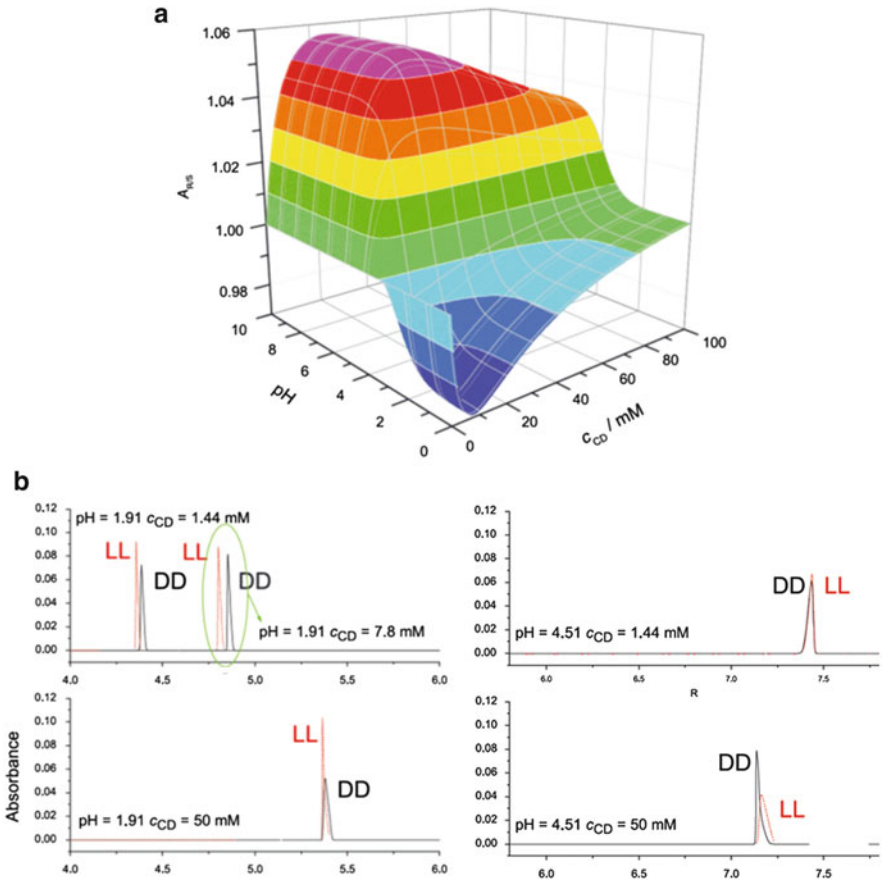

Fig. 12 Modeling of the enantioseparation of Ala-Tyr using 2,6-dimethyl-β-CD as chiral selector by Simul 5 Complex. (**a**) 3D contour plot of the separation selectivity as a function of the pH of the background electrolyte and the concentration of the chiral selector and (**b**) calculated electropherograms at pH 1.91 and pH 4.51 at CD concentrations of 1.44 and 50 mM. The *black solid line* represents D-Ala-D-Tyr while the *red dashed line* represents L-Ala-L-Tyr. (Adapted with permission of Wiley from [109] © 2012)

steroids, amino acids, tartaric acid, or glycosides [23, 24, 110]. Depending on the chiral selector and the analyte enantiomers, formation of the diastereomeric selector–selectand complexes is driven by several types of interactions including ionic interactions, ion-dipole or dipole-dipole interactions, hydrogen bonds, van der Waals interactions, or π–π interactions. Ionic interactions are strong and may be primarily involved in the "initial" contact because of their long range nature. However, they may not be stereoselective because both enantiomers are able to establish such interactions in contrast to short range interactions such as hydrogen bonds or π–π interactions. For an enantioseparation at least one interaction between selector and the analyte enantiomers has to be stereoselective. Finally, selector–selectand interactions

may be attractive or repulsive and at least one attractive interaction must exist in order to allow the formation of one of the two possible diastereomeric complexes. The following part will briefly highlight the most frequently applied chiral selectors and the current understanding of their chiral recognition mechanisms. A comprehensive summary of the chiral recognition mechanisms of chiral selectors can be found in [111–114].

Besides structure-separation studies, varying either the structure of the analytes or the selectors, spectroscopic techniques including UV spectroscopy, fluorimetry, Fourier transformation and attenuated total reflectance IR spectroscopy, NMR spectroscopy as well as circular dichroism and vibrational circular dichroism (VCD) spectroscopy have been employed. Especially NMR techniques, including nuclear Overhauser effect (NOE) and rotating-frame Overhauser enhancement spectroscopy (ROESY), have the advantage of allowing conclusions about the spatial proximity of atoms or substitutents [115–119]. The structure of the selectand–selector complex in the solid state can be obtained by X-ray crystallography while molecular modeling is very useful for the illustration of selector–selectand complexes [120]. Finally, chemoinformatic methods have also been applied [121].

4.1 Cyclodextrins

CDs are by far the most often applied chiral selectors in CE as documented in many reviews [122–129]. This is due to their UV-transparency as well as enantiodifferentiation ability towards compounds with a broad structural variety and commercial availability. Numerous separation scenarios can be realized.

CDs are cyclic oligosaccharides composed of α(1 → 4) linked D-glucose molecules. The most important CDs are α-CD, β-CD, and γ-CD consisting of 6, 7, and 8 glucose units, respectively, which form a hollow torus with a lipophilic cavity and a hydrophilic outside. The wider rim is formed by the secondary 2- and 3-hydroxyl groups of the glucose molecules while the primary 6-hydroxyl groups form the primary rim. The top (secondary rim) and bottom (primary rim) diameters of the cavities of the CDs are approximately 5.3 and 4.7 Å in the case of α-CD, 6.5 and 6.0 Å for β-CD, and 8.3 and 7.5 Å for γ-CD [130]. The hydroxyl groups can be derivatized yielding a large variety of CD derivatives containing uncharged or charged substituents (Table 3). Native CDs and CD derivatives have been used for enantioseparations in EKC employing aqueous and non-aqueous background electrolytes as well as in MEKC and MEEKC.

Numerous techniques including thermodynamics, mass spectrometry, X-ray crystallography, molecular modeling, and especially NMR spectroscopy [115–117] have contributed to the current understanding of the structures of CD–analyte complexes. The 1:1 complexes are generally assumed but complexes with other stoichiometry such as 2:1, 2:2, or higher order equilibria also exist. Complexation often involves inclusion of lipophilic parts of the analytes into the CD cavity displacing solvent molecules (in most cases water) from the cavity [130]. Hydrophobic and van der Waals interactions are believed to be primarily involved but hydrogen bonding

Table 3 Examples of commercially available CDs

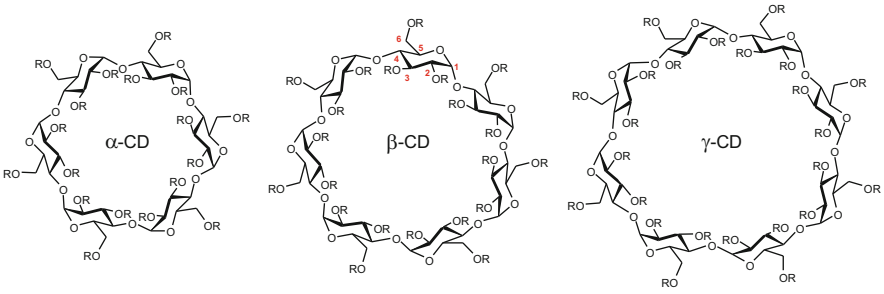

Derivative	Substituents
Native CDs	
α-CD	H
β-CD	H
γ-CD	H
Neutral CDs	
Methyl-α-CD	CH_3, randomly substituted
Methyl-β-CD	CH_3, randomly substituted
Heptakis-2,6-dimethyl-β-CD	CH_3 in positions 2 and 6
Heptakis-2,3,6-trimethyl-β-CD	CH_3 in positions 2, 3 and 6
Hydroxypropyl-α-CD	CH_2–CH_2–CH_2–OH, randomly substituted
Hydroxypropyl-β-CD	CH_2–CH_2–CH_2–OH, randomly substituted
Hydroxypropyl-γ-CD	CH_2–CH_2–CH_2–OH, randomly substituted
Negatively charged CDs	
Carboxymethyl-β-CD	CH_2–COONa, randomly substituted
Sulfated α-CD	SO_3Na, randomly substituted
Sulfated β-CD	SO_3Na, randomly substituted
Sulfated γ-CD	SO_3Na, randomly substituted
Sulfobutyl-β-CD	CH_2–CH_2–CH_2–CH_2–SO_3Na, randomly substituted
Heptakis-6-sulfo-β-CD	SO_3Na in position 6
Heptakis-(2,3-diacetyl-6-sulfo)-β-CD	CH_3CO in positions 2 and 3, SO_3Na in position 6
Heptakis-(2,3-methyl-6-sulfo)-β-CD	CH_3 in positions 2 and 3, SO_3Na in position 6
Positively charged CDs	
2-Hydroxy-3-trimethylammoniopropyl-β-CD	CH_2–CH(OH)–CH_2–$N(CH_3)_3Cl$, randomly substituted
6-Monodeoxy-6-monoamino-β-CD	NH_2 instead of one 6-OH group

with the glucose hydroxyl groups and steric factors also contribute. In the case of CD derivatives, interactions with the substituents also have to be considered, such as ionic interactions for CDs containing charged substituents. The increased strength of the complexation based on ionic interactions between oppositely charged analytes and CDs often allows the use of very low selector concentrations. Depending on the analyte, the inclusion into the cavity can occur from the narrow primary side or the wider secondary side. For example, opposite enantiomer migration order of the enantiomers of ephedrine was observed using β-CD as compared to α-CD and the negatively charged heptakis(2,3-di-*O*-acetyl-6-*O*-sulfo)-β-CD as chiral selectors in an

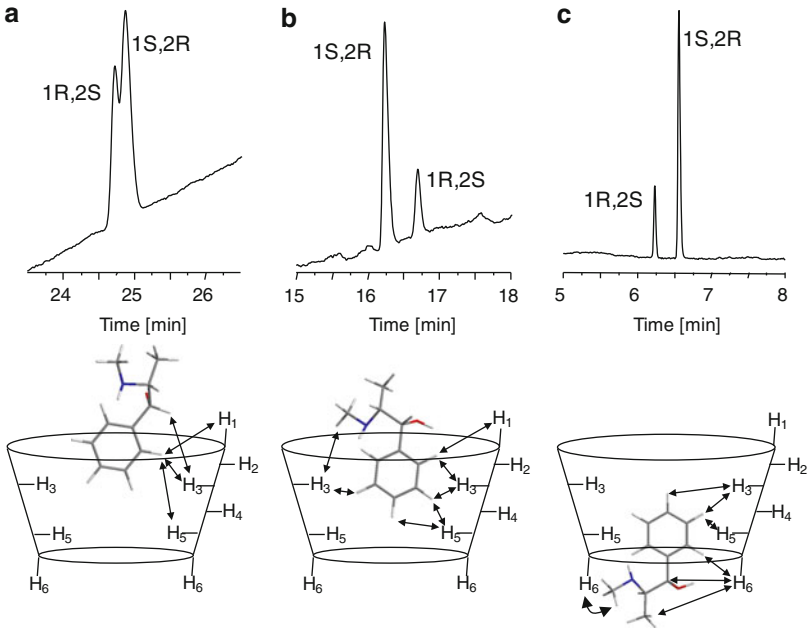

Fig. 13 Separation of the enantiomers of ephedrine in 200 mM sodium phosphate buffer, pH 2.5, as background electrolyte (*top*) and schematic structures of the cyclodextrin–ephedrine complexes as derived from ROESY measurements (*bottom*). The *arrows* indicate the NOE observed upon irradiation of the respective protons. (**a**) α-CD, (**b**) β-CD, and (**c**) heptakis(2,3-di-*O*-acetyl-6-*O*-sulfo)-β-CD. (Reproduced with permission of Wiley from [52] © 2011)

acidic background electrolyte (Fig. 13) [52]. As derived from subsequent NMR studies, the aromatic ring of ephedrine was included only partially into the cavity of α-CD from the secondary wider opening (Fig. 13a), while it penetrated β-CD more deeply also from the secondary side (Fig. 13b). In contrast, the compound entered heptakis(2,3-di-*O*-acetyl-6-*O*-sulfo)-β-CD from the narrower, primary side (Fig. 13c). Thus, the enantiomer migration order cannot be established from the structures of the complexes and, furthermore, small differences such as the depth of inclusion may result in opposite migration order as shown for α-CD and β-CD. The negatively charged derivative heptakis(2,3-di-*O*-acetyl-6-*O*-sulfo)-β-CD led to the same migration order as compared to α-CD under otherwise identical experimental conditions, i.e., a migration order opposite to the order observed for the underivatized native analogue β-CD. However, the structure of the analyte–CD complex was entirely different from the native CDs because the aromatic moiety was inserted into the cavity from the narrower primary side. Similar observations were made for the related analyte norephedrine [53]. Another example for the formation of inclusion complexes either via the wider or the narrower opening is the interaction between propranolol and β-CD or heptakis(6-*O*-sulfo)-β-CD where inclusion of the naphthyl ring occurs from the secondary side in the case of β-CD and from the narrow primary side in the case of heptakis(6-*O*-sulfo)-β-CD [131]. Furthermore, different moieties of a molecule may

interact with different CDs as shown for the combination of clenbuterol with β-CD and heptakis(2,3-di-*O*-acetyl)-β-CD, respectively [132]. The phenyl ring of the drug enters β-CD through the wider opening while the *tert*-butyl moiety of the compound is included in the cavity of heptakis(2,3-di-*O*-acetyl)-β-CD, also from the wider side. Opposite enantiomer migration order was observed. Different complex structures and, consequently, different migration order were also found for ketoprofen and 2,3,6-trimethyl derivatives of α-CD, β-CD, and γ-CD [54].

It has also been demonstrated that inclusion complexation is not a prerequisite for CD-mediated enantioseparations. Thus, effective resolution of the enantiomers propranolol [62] and bupivacaine [64] in the presence of heptakis(2,3-di-*O*-acetyl-6-*O*-sulfo)-β-CD as chiral selector were noted in CE experiments while no apparent interaction with the cavity of the CDs could be observed by NMR in the respective studies. Similar results were found for talinolol and heptakis(2,3-di-*O*-methyl-6-*O*-sulfo)-β-CD in aqueous background electrolytes as well as heptakis(2,3-di-*O*-acetyl-6-*O*-sulfo)-β-CD in non-aqueous electrolyte solutions [56]. Moreover, the structure of the complex can depend on the nature of the background electrolyte as demonstrated for propranolol and sulfated β-CD derivatives in aqueous and non-aqueous buffers [62]. Thus, inclusion of the aliphatic side chain of propranolol into the cavity of heptakis(2,3-di-*O*-acetyl-6-*O*-sulfo)-β-CD from the wider opening occurred in a non-aqueous background electrolyte while only an external complex was formed between propranolol and the CD in aqueous buffers. In the case of heptakis(2,3-di-*O*-methyl-6-*O*-sulfo)-β-CD, the opposite behavior was observed, i.e., an inclusion complex in aqueous electrolyte solutions and an external complex in a methanol-based background electrolyte. Moreover, the naphthyl moiety was enclosed via the narrower rim into the cavity of heptakis(2,3-di-*O*-methyl-6-*O*-sulfo)-β-CD. In the case of heptakis(2,3-di-*O*-methyl-6-*O*-sulfo)-β-CD, opposite enantiomer migration order was observed in aqueous and non-aqueous background electrolytes which could be rationalized based on the complex structures under the respective conditions. Only a few studies also reported spectroscopic proof of structural differences between the diastereomeric complexes. Enantioselective peak splitting due to non-equivalence of the complexation-induced chemical shifts for the propranolol enantiomers in the presence of heptakis(2,3-di-*O*-acetyl-6-*O*-sulfo)-β-CD was observed in aqueous as well as non-aqueous solutions, clearly indicating different complex geometries in the case of the aqueous solutions where an inclusion complex is apparently not formed [63]. With regard to the inclusion complex formed in non-aqueous electrolytes, (*S*)-propranolol apparently formed a tighter complex as the side chain of the molecule was inserted deeper into the CD cavity compared to the (*R*)-enantiomer. The data obtained from NMR measurements were supported by a molecular modeling study [64]. A higher interaction energy was calculated for the complex between heptakis-(2,3-di-*O*-acetyl-6-*O*-sulfo)-β-CD and (*S*)-propranolol than for the respective complex with (*R*)-propranolol, indicating the formation of a stronger complex in the case of the (*S*)-enantiomer. The modeling structures of the complexes are shown in Fig. 14. In accordance with the NMR data [63], the side chain of the (*S*)-enantiomer deeply penetrates the CD cavity through the wider secondary side. An electrostatic interaction appears to exist between the

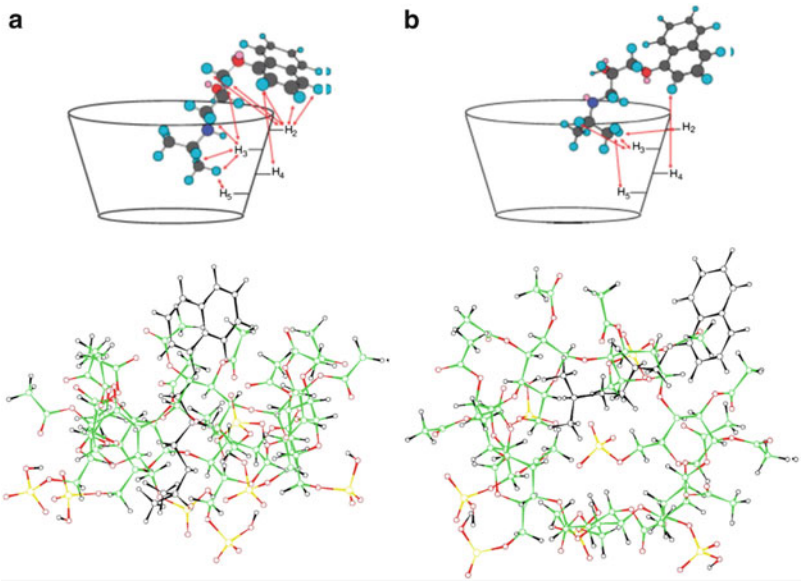

Fig. 14 Structures of the complexes of (*S*)-propranolol (**a**) and (*R*)-propranolol (**b**) with heptakis (2,3-di-*O*-acetyl-6-*O*-sulfo)-β-CD. *Top*: Schematic structures as derived from ROESY experiments. The *arrows* indicate the NOE observed upon irradiation of the respective protons. *Bottom*: Molecular modeling structure of the complexes. The atoms of propranolol are shown in *black*, the carbon, hydrogen, oxygen, and sulfur atoms are colored in *green*, *black*, *red*, and *yellow*, respectively. (Top structures reproduced with permission of Wiley from [63] © 2011; bottom structures reproduced with permission of Elsevier from [64] © 2012)

extended side chain and the sulfate groups located at the primary rim of the CD. In the case of the (*R*)-enantiomer, the side chain enters the cavity less deeply. Stereoselective complexation of the dipeptides Ala-Phe and Ala-Tyr by β-CD and sulfated derivatives was also derived from NMR studies [133, 134].

Finally, buffer additives can also affect the structure of the analyte–CD complex. Thus, it was shown by NMR measurements and molecular modeling that the enantiomers of the dipeptide Ala-Tyr in the protonated state penetrated deeper into the cavity of β-CD in the presence of urea compared to in the absence of urea [133]. This resulted in higher peak resolution in β-CD-mediated CE enantioseparations in the presence of urea in the background electrolyte. Another example is the complex between β-CD and naproxen when adding 1,2-dibromoethane [135]. In the presence of 1,2-dibromoethane naproxen enters the CD cavity from the wider secondary side while inclusion from the narrower primary side of β-CD occurs in the absence of 1,2-dibromoethane.

Summarizing, substantial structural differences between the analyte–CD complexes as derived from NMR spectroscopy or molecular modeling can rationalize the migration behavior observed in CE experiments. However, minor differences in complex structure (such as depth of insertion into the cavity) may also affect the chiral recognition of selectors towards analyte enantiomers which is translated into opposite enantiomer migration order in CE. In other cases entirely different types of

complexes had no apparent effect on the migration behavior. Therefore, significant differences in the enantiomer–CD complex structures do not appear to be a prerequisite in order to observe reversed enantiomer migration order in CE.

4.2 Macrocyclic Antibiotics

Macrocyclic glycopeptides are also called macrocyclic antibiotics due to their medical applications. The most important representatives used as chiral selectors in CE are vancomycin, ristocetin, teicoplanin, and the teicoplanin aglycone. The common structural feature of this class of compounds is a heptapeptide as a set of interconnected macrocylces each composed of two aromatic rings and a peptide sequence. Vancomycin contains three macrocycles while teicoplanin and ristocetin A are composed of four. The macrocycles form a three-dimensional, C-shaped basket-like structure with the carbohydrate moieties positioned at the surface. Due to the presence of ionizable groups, such as a carboxylic acid group or amino groups, a large number of interactions between analyte molecules and the glycopeptides antibiotics are possible, including hydrogen bonds, π–π, dipole–dipole, and ionic interactions depending on the experimental conditions [136]. The detailed recognition mechanism on a molecular basis has not been studied in detail yet. Mechanisms deduced from structure-separation studies using various classes of analytes were examined. However, detailed NMR studies or X-ray crystallographic studies with respect to chiral separations have not been published to date except for vancomycin and small ligands such as D-lactic acid, *N*-acetyl-Ala or *N*-acetyl Gly [137], or vancomycin with the tripeptide ligand N_{α},N_{ω}-diacetyl-L-Lys-D-Ala-D-Ala [138] as shown in Fig. 15, as well as the glycopeptide balhimycin and D-Ala-D-Ala [139]. A molecular docking has been performed for macrocyclic antibiotic selectors and chiral xanthone analytes [140]. The application of macrocyclic glycopeptides as chiral selectors in CE has been summarized [11, 141, 142].

4.3 Crown Ethers

Chiral crown ethers form complexes with protonated primary amines so that their use is essentially limited to this group of analytes, although some exceptions have been reported. In CE only (+)-(18-crown-6)-2,3,11,12-tetracarboxylic acid [(+)-18C6H4] has been employed as summarized in [143, 144]. Complex formation is due to hydrogen bonds between the protonated amino group and oxygen atoms of the crown ether. For chiral recognition (+)-18C6H4 adopts an asymmetric C1-type conformation exhibiting a bowl-like shape with the N–H and Cα-H protons of the amino acid interacting with the oxygen atoms of the ring system as well as the carboxylate groups [145]. This asymmetric C1-type shape is assumed to result from a conformational sequence of successive rotations in the macrocycle which appear to be promoted by protons. The diastereomeric complexes between the analyte enantiomers and

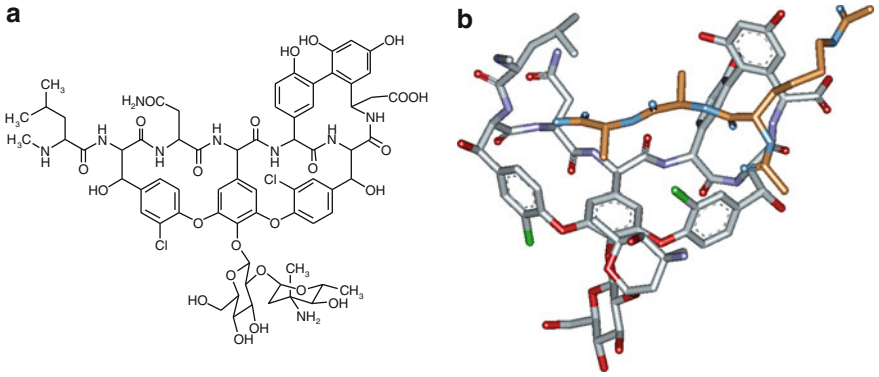

Fig. 15 Structure of vancomycin (**a**) and X-ray crystal structure of the complex of vancomycin with N_{α},N_{ω}-diacetyl-L-Lys-D-Ala-D-Ala (**b**). Vancomycin is shown in *gray* and the ligand in *orange*. Oxygen, nitrogen, and chlorine atoms are colored in *red*, *blue* (ligand) or *violet* (vancomycin), and *green*, respectively. The X-ray structure image was generated with the Accelrys Discovery Studio Visualizer 2.5 software from the coordinates deposited in the Brookhaven Protein Data Bank (www.rcbs.org/pdb, file 1FVM)

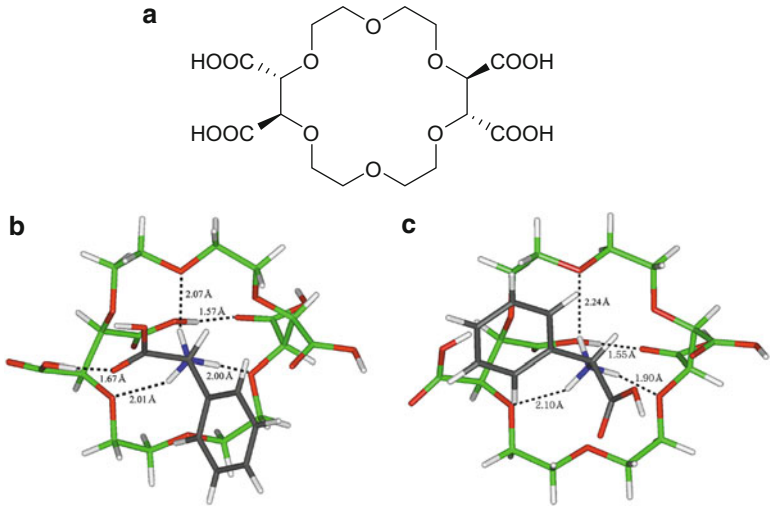

Fig. 16 Structure of (+)-(18-crown-6)-2,3,11,12-tetracarboxylic acid (**a**) and modeling structures of the complexes of the crown ether with protonated D-phenylglycine (**b**) and L-phenylglycine (**c**). The modeling structures were generated from NOE and molecular dynamics calculations. Hydrogen bonds are shown as *dotted lines*. (**a** and **b** reproduced with permission of The Royal Society of Chemistry from [146] © 2001)

(+)-18C6H4 displayed differences. For example, as demonstrated for phenylglycine, the more strongly complexed D-enantiomer exhibited a more favorable complex geometry and an additional hydrogen bond compared to the more weakly bound L-enantiomer as derived from NMR and molecular modeling (Fig. 16) [146]. A slightly different

structure of the more weakly bound L-phenylglycine featuring two hydrogen bonds with ring oxygen atoms and one with a carboxylic acid group has also been derived [147]. Further examples of differences in the structures of complexes between (+)-18C6H4 and amino acid enantiomers have been reported [148–150].

4.4 Ligand Exchange

Chiral ligand exchange was the first principle applied in CE for analyte enantioseparations [3]. This technique is based on the formation of ternary chelate complexes between ligands and a central metal atom. Amino acid derivatives are most frequently employed as chelating agents although D-quinic acid, D-gluconic acid, D-saccharic acid, or L-threonic acid have also been used as complexation agents [151]. The metal ions include divalent metal ions such as Cu^{2+}, Zn^{2+}, or Ni^{2+}. Enantioseparation by ligand exchange is restricted to analytes with two or three electron-donating groups such as amino acids, hydroxy acids, amino alcohols, or diols. In addition, borate can serve as central ion in a CE ligand exchange system in combination with diols as ligands for the separation of the enantiomers dihydroxy analytes [152]. Applications of ligand exchange for CE enantioseparations have been summarized, for example, in [151–154].

Ligand exchange is based on the reversible coordination of a chiral analyte into the sphere of a metal ion which is complexed with an enantiopure chelator, resulting in a selectand–metal ion–selector complex. The resulting diastereomeric chelates possess different thermodynamic formation ratios or stabilities. It is assumed that ternary complexes with a 1:1:1 stoichiometry are formed, although complexes with other stoichiometries such as 1:2:1 have also been reported for the system D-quinic acid–Cu(II)-tartrate depending on the configuration of the tartrate analyte [104]. Moreover, it should be kept in mind that the ligand exchange process does not necessarily has to be ascribed to the ligand in the Me–$(ligand)_2$ complex but can also occur by exchange with water molecules that complete for the coordination sphere of the metal ion, i.e., the Me–ligand–$(H_2O)_2$ complex [155, 156]. In addition, the ternary complex between selector, central ion, and analyte is uncharged and therefore does not possess an electrophoretic mobility in CE in contrast to the binary complex $[Me–analyte]^+$ [156]. Consequently, the different stabilities of the diastereomeric complexes result in a different distribution of charged species (free analyte and binary complexes) of the enantiomers. It has also been demonstrated that the ionization status of the analyte ligand may affect the stability of the diastereomeric mixed complexes. Thus, different stereoselectivities of complex formation have been observed whether the analyte enantiomers are charged or uncharged [157, 158]. The structures of the diastereomeric ternary complexes L-Pro–Cu(II)–L/D-Thr are shown in Fig. 17 as an example [159].

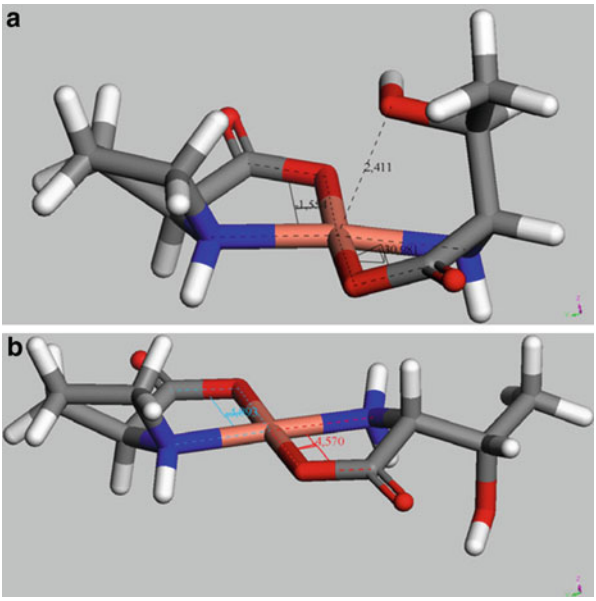

Fig. 17 Molecular modeling structure of the ternary L-proline–Cu(II)–threonine complex containing (**a**) L-threonine and (**b**) D-threonine. (Reproduced with permission of Elsevier from [159] © 2010)

4.5 Chiral Surfactants

Chiral micelles are formed from monomeric chiral surfactants in aqueous solution at concentrations above the critical micelle concentration. Furthermore, polymeric micelles (molecular micelles) have been developed [46, 160] in order to overcome the disadvantages of "classical" micelles such as the dynamic equilibrium between the surfactant monomers in the aqueous phase and the micelles. Polymeric micelles are obtained by polymerization of suitably functionalized surfactants via the hydrophobic tails. Chiral surfactants with a large structural variety are available including bile acid derivatives or surfactants derived from amino acids or carbohydrates (Fig. 18a). Molecular micelles are based on surfactants derived from amino acids or dipeptides (Fig. 18b). Reviews on the application of chiral micelles in enantioseparations can be found, for example, in [161, 162].

The chiral recognition process for chiral micelles has been less frequently addressed, probably due to the complex and dynamic structure of micelles that are difficult to assess by spectroscopic techniques. Compared to the (*R*)-enantiomer, the (*S*)-enantiomer of 1,1′-binaphthyl-2,2′-diyl hydrogen phosphate (BNDHP) appeared to interact more strongly with micelles formed by sodium cholate as derived from NMR experiments in accordance with the elution order in MEKC [163]. The naphthyl moieties are inserted into the micelle, leading to a discrimination of the analyte enantiomers.

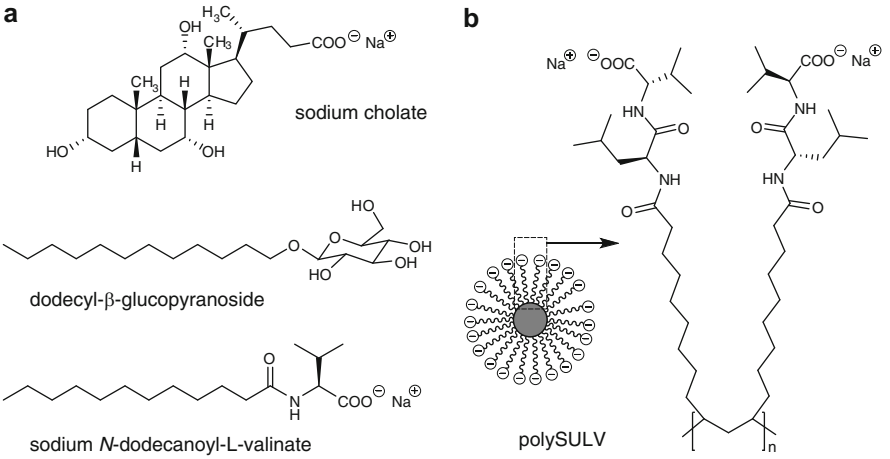

Fig. 18 Structures of chiral surfactants (**a**) and schematic representation of a chiral polymeric micelle of poly(sodium *N*-undecanoyl-L-leucyl-L-valinate (**b**)

Dipeptide-based surfactants seem to adopt a folded conformation in aqueous solutions, creating a chiral pocket into which analytes can be accommodated. In the case of BNDHP, the N-terminal amino acid of the dipeptide head group appears to be the primary site of chiral recognition in monomeric [164] as well as polymeric surfactants [165, 166]. As a consequence, the configuration of the amino acid also affected the elution order of the BNDHP enantiomers. In the case of an L-configured amino acid (*R*)-BNDHP was complexed more strongly and eluted faster in MEKC experiments [167]. When the configuration of the "inner" amino acid was changed to the D-configuration the elution order was reversed with the (*S*)-enantiomer of BNDHP eluting first. The stereochemistry of the C-terminal amino acid did not affect the enantiomer elution order of BNDHP. It did, however, influence the magnitude of the chiral resolution. Tröger's base and propranolol bind to the chiral pocket of the molecular micelle in a mode comparable to BNDHP while Dns-amino acids appeared to interact primarily with the C-terminal amino acid of poly(*N*-undecanoyl-L-leucine-L-valine) [166]. Molecular micelles obtained from surfactants containing a single amino acid as polar head group also created a chiral pocket which was able to adopt BNDHP [168].

4.6 Miscellaneous Selectors

Apart from the more often applied chiral selectors discussed above, many types of complex forming agents have been evaluated as chiral selectors in CE [14–16, 20, 23, 110]. However, in most cases only proof of concept, i.e., the application to enantioseparations, has been reported and only mechanistic studies for a few further groups of selectors were performed.

While being the most successful chiral selectors in HPLC, polysaccharide have not been frequently used as chiral selectors in CE, although successful applications have been reported such as [169–174]. Based on the fact that CE enantioseparations using native amylose as chiral selector deteriorated upon increasing the capillary temperature from 25°C to 60°C in the case of analytes with a molecular size smaller than 0.78 nm while chiral separations of larger analytes was not affected by temperature, it has been concluded that the chiral recognition of amylose possesses a helical and an ahelical component [175]. Addition of iodine, which is known to be included in the helices of polysaccharides, led to the same observation. Thus, small molecules appear to be stereoselectively included into helical groves of amylose while the stereoselective complexation of larger molecules appears to occur via other interactions.

Cyclofructans (CFs) are cyclic oligosaccharides composed of β(2 → 1) linked D-fructofuranose units. Derivatives containing 6 (CF6) or 7 (CF7) fructose units have been employed in separation sciences to date. These CFs possess a disk-type structure, the inner core having the structure of a crown ether. In the case of CF6 the fructose units are arranged in a spiral array around the 18-crown-6 core with alternating "inward" and "outward" orientation [176] so that three of the OH groups in position 3 of the fructofuranose moieties point towards the inner core blocking its access due to hydrogen bonding [177]. As a consequence, only poor or no enantioseparations have been observed using native CF6 in CE [178] due to the limited interaction possibilities with analytes. In contrast, sulfated CF6 proved to be an effective chiral selector in CE enantioseparations [178].

The stereoselective interaction of proteins with chiral compounds is a well-known phenomenon in nature. Consequently, proteins have been used as chiral selectors in separation sciences including CE [179, 180]. However, the fact that proteins tend to adsorb to the capillary inner surface somewhat limits their applications as chiral selectors in CE, often necessitating special measures such as coating of the capillary wall. Due to the complexity of the protein selectors a number of molecular interactions including hydrogen bonds, π–π, dipole, and ionic interactions contribute to the complexation of the analyte enantiomers.

Chiral ionic liquids have been recently introduced as chiral selectors in CE. Ionic liquids are salts that are liquid at or close to room temperature. Either the cation or the anion or both may be chiral [181]. Due to their high aqueous solubility chiral ionic liquids have been used as chiral background electrolyte or chiral selector in CE [182, 183] including MEKC [184] and ligand exchange [185, 186]. Ionic and ion-pair interactions between analyte and selector predominate in the case of these selectors. Enantiomeric differentiation by chiral ionic liquids has been demonstrated by spectroscopic techniques [187, 188] but the structures of the complexes formed between ionic liquids and the analyte enantiomers are currently unknown.

Aptamers are single stranded RNA or DNA oligonucleotides which are obtained by the iterative process of systematic evolution of ligands by exponential enrichment (SELEX) [189] which act as target-specific chiral selectors binding one enantiomer with high enantioselectivity. Aptamers possess a complex three-dimensional shape

containing structural motifs including stems, loops, bulges, hairpins, triplexes, or quadruplexes, and can bind a large variety of target compounds with an affinity, specificity, and selectivity comparable to antibodies. Complexation of the target molecules occurs via an adaptive conformational change of the aptamer in a so-called induced-fit process which results in a tight aptamer–solute complex with maximal complementarity between the aptamer and the preferred enantiomer [190–192]. The other enantiomer forms less stabilizing contacts yielding a lower binding affinity. Depending on the structure and functional groups of the target molecules, hydrogen bonding, electrostatic interactions, stacking interactions, or hydrophobic interactions contribute to this process. According to a molecular modeling study, the aptamer folds from a relatively disordered structure into a defined binding pocket encapsulating the target molecule [193]. For a summary of the use of aptamers in separation sciences see [194].

5 Modes of CE Enantioseparation: Selected Examples

As stated above, in CE enantioseparations the chiral selector is added to the background electrolyte performing as a mobile, pseudostationary phase. As in chromatography, chiral recognition is due to stereoselective interactions between the analyte enantiomers and the chiral selector while transport to the detector is achieved by electrokinetic phenomena. Differences in the formation equilibria of the diastereomeric complexes between the chiral selector and the analyte enantiomers and/or differences in the mobilities of the diastereomeric complexes result in enantioseparations (see Sect. 2). Combined with the different modes of CE, many separation scenarios can be envisioned. CE has been applied to the determination of the enantiomers including the enantiomeric composition of compounds in chemical, pharmaceutical, forensic, or environmental analysis, as well as bioanalysis. Many assays displayed enantioselectivity and chemoselectivity allowing the simultaneous analysis of chiral as well as achiral impurities in drug substances. The most frequently employed CE enantioseparation modes, i.e., EKC, MEKC, and MEEKC, will be briefly addressed.

5.1 Electrokinetic Chromatography

The EKC mode is the most often applied technique for CE enantioseparations as documented by numerous publications, many reviews [14–22] or monographs [23, 24]. The term EKC describes a system with a chiral selector in a background electrolyte without the presence of a further pseudostationary phase such as micelles or a microemulsion. It is often (incorrectly) also referred to as chiral CE. The selector may be charged, thus exhibiting an electrophoretic self-mobility allowing the enantioseparation of neutral analytes, or uncharged so that it is transported with the EOF. This enables many separation scenarios, some of which are schematically shown in Fig. 2. Many structurally diverse compounds have been utilized as chiral

selectors in CE including CDs, macrocyclic glycopeptide antibiotics, proteins, crown ethers, chiral ligand-exchangers, chiral ionic liquids, aptamers as well as chiral surfactants derived from steroids, amino acids, tartaric acid or glycosides [14, 16, 23, 24, 110]. When evaluating a specific chiral selector, the compound is typically investigated with regard to its enantioseparation ability towards a certain class of analytes. Conversely, the identification of the most suitable selector for a given class of analytes from a large library of potential selectors may also be applied by screening the entire library with subsequent deconvolution as described for cyclic peptides [195, 196]. The identification of selectors via combinatorial strategies has also been applied to the development of aptamer selectors [197].

Although some selectors appear to be limited to a certain group of analytes, for example chiral crown ethers for the enantioseparation of primary amines, there is no general rule for the application of certain selectors. Thus the choice of a specific selector currently depends on the experience and/or preferences of the analyst. Due to the large variety of derivatives as well as commercial availability, CDs are by far the most often applied chiral selectors in CE [110, 122–129]. Consequently, general strategies for screening approaches utilizing CDs have been published in order to find generalized starting conditions without excessive testing of a large number of CDs. Many analysts prefer negatively charged CDs as they can be used for charged and uncharged compounds [198–200]. At low pH, basic analytes are protonated and migrate to the cathode while the negatively charged CDs migrate to the anode. Neutral compounds interacting with the negatively charged CDs are transported to the anode and can be detected upon reversing the polarity of the applied voltage. Most acidic analytes are protonated at low pH and behave as neutral compounds. Strategies for dual CD systems have also been published [201, 202]. In these systems, both chiral selectors may cooperate in a synergistic manner or counteract each other. An improvement in separation selectivity compared to the use of a single selector is observed when both selectors display opposite affinity towards the analyte enantiomers. Alternatively, increased selectivity also occurs if one CD accelerates the analyte while the other either decelerates it or has no effect on the analyte mobility [203]. Analogous effects may be achieved if one of the selectors is immobilized on the inner wall of the capillary [204, 205].

As discussed above, opposite enantiomer migration order may be observed when switching from one CD to another. Moreover, pure single isomers of CD derivatives are not necessarily required for successful enantioseparations. In fact, many enantioseparations have been achieved using randomly substituted derivatives [43]. However, randomly substituted CDs are a mixture of isomers differing in their degree of substitution, i.e., the number and position of the substituents. Therefore, randomly substituted CDs from various suppliers may differ in this respect and differences may even be observed from batch to batch for a given CD from the same supplier. Literature examples clearly demonstrate that the source of the CD and the degree of substitution may affect the enantioseparation of one compound while this may have no effect for another analyte [206–208]. In addition, it cannot be predicted whether a higher or lower degree of substitution of a given CD results in a better enantioseparation.

Most CE enantioseparations were achieved in aqueous background electrolytes. However, it has been shown that nonaqueous conditions employing organic solvents for electrolyte preparation may be a valuable alternative. Organic solvents possess advantages in terms of higher dissolution of lipophilic analytes, increased stability of water-sensitive analytes, and shift of analyte pK_a or analyte–selector complexation equilibria, among others [209]. Consequently, many successful CE enantioseparations in nonaqueous background electrolytes have been reported [210].

The fact that the chiral selector is dissolved in the background electrolyte is often considered an advantage in terms of the ease of changing the experimental conditions, including the type of the chiral selector. However, this may become a disadvantage when CE is hyphenated with a mass spectrometer. Most selectors are not volatile and contaminate the ion source of the mass spectrometer when entering it. Two strategies have been implemented in order to prevent the entrance of the selector into the ion source [211–213]. The first called the counter migration technique exploits the self-mobility of a chiral selector migrating in the opposite direction of the mass spectrometer. The capillary is initially filled with the background electrolyte containing the chiral selector. Upon application of the separation voltage the analytes migrate towards the mass spectrometer while the selector migrates in the opposite direction. Interaction between analyte and selector results in the enantioseparation. This method is limited to charged chiral selectors. The second approach is the partial filling technique. In this case, only part of the capillary is filled with the background electrolyte containing the selector while the remainder contains a selector-free electrolyte. The experimental conditions have to be chosen in such a way that the analytes migrating through the zone containing the chiral selector have to exhibit a higher velocity towards the mass spectrometer compared to the selector zone so that the analytes reach the mass spectrometer before the selector can enter the ion source. Careful control of the EOF is required. Successful enantioseparations with mass spectrometric detection have been reported applying both approaches [211–213]. It has also been shown that background electrolytes with low concentrations of the chiral selector may be used in CE hyphenated to mass spectrometry without significant loss of sensitivity despite the entrance of the selector into the ion source [214].

A well-known phenomenon in CE is the fact that the peak area in CE depends on the migration velocity of the compounds and, subsequently, the area ratio of the enantiomers of a racemic compound differs from 1:1. This may be compensated by using the corrected peak area by dividing the peak area by the analyte migration time. It has also been shown that complexation of the enantiomers by a chiral selector may result in different detector responses for the individual enantiomers. As demonstrated for the hypnotic drug zopiclone, the drug–β-CD complex displays higher fluorescence intensity as compared to the non-complexed drug [215]. Consequently, in a CE enantioseparation using laser-induced fluorescence detection the more strongly complexed second migrating enantiomer of zopiclone possessed a significantly larger peak area than the faster migrating first enantiomer. This was explained by the fact that the slower migrating enantiomer passes the detector with a higher molar fraction in the complexed form compared to the faster migrating

enantiomer. Although different detector response of enantiomers does not appear to be a common phenomenon, especially when using UV detection, it should be kept in mind that analyte complexation may alter the spectroscopic properties of the compounds and, consequently, affect analyte quantitation.

The aim of any method development for an analytical separation is to obtain an assay allowing the separation of the analytes in a short period of time. Apart from the physicochemical characteristics of the analytes, experimental factors such as type and concentration of the chiral selector, type, pH, and concentration of the background electrolyte, as well as additives such as organic solvents or surfactants, applied voltage, or capillary temperature, and capillary rinsing procedures affect enantioseparations in CE. All these factors have to be optimized and properly validated. The univariate approach, i.e., optimizing one variable at a time while keeping all other variables constant, results in a large number of experiments. Typically, this approach only leads to a local optimum of the conditions. Therefore, chemometric methods have been increasingly used in order to find the global optimal conditions of the experimental variables [216–219]. In such approaches, the variables which significantly affect a separation are first identified by an experimental design and subsequently optimized using another type of design. Testing of the robustness of the analytical method can also be addressed by chemometrics. General practical considerations for obtaining a robust CE method can be found in [220].

An example illustrating the stereoselectivity and chemoselectivity of CE is the separation of the etomidate exhibiting (*R*)-configuration from its (*S*)-enantiomer as well as the related substances metomidate and etomidate acid (Fig. 19) [221]. All analytes could be detected at the cathodic end of the capillary using a 100 mM phosphate buffer, pH 2.1, as background electrolyte (Fig. 19a). The enantiomers of etomidate and metomidate could be separated using 30 mg/mL β-CD while the enantiomers of the acid comigrated under these conditions (Fig. 19b). Addition of 30 mg/mL α-CD only resulted in poor separation of the enantiomers of etomidate (Fig. 19c). However, α-CD also led to an increased resolution between metomidate and etomidate. Exploiting the carrier ability of sulfated β-CD and reversing the polarity of the applied voltage, i.e., detecting the analytes at the anodic end of the capillary, resulted in the separation of all enantiomers with large resolution values, R_S, at a concentration of 20 mg/mL of the CD (Fig. 19d). However, when overloading the system by injecting high concentrations of etomidate in order to achieve the required sensitivity for the detection of the impurities at the 0.1% level, peak splitting and peak distortion were observed. Finally, the combination of 30 mg/mL α-CD and 4.6 mg/mL sulfated β-CD allowed the determination of all potential impurities of the drug in the presence of a large excess of etomidate (Fig. 19e). The system allows the separation of all enantiomers (Fig. 19f) but the peak of the (*S*)-enantiomer of metomidate is "covered" by the peak of etomidate when high concentrations of the drug are injected (Fig. 19e). In the present case this was considered insignificant as (*S*)-metomidate is a very unlikely impurity of etomidate. In the dual CD system the enantioselectivity is achieved by sulfated

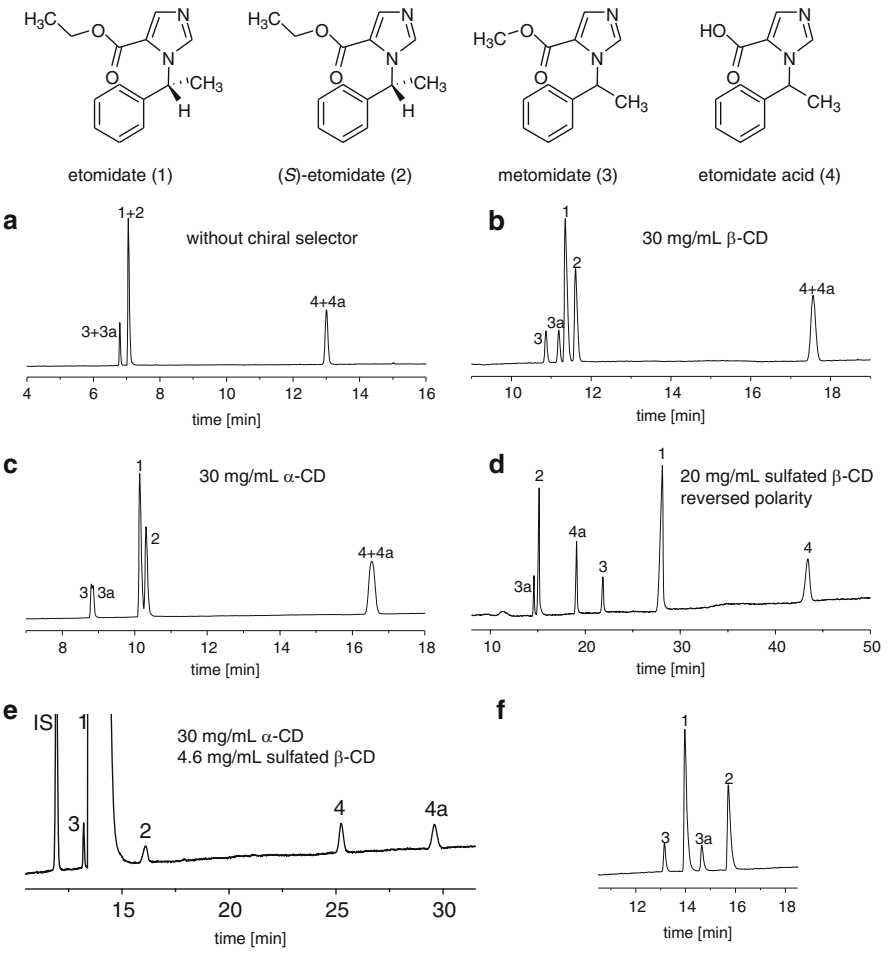

Fig. 19 Simultaneous separation of the enantiomers of etomidate, metomidate, and etomidate acid (**a**) in the absence of a chiral selector and in the presence of (**b**) β-CD, (**c**) α-CD, (**d**) sulfated β-CD and (**e**, **f**) a combination of α-CD and sulfated β-CD. Experimental conditions: 50.2/40 cm, 50 μm id fused-silica capillary, 100 mM sodium phosphate buffer, pH 2.1, 20°C, 20 kV. Peak assignment: (*1*) etomidate, (*2*) (*S*)-etomidate, (*3*) (*R*)-metomidate, (*3a*) (*S*)-metomidate, (*4*) (*R*) etomidate acid, (*4a*) (*S*)-etomidate acid. Sample concentration in (**e**): 5.4 mg/mL etomidate containing approximately 40–80 μg/mL of the related substances. (Adapted with permission of Wiley from [221] © 2006)

β-CD while α-CD contributes to the chemoselectivity of the system by assisting the separation of etomidate and metomidate. The CE assay was subsequently validated and applied to the simultaneous analysis of etomidate with regard to the stereochemical purity as well as related substances. Concentrations of the impurities as low as 0.01% could be detected with the CE method [221].

5.2 Micellar Electrokinetic Chromatography

MEKC has been introduced as a method allowing the analysis of uncharged compounds [10–13] but the technique is equally suitable for charged analytes. MEKC enantioseparations can be carried out using two basic systems. The first mode employs a chiral surfactant used in concentrations above the critical micelle concentration. These surfactants comprise bile salts or charged or neutral compounds derived from glucopyranosides or *N*-acylamino acids surfactants [222]. Mixed micelles composed of chiral and achiral surfactants have also been used. The separation mechanism using chiral micelles is based on the stereoselective interaction of the analyte enantiomers with the selector upon partitioning between the aqueous and the micellar phases.

A further development is the introduction of polymeric surfactants (polymeric micelles) by the groups of Warner [46] and Dobashi [160]. These are obtained by polymerization of the hydrocarbon chain of *N*-acyl amino acids or *N*-alkyloxycarbonyl derivatives of amino acids or dipeptides. The polymeric micelles overcome the limitations caused by the dynamic nature of conventional micelles and instability upon addition of higher concentrations of organic solvents. Furthermore, lower Joule heating is observed for polymeric micelles as compared to micelles formed from monomeric surfactants. Limitations of the polymeric micelles may be the presence of impurities originating from the polymerization process or slow mass transfer kinetics in the case of a high polydispersity of the polymers. Comparison of the separation selectivity of amino acid-based chiral surfactants and their polymeric analogs revealed a significant influence of steric effects as well as the orientation and charge of the headgroup [223–225].

In the second approach achiral micelles are combined with a chiral selector. A frequently employed combination is the use of SDS as surfactant combined with cyclodextrins. Also termed CD-modified MEKC, this system is based on several equilibria, i.e., the partitioning of the analyte between the (achiral) micelles and the aqueous phase as well as the stereoselective complexation of the enantiomers by the selector. Furthermore, distribution of the CD–analyte complexes into the micelles may be considered as well as the binding of the enantiomers by CDs associated with the micelles. The latter may differ from the complexation between CD and analyte in the aqueous phase. Furthermore, it has been shown by CE, spectroscopic techniques and molecular modeling that the hydrocarbon chain of SDS can be incorporated into the cavity of CDs, thereby modulating the binding affinity towards the analyte molecules [226–228]. Although not yet experimentally proven, the incorporation of surfactants other than SDS into the cavity of CDs can be expected. Conversely, CDs may affect the micellization of surfactants [226, 227], emphasizing the importance of a profound understanding of the interactions between surfactants and CDs in order to design proper separation systems.

Both modes, i.e., MEKC using chiral micelles and CD-modified MEKC, have been successfully applied to the enantioseparations of many basic, acidic, or neutral compounds [222]. An interesting characteristic of the polymeric micelles is their

compatibility with MS detection [211, 229]. MEKC employing monomeric chiral surfactants or achiral surfactants combined with CDs is not suitable for this purpose. Major concerns are signal suppression, poor volatility, interactions between surfactant and analytes, as well as the production of interfering background ions. The use of polymeric micelles has several advantages. First, as they do not possess a critical micelle concentration they may be used at relatively low concentrations in the background electrolyte, minimizing the deteriorating effects on the MS detection. Second, as the molecular organization of polymeric micelles is not affected by organic solvents, a high content of organic solvent may be used in the background electrolyte. Third, they do not interfere in the low molecular mass range due to their high molecular mass. Finally, their low surface activity provides a stable electrospray and consequently less suppression of the analyte signal. MEKC enantioseparations with MS detection using polymeric micelles has been reported for a number of structurally diverse analytes [230–232]. A recent illustrative example of MEKC-MS is the stereoselective analysis of warfarin and its metabolite hydroxywarfarin in serum samples [233]. The simultaneous separation of the drug and five hydroxylated metabolites upon optimization of the background electrolyte is shown in Fig. 20a. Except for 8-hydroxywarfarin, all enantiomers could be separated in the presence of 25 mM poly(sodium *N*-undecenoyl-L-leucyl-L-valinate) in an ammonium acetate buffer containing 15 vol.% methanol. Tandem mass spectrometry allowed limits of detection between 0.5 and 3 ng/mL depending on the analyte. The assay allowed the stereoselective analysis of plasma samples from patients (Fig. 20b) and the sensitive determination of metabolites that were apparently not detected in previous studies, illustrating the fact that MEKC-electrospray ionization-tandem mass spectrometry employing polymeric micelles is well suited to the bioanalysis with MS detection. Moreover, differences between the stereoselective metabolism of subjects possessing a mutant of the cytochrome enzyme CYP2C9 could be identified (Fig. 20b) [233].

5.3 Microemulsion Electrokinetic Chromatography

MEEKC was introduced in 1991 [234] and can be regarded as analogous to MEKC using microemulsion droplets as pseudostationary phase as compared to micelles in MEKC. The microemulsion is formed by a water immiscible organic liquid stabilized by a surfactant and a co-surfactant. The droplets of the microemulsion are typically charged due to the use of a negatively charged surfactant so that they migrate towards the anode. There has been much debate about both techniques with regard to enhanced stability, solubilization capacity, or higher mass transfer efficiency of the microemulsion vs the micelles. However, the literature published to date suggests that the answer regarding the superior separation mode may be analyte dependent, especially in the light of solvent-modified MEKC. Recent work on the achiral separation of steroids comparing MEEKC and MEKC with the addition of 1-butanol yielded comparable results with regard to separation performance [235].

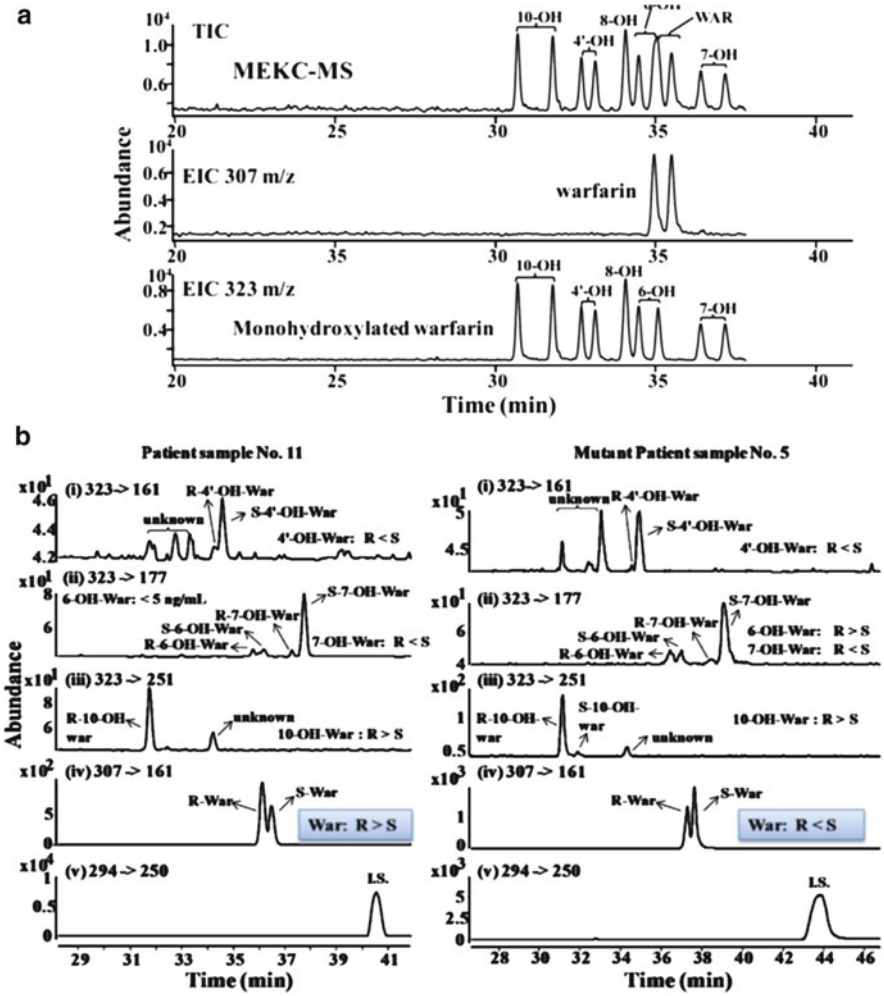

Fig. 20 MEKC-MS analysis of warfarin and its hydroxylated metabolites. (**a**) Analysis of standards showing the total ion chromatogram (TIC), the mass trace m/z 307 representing warfarin and the mass trace m/z 323 of the hydroxy metabolites. (**b**) Tandem MS extracted ion chromatograms of plasma samples. Patient sample 5 represents a subject with polymorphism of cytochrome CYP2C9. Experimental conditions: 118 cm, 50 μm id fused-silica capillary, 25 mM poly(sodium *N*-undecenoyl-L-leucyl-L-valinate) in 25 mM ammonium acetate, pH 5.0, containing 15 vol.% methanol, 30 kV. Spray chamber parameters: nebulizer pressure: 4 psi, drying gas temp.: 200°C, drying gas flow: 6 L/min, capillary voltage: −3,000 V, fragmentor voltage: 91 V. (Reproduced with permission of Elsevier from [233] © 2013)

For MEEKC enantioseparations, two general approaches have been realized. The first employs chiral components forming the microemulsion. For example, *N*-dodecoxycarbonyl-L-valine was used as chiral surfactant [236–238], chiral alkanols such as (2*R*)-pentanol or (2*R*)-hexanol as chiral co-surfactants [239], or

chiral oil phases such as dibutyl L-tartrate [240, 241]. Combinations of two [242–244] or three [245] chiral components have also been employed. Interestingly, effective separations of the enantiomers of β-blockers have also been obtained using a neutral microemulsion composed of Tween 20 and dibutyl L-tartrate in a sodium tetraborate buffer [246]. The mechanism of the enantioseparations using a chiral oil droplet is based on the partitioning equilibria of the analyte enantiomers between the aqueous phase and the chiral oil phase.

The second approach uses an achiral microemulsion in combination with a chiral selector such as a CD. In this case the microemulsion is composed of a water-immiscible organic solvent such as *n*-hexane, *n*-heptane, or ethyl acetate, a surfactant such as SDS, and a co-surfactant such as 1-butanol or 1-octanol. As chiral selectors, neutral [247] as well as negatively charged CD derivatives [248–251] have been employed. In these systems two equilibria have to be considered – the partitioning of the analyte between the aqueous phase and the lipid phase as well as the stereospecific complexation of the enantiomers by the CDs. The partitioning of the diastereomeric enantiomer–CD complexes may, in principle, also take place. It has been shown by NMR and molecular modeling that SDS used for the preparation of the microemulsion can also form complexes with CDs, modulating the interaction between the selector and analyte enantiomers [228].

In this context it is interesting to note that the way of preparation of the microemulsion, specifically the time of the addition of the chiral selector, may affect the performance of the separation system. Thus, a MEEKC method allowing the simultaneous separation of the enantiomers of amphetamine, i.e., dexamphetamine and levoamphetamine, as well as related substances was developed using a microemulsion composed of 1.5 wt% SDS, 0.5 wt% ethyl acetate, 3.5 wt% 1-butanol, 2.5 wt% 2-propanol, and 92 wt% 50 mM sodium phosphate buffer, pH 3.0, containing 5.5 wt% sulfated β-CD [251]. Superior separation of the amphetamine enantiomers and the related substances phenylacetone *E*-oxime and (1*S*,2*S*)-(+)-norpseudoephedrine was observed when sulfated β-CD was added to the phosphate buffer prior to the preparation of the microemulsion by sonication (Fig. 21a) as compared to addition of the chiral selector after preparation of the microemulsion (Fig. 21b). At present, the origin of the phenomenon is not clear. It may be speculated that it is due either to inclusion of SDS or other components of the microemulsion into the cavity of the CD or to association of the CD with the microemulsion droplets during the preparation. In any case, such effects have to be considered when developing methods for routine analysis. For recent reviews on MEEKC, including the use for enantioseparations, see, for example, [252, 253].

6 Concluding Remarks

Within the 30 years since its introduction CE has developed into a mature technique for the analysis of a large variety of analytes. Theoretical knowledge and understanding of the underlying mechanisms of CE separations has been compiled. Due to the different separation mechanisms, HPLC and CE are complimentary techniques where each has its own advantages and disadvantages so that the user

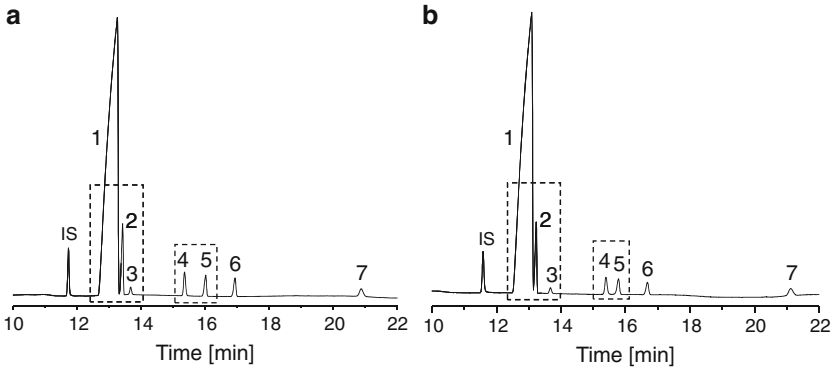

Fig. 21 Effect of the preparation of the microemulsion background electrolyte on analyte separation. (**a**) Addition of sulfated β-CD prior to the phosphate buffer preparation of the microemulsion by sonication and (**b**) addition of sulfated β-CD after preparation of the microemulsion. Experimental conditions: 50.2/40 cm, 50 μm id fused-silica capillary, 20°C, −14 kV, UV detection at 200 nm; background electrolyte: 1.5 wt% SDS, 0.5 wt% ethyl acetate, 3.5 wt% 1-butanol, 2.5 wt% 2-propanol, and 92 wt% 50 mM sodium phosphate buffer, pH 3.0, containing 5.5 wt% sulfated β-CD. Peak assignment: (IS) internal standard, (*1*) dexamphetamine, (*2*) levoamphetamine, (*3*) phenylacetone *Z*-oxime, (*4*) phenylacetone *E*-oxime, (*5*) (1*S*,2*S*)-(+)-norpseudoephedrine, (*6*) (1*R*,2*S*)-(−)-norephedrine, (*7*) phenylacetone. (Reproduced with permission of Wiley from [251] © 2010)

may have to choose between both techniques for a certain separation problem. CE offers many modes, chiral selectors, and migration options, making it a highly flexible and versatile technique. However, this flexibility may also be the reason why CE is often considered a less robust technique compared to HPLC. Consequently, CE is less accepted for routine analysis and sometimes referred to as an "academic" technique. This may be due to the fact that most analytical chemists are trained in chromatography and not in CE, so that the basic understanding of CE may not be as widespread as of chromatography. For example, the fused-silica capillary surface is often considered inert which does not apply. The ionization state of silanol groups on the surface generates the EOF. Therefore, understanding of the influencing factors and the EOF, which includes all rinsing steps and, consequently, properly controlling the EOF is the key to a successful method. In fact, it has been shown that properly validated CE methods perform as well as HPLC methods with regard to precision and robustness.

Another often mentioned fact is the relatively low UV-detection sensitivity of CE compared to HPLC because detection is performed on column which results in a low optical path length. Besides using specific capillaries with extended optical path lengths (bubble cells or Z-cells), detection modes other than UV may be employed such as laser-induced fluorescence or mass spectrometric detection. Moreover, on-column sample stacking techniques based on electrophoretic phenomena have been developed, resulting in an up to 1,000-fold increase in sensitivity as summarized, for example, in [254–257].

CE methods have been included in the documentation submitted to regulatory authorities such as the US Food and Drug Administration (FDA) or the European Medicines Agency (EMA). Furthermore, CE has been implemented in the draft guidance for industry of the FDA [258, 259] as well as in monographs of the United States Pharmacopeia (USP) and the European Pharmacopoeia (Ph. Eur.) [259, 260]. Within the pharmaceutical industry CE has seen an increase in recent years, especially in the biotechnological sector. This may be primarily due to the use of well defined commercial kits for specific applications such as CE-gel electrophoresis or capillary isoelectric focusing for biomolecules [260]. In the author's opinion, CE is also an excellent technique for small molecule analysis, especially for enantioseparations if such methods are properly validated. This has been shown in some of the examples discussed above where the simultaneous analysis of the stereochemical purity of a drug and of its related substances has been demonstrated, for example in [208, 221, 251], as well as the implementation of CE enantioseparation methods in international pharmacopeias. Further acceptance of CE, especially for routine analysis, will require trained laboratory staff with a profound understanding of the technique. CE is not just "like HPLC in capillaries" but a technique based on different phenomena compared to chromatography.

References

1. Kant I (1783) Prolegomena zu einer jeden künftigen Metaphysik die als Wissenschaft wird auftreten können. English translation: Hatfield G (1997) Prolegomena to any future metaphysics that will be able to come forward as science. Cambridge University Press, New York
2. Jorgenson JW, Lukacs KA (1981) Free zone capillary electrophoresis in open-tubular glass capillaries. Anal Chem 53:1298–1302
3. Gassmann E, Kuo JE, Zare R (1985) Electrokinetic separation of chiral compounds. Science 230:813–814
4. Cohen AS, Paulus A, Karger BL (1987) High-performance capillary electrophoresis using open tubes and gels. Chromatographia 24:15–24
5. Snopek J, Jelinek I, Smolkova-Keulemansova E (1988) Use of cyclodextrins in isotachophoresis: IV. The influence of cyclodextrins on the chiral resolution of ephedrine alkaloid enantiomers. J Chromatogr 438:211–218
6. Snopek J, Jelinek I, Smolkova-Keulemansova E (1988) Use of cyclodextrins in isotachophoresis: V. The separation of ketotifen and its polar intermediate enantiomers. J Chromatogr 439:386–392
7. Jelinek I, Dohnal J, Snopek J, Smolkova-Keulemansova E (1989) Use of cyclodextrins in isotachophoresis: VII. Resolution of structurally related and chiral phenothiazines. J Chromatogr 464:139–147
8. Guttman A, Paulus A, Cohen AS, Grinberg N, Karger BL (1988) Use of complexing agents for selective separation in high-performance capillary electrophoresis: chiral resolution via cyclodextrins incorporated within polyacrylamide gel columns. J Chromatogr 448:41–53
9. Fanali S (1989) Separation of optical isomers by capillary zone electrophoresis based on host-guest complexation with cyclodextrins. J Chromatogr 474:441–446
10. Terabe S (1989) Electrokinetic chromatography: an interface between electrophoresis and chromatography. Trends Anal Chem 8:129–134
11. Terabe S, Shibata M, Miyashita Y (1989) Chiral separation by electrokinetic chromatography with bile salt micelles. J Chromatogr 480:403–411

12. Dobashi A, Ono T, Hara S (1989) Optical resolution of enantiomers with chiral mixed micelles by electrokinetic chromatography. Anal Chem 61:1984–1986
13. Dobashi A, Ono T, Hara S, Yamaguchi J (1989) Enantioselective hydrophobic entanglement of enantiomeric solutes with chiral functionalized micelles by electrokinetic chromatography. J Chromatogr 480:413–420
14. Van Eeckhaut A, Michotte Y (2006) Chiral separations by capillary electrophoresis: recent developments and applications. Electrophoresis 27:2880–2895
15. Chankvetadze B (2007) Enantioseparations by using capillary electrophoretic technique. J Chromatogr A 1168:45–70
16. Gübitz G, Schmid MG (2008) Chiral separation by capillary electromigration techniques. J Chromatogr A 1204:140–156
17. Mikus P, Marakova K (2009) Advanced CE for chiral analysis of drugs, metabolites and biomarkers in biological samples. Electrophoresis 30:2773–2802
18. Preinstorfer B, Lämmerhofer M, Lindner W (2009) Advances in enantioselective separations using electromigration capillary techniques. Electrophoresis 30:100–132
19. Caslavska J, Thormann W (2011) Stereoselective determination of drugs and metabolites in body fluids, tissues and microsomal preparations by capillary electrophoresis (2000–2010). J Chromatogr A 1218:588–601
20. Scriba GKE (2011) Fundamental aspects of chiral electromigration techniques and application in pharmaceutical and biomedical analysis. J Pharm Biomed Anal 55:688–701
21. Scriba GKE (2011) Chiral electromigration techniques in pharmaceutical and biomedical analysis. Bioanal Rev 3:95–114
22. Lu H, Chen G (2011) Recent advances of enantioseparations in capillary electrophoresis and capillary electrochromatography. Anal Methods 3:488–508
23. Chankvetadze B (1997) Capillary electrophoresis in chiral analysis. Wiley, Chichester
24. Van Eeckhaut A, Michotte Y (eds) (2010) Chiral separations by capillary electrophoresis. CRC, Boca Raton
25. Chankvetadze B (1997) Separation selectivity in chiral capillary electrophoresis with charged selectors. J Chromatogr A 792:269–295
26. Sänger-van de Griend CE, Gröningsson K, Arvidsson T (1997) Enantiomeric separation of a tetrapeptide with cyclodextrin extension of the model for chiral capillary electrophoresis by complex formation of one enantiomer molecule with more than one chiral selector molecules. J Chromatogr A 782:271–279
27. Bowser MT, Kranack AR, Chen DDY (1998) Properties of multivariate binding isotherms in capillary electrophoresis. Anal Chem 70:1076–1084
28. Bowser MT, Chen DDY (1998) Higher order equilibria and their effect on analyte migration behavior in capillary electrophoresis. Anal Chem 70:3261–3270
29. Scriba GKE (2002) Selected fundamental aspects of chiral electromigration techniques and their application to pharmaceutical and biomedical analysis. J Pharm Biomed Anal 27: 373–399
30. Rizzi A (2001) Fundamental aspects of chiral separations by capillary electrophoresis. Electrophoresis 22:3079–3106
31. Wren SAC, Rowe RC (1992) Theoretical aspects of chiral separation in capillary electrophoresis. I. Initial evaluation of a model. J Chromatogr A 603:235–241
32. Stepanova ND, Stepanov AV (1969) Influence of temperature on the effectiveness of the electromigration separation of calcium and strontium in citric acid solutions. Zh Prikl Khimii (Russ J Appl Chem Engl Ed) 42:1670–1673
33. Chankvetadze B, Lindner W, Scriba GKE (2004) Enantiomer separations in capillary electrophoresis in the case of equal binding constants of the enantiomer with a chiral selector: commentary on the feasibility of the concept. Anal Chem 76:4256–4260
34. Lomsadze K, Martinez-Giron AB, Castro-Puyana M, Chankvetadze L, Crego AL, Salgado A, Marina ML, Chankvetadze B (2009) About the role of enantioselective selector-selectand

interactions and the mobilities of diastereomeric associates in enantiomer separations using CE. Electrophoresis 30:2803–2811
35. Süß F, Sänger-van de Griend CE, Scriba GKE (2003) Migration order of dipeptides and tripeptide enantiomers in the presence of single isomer and randomly sulfated cyclodextrins as a function of pH. Electrophoresis 24:1069–1076
36. Rizzi AM, Kremser L (1999) pK_a shift-associated effects in enantioseparations by cyclodextrin-mediated capillary zone electrophoresis. Electrophoresis 20:2715–2722
37. Rawjee YY, Staerk DU, Vigh G (1993) Capillary electrophoretic chiral separations with cyclodextrin additives: I. acids: chiral selectivity as a function of pH and the concentration of β-cyclodextrin for fenoprofen and ibuprofen. J Chromatogr 635:291–306
38. Rawjee YY, Williams RL, Vigh G (1993) Capillary electrophoretic chiral separations using β-cyclodextrin as resolving agent II. Bases: chiral selectivity as a function of pH and the concentration of β-cyclodextrin. J Chromatogr A 652:233–245
39. Rawjee YY, Williams RL, Vigh G (1994) Capillary electrophoretic chiral separations using cyclodextrin additives: III. Peak resolution surfaces for ibuprofen and homatropine as a function of the pH and the concentration of β-cyclodextrin. J Chromatogr 680:599–607
40. Williams BA, Vigh G (1977) A dry look at CHARM (charged resolving agent migration) model of enantiomer separations by capillary electrophoresis. J Chromatogr A 777:295–309
41. Zhu W, Vigh G (2000) Experimental verification of a predicted, hitherto unseen separations electivity pattern in the nonaqueous capillary electrophoretic separation of weak base enantiomers by oktakis (2,3-diacetyl-6-sulfato)-γ-cyclodextrin. Electrophoresis 21: 2016–2024
42. Dubsky P, Svobodova J, Gas B (2008) Model of CE enantioseparation systems with a mixture of chiral selectors. Part I. Theory of migration and interconversion. J Chromatogr B 875: 30–34
43. Dubsky P, Svobodova J, Tesarova E, Gas B (2010) Enhanced selectivity in CZE multi chiral selector enantioseparation systems: proposed separation mechanism. Electrophoresis 31: 1435–1441
44. Chankvetadze B, Schulte G, Blaschke G (1997) Nature and design of enantiomer migration order in chiral capillary electrophoresis. Enantiomer 2:157–179
45. Chankvetadze B (2002) Enantiomer migration order in chiral capillary electrophoresis. Electrophoresis 23:4022–4035
46. Wang J, Warner IM (1994) Chiral separations using micellar electrokinetic capillary chromatography and a polymerized chiral micelle. Anal Chem 66:3773–3776
47. Zheng Z, Lin J, Qu F, Hobo T (2003) Chiral separation with ligand-exchange micellar electrokinetic chromatography using a D-penicillamine-copper(II) ternary complex as chiral selector. Electrophoresis 24:4221–4226
48. Tano C, Son SH, Furukawa J, Furuike T, Sakairi N (2008) Dodecyl thioglycopyranoside sulfates: novel sugar-based surfactants for enantiomeric separations by micellar electrokinetic capillary chromatography. Electrophoresis 29:2869–2875
49. Lee W, La S, Choi Y, Kim KR (2003) Chiral discrimination of aromatic amino acids by capillary electrophoresis in (+)- and (−)-(18-crown-6)-2,3,11,12-tetracarboxylic acid selector modes. Bull Korean Chem Soc 24:1232–1234
50. Vaccher MP, Lipka E, Bonte JP, Foulon C, Groossens JF, Vaccher C (2005) Enantiomeric analysis of baclofen by capillary zone electrophoresis, using highly sulfated cyclodextrins: inclusion ionization constant pK_a determination. Electrophoresis 26:2974–2983
51. Lipka E, Charton J, Vaccher MP, Folly-Klan M, Bonte JP, Vaccher C (2009) Enantioseparation of chiral benzimidazole derivatives by electrokinetic chromatography using sulfated cyclodextrins. J Sep Sci 32:1907–1915
52. Dominguez Vega E, Lomsadze K, Chankvetadze L, Salgado A, Scriba GKE, Calvo E, López JA, Crego AL, Marina ML, Chankvetadze B (2011) Separation of enantiomers of ephedrine by capillary electrophoresis using cyclodextrins as chiral selectors: comparative CE, NMR and high resolution MS studies. Electrophoresis 32:2640–2647

53. Lomsadze K, Domínguez Vega E, Salgado A, Crego AL, Scriba GKE, Marina ML, Chankvetadze B (2012) Separation of enantiomers of norephedrine by capillary electrophoresis using cyclodextrins as chiral selectors: comparative CE and NMR studies. Electrophoresis 33:1637–1647
54. Samakashvili S, Salgado A, Scriba GKE, Chankvetadze B (2013) Comparative enantioseparation of ketoprofen with trimethylated α-, β- and γ-cyclodextrin in capillary electrophoresis and study of related selector-selectand interactions using nuclear magnetic resonance spectroscopy. Chirality 25:79–88
55. Chankvetadze B, Burjanadze N, Breitkreutz J, Bergander K, Bergenthal D, Kataeva O, Fröhlich R, Luftmann H, Blaschke G (2002) Mechanistic study of the opposite migration order of the enantiomers of ketamine with α- and β-cyclodextrin in capillary electrophoresis. J Sep Sci 25:1155–1166
56. Chankvetadze L, Servais AC, Fillet M, Salgado A, Crommen J, Chankvetadze B (2012) Comparative enantioseparation of talinolol in aqueous and non-aqueous capillary electrophoresis and study of related selector-selectand interactions by nuclear magnetic resonance spectroscopy. J Chromatogr A 1267:206–216
57. Süß F, Poppitz W, Sänger-van de Griend CE, Scriba GKE (2001) Influence of the amino acid sequence and nature of the cyclodextrin on the separation of small peptide enantiomers by capillary electrophoresis using randomly substituted and single isomer sulfated and sulfonated cyclodextrins. Electrophoresis 22:2416–2423
58. Fillet M, Chankvetadze B, Crommen J, Blaschke G (1999) Designed combination of chiral selectors for adjustment of enantioseparation selectivity in capillary electrophoresis. Electrophoresis 20:2691–2697
59. Scriba GKE (2003) Recent advances in enantioseparations of peptides by capillary electrophoresis. Electrophoresis 24:4063–4077
60. Li J, Waldron KC (1999) Estimation of the pH-independent binding constants of alanylphenylalanine and leucylphenylalanine stereoisomers with β-cyclodextrin in the presence of urea. Electrophoresis 20:171–179
61. Sabbah S, Süß F, Scriba GKE (2001) pH-dependence of complexation constants and complex mobility in capillary electrophoresis separations of dipeptide enantiomers. Electrophoresis 22:3163–3170
62. Servais AC, Rousseau A, Fillet M, Lomsadze K, Salgado A, Crommen J, Chankvetadze B (2010) Separation of propranolol enantiomers by CE using sulfated β-CD derivatives in aqueous and non-aqueous electrolytes; comparative CE and NMR study. Electrophoresis 31:1467–1474
63. Lomsadze K, Salgado A, Calvo E, Antonio Lopez J, Chankvetadze B (2011) Comparative NMR and MS studies on the mechanism of enantioseparation of propranolol with hepatakis (2,3-diacetyl-6-sulfo)-β-cyclodextrin in capillary electrophoresis with aqueous and non-aqueous electrolytes. Electrophoresis 32:1156–1163
64. Servais AC, Rousseau A, Dive G, Frederich M, Crommen J, Fillet M (2012) Combination of capillary electrophoresis, molecular modelling and nuclear magnetic resonance to study the interaction mechanisms between single-isomer anionic cyclodextrin derivatives and basic drug enantiomers in a methanolic background electrolyte. J Chromatogr A 1232:59–64
65. Qi L, Yang G (2009) Enantioseparation of dansyl amino acids by ligand-exchange capillary electrophoresis with zinc(II)-L-phenylalaninamide complex. J Sep Sci 32:3209–3214
66. Chen Z, Niitsuma M, Nakagama T, Uchiyama K, Hobo T (2002) Enantioseparations of dansyl amino acids by capillary electrophoresis using Cu(II) complexes with L-amino acylamides as chiral selectors in electrolytes. J Sep Sci 25:1197–1201
67. Chankvetadze B, Schulte G, Blaschke G (1996) Reversal of enantiomer elution order in capillary electrophoresis using charged and neutral cyclodextrins. J Chromatogr A 732: 183–187
68. Schmitt T, Engelhardt H (1995) Optimization of enantiomeric separations in capillary electrophoresis by reversal of the migration order and using different derivatized cyclodextrins. J Chromatogr A 697:561–570

69. Chankvetadze B, Schulte G, Blaschke G (1997) Selected applications of capillaries with dynamic or permanent anodal electroosmotic flow in chiral separations by capillary electrophoresis. J Pharm Biomed Anal 15:1577–1584
70. Knob R, Maier V, Ranc V, Znaleziona J, Sevcik J (2010) Dopa and tyrosine enantiomers migration order reversal using uncoated and polypyrrole-coated capillaries. Glob J Anal Chem 1:228–232
71. Werner A, Nassauer T, Kiechle P, Erni F (1994) Chiral separation by capillary zone electrophoresis of an optically active drug and amino acids by host-guest complexation with cyclodextrins. J Chromatogr A 666:375–379
72. Baumy P, Morin P, Dreux M, Viaud MC, Boye S, Gullmant G (1995) Determination of β-cyclodextrin inclusion complex constants for 3,4-dihydro-2*H*-1-benzopyran enantiomers by capillary electrophoresis. J Chromatogr A 707:311–325
73. Sabah S, Scriba GKE (1998) Electrophoretic stereoisomer separation of aspartyl dipeptides and tripeptides in untreated fused-silica and polyacrylamide-coated capillaries using charged cyclodextrins. J Chromatogr A 822:137–145
74. Liu L, Nussbaum MA (1995) Control of enantiomer migration order in capillary electrophoresis separations using sulfobutyl ether beta-cyclodextrin. J Pharm Biomed Anal 14: 65–72
75. Tamisier-Karolak SL, Stenber MA, Bommart A (1999) Enantioseparation of β-blockers with two chiral centers by capillary electrophoresis using sulfated β-cyclodextrins. Electrophoresis 20:2656–2663
76. Lin CE, Cheng HT, Fang IJ, Liu YD, Kuo CM, Lin WY, Lin CH (2006) Strategies for enantioseparations of catecholamines and structurally related compounds by capillary zone electrophoresis using sulfated β-cyclodextrins as chiral selectors. Electrophoresis 27: 3443–3451
77. Rudaz S, Geiser L, Sourverain S, Prat J, Veuthey JL (2005) Rapid stereoselective separations of amphetamine derivatives with highly sulphated γ-cyclodextrin. Electrophoresis 26: 3910–3920
78. Ha PTT, Van Schepdael A, Hauta-Aho T, Roets E, Hoogmartens J (2002) Simultaneous determination of DOPA and carbidopa enantiomers by capillary zone electrophoresis. Electrophoresis 23:3404–3409
79. Schulte G, Chankvetadze B, Blaschke G (1997) Enantioseparation in capillary electrophoresis using 2-hydroxypropyltrimethylammonium salt of β-cyclodextrin as chiral selector. J Chromatogr A 771:259–266
80. Süß F, Poppitz W, Scriba GKE (2002) Separation of dipeptide and tripeptide enantiomers in capillary electrophoresis by the cationic cyclodextrin derivative 2-hydroxypropyltrimethylammonium-β-cyclodextrin and by neutral β-cyclodextrin derivatives at alkaline pH. J Sep Sci 25:1147–1154
81. Schmitt T, Engelhardt H (1993) Charged and uncharged cyclodextrins as chiral selectors in capillary electrophoresis. Chromatographia 37:475–481
82. Sabbah S, Scriba GKE (2001) Separation of dipeptide and tripeptide enantiomers in capillary electrophoresis using carboxymethyl-β-cyclodextrin and succinyl-β-cyclodextrin: influence of the amino acid sequence, nature of the cyclodextrin and pH. Electrophoresis 22:1385–1393
83. Zhu X, Ding Y, Lin B, Jakob A, Koppenhöfer B (2000) Transient state of chiral recognition in a binary mixture of cyclodextrins in capillary electrophoresis. J Chromatogr A 888:241–250
84. Calvet C, Cuberes R, Perez-Maseda C, Frigola J (2002) Enantioseparation of novel COX-2 anti-inflammatory drugs by capillary electrophoresis using single and dual cyclodextrin systems. Electrophoresis 23:1702–1708
85. Lin CE, Lin SL, Liao WS, Liu YC (2004) Enantioseparation of benzoins and enantiomer migration reversal of hydrobenzoin in capillary zone electrophoresis with dual cyclodextrin systems and borate complexation. J Chromatogr A 1032:227–235

86. Lin CE, Liao WS, Cheng HT, Kuo CM, Liu YC (2005) Enantioseparation of phenothiazines in cyclodextrin-modified capillary zone electrophoresis using sulfated cyclodextrins as chiral selectors. Electrophoresis 26:3869–3877
87. Liao WS, Lin CH, Chen CY, Kuo CM, Liu YC, Wu JC, Lin CE (2007) Enantioseparation of phenothiazines in CD-modified CZE using single isomer sulfated CD as a chiral selector. Electrophoresis 28:3922–3929
88. Valle BC, Billot FH, Shamsi SA, Zhu Y, Powe AM, Warner IM (2004) Combination of cyclodextrins and polymeric surfactants for chiral separations. Electrophoresis 25:743–752
89. Lin JM, Hobo T (2001) Inspection of the reversal of enantiomer migration order in ligand exchange micellar electrokinetic capillary chromatography. Biomed Chromatogr 15:207–211
90. Rundlett KL, Armstrong DW (1995) Effect of micelles and mixed micelles on efficiency and selectivity of antibiotic-based capillary electrophoretic enantioseparations. Anal Chem 67: 2088–2095
91. Wan H, Engstrom A, Blomberg E (1996) Direct chiral separation of amino acids derivatized with 2-(9-anthryl)ethyl chloroformate by capillary electrophoresis using cyclodextrins as chiral selectors. Effect of organic modifiers on resolution and enantiomeric elution order. J Chromatogr A 731:283–292
92. Schmitt T, Engelhardt H (1993) Derivatized cyclodextrins for the separation of enantiomers in capillary electrophoresis. J High Resolut Chromatogr 16:525–529
93. Lin CE, Liao WS, Chen KH (2003) Enantioseparation of phenothiazines in cyclodextrin-modified capillary zone electrophoresis: reversal of migration order. Electrophoresis 24:3139–3146
94. Zhu H, Wu E, Chen J, Yang YS, Kang W, Choi JK, Lee W, Kang JS (2011) Reverse migration order of sibutramine enantiomers as a function of cyclodextrin concentration in capillary electrophoresis. J Pharm Biomed Anal 54:1007–1012
95. Krajian H, Mofaddel N, Villemin D, Desbene PL (2009) A new example of reversal of the order of migration of enantiomers, as a function of cyclodextrin concentration and pH, by cyclodextrin-modified capillary zone electrophoresis: enantioseparation of 6,6′-dibromo-1,1′-binaphthyl-2,2′-diol. Anal Bioanal Chem 394:2193–2201
96. Castro-Puyana M, Crego AL, Marina ML, Garcia-Ruiz C (2007) Enantioselective separation of azole compounds by EKC. Reversal of migration order of enantiomers with CD concentration. Electrophoresis 28:2667–2674
97. Mofaddel N, Krajian H, Villemin D, Desbene PL (2009) Enantioseparation of binaphthol and its monoderivatives by cyclodextrin-modified capillary zone electrophoresis: a mathematical approach. Talanta 78:631–637
98. Wren SAC (1997) Mobility measurements on dansylated amino acids. J Chromatogr A 768: 153–159
99. Sabbah S, Scriba GKE (1999) pH-dependent reversal of the chiral recognition of an aspartyl tripeptide by carboxymethyl-β-cyclodextrin. J Chromatogr A 833:261–266
100. Sabbah S, Scriba GKE (2000) Influence of the structure of cyclodextrins and amino acid sequence of dipeptides and tripeptides on the pH-dependent reversal of the migration order in capillary electrophoresis. J Chromatogr A 894:267–272
101. Sungthong B, Ivanyi R, Bunz SC, Neusüß C, Scriba GKE (2010) CE-MS characterization of negatively charged α-, β- and γ-CD derivatives and their application to the separation of dipeptide and tripeptide enantiomers by CE. Electrophoresis 31:1498–1505
102. Terekhova IV, Hammitzsch-Wiedemann M, Shi J, Sungthong B, Scriba GKE (2010) Investigation of the pH-dependent complex formation between β-cyclodextrin and dipeptides enantiomers by capillary electrophoresis and calorimetry. J Sep Sci 33:2499–2505
103. Kodama S, Aizawa S, Taga A, Yamashita T, Kemmei T, Suzuki KHY, Yamamoto A (2010) Metal(II)-ligand molar ratio dependence of enantioseparation of tartaric acid by ligand exchange CE with Cu(II) and Ni(II)-D-quinic acid systems. Electrophoresis 31:1051–1054
104. Aizawa S, Kodama S (2012) Mechanism of change in enantiomer migration order of enantioseparation of tartaric acid by ligand exchange capillary electrophoresis with Cu(II) and Ni(II)-D-quinic acid systems. Electrophoresis 33:523–527

105. Hammitzsch-Wiedemann M, Scriba GKE (2009) Mathematical approach by a selectivity model for rationalization of pH- and selector concentration-dependent reversal of the enantiomer migration order in capillary electrophoresis. Anal Chem 81:8765–8773
106. Hammitzsch-Wiedemann M, Scriba GKE (2010) Mathematical approach by a selectivity model for rationalization of pH- and selector concentration-dependent reversal of the enantiomer migration order in capillary electrophoresis – correction. Anal Chem 82:6744
107. Hruska V, Benes M, Svobodova J, Zuskova I, Gas B (2012) Simulation of the effects of complex-formation equilibria in capillary electrophoresis: I. Mathematical model. Electrophoresis 33:938–947
108. Svobodova J, Benes M, Hruska V, Uselova K, Gas B (2012) Simulation of the effects of complex-formation equilibria in capillary electrophoresis: II. Experimental verification. Electrophoresis 33:948–957
109. Svobodova J, Benes M, Dubsky P, Vigh G, Gas B (2012) Simulation of the effects of complex-formation equilibria in electrophoresis: III. Simultaneous effects of chiral selector concentration and background electrolyte pH. Electrophoresis 33:3012–3020
110. Tsioupi DA, Stefan-van Staden RI, Kapnissi-Christodoulou CP (2013) Chiral selectors in CE: recent developments and applications. Electrophoresis 34:178–204
111. Lämmerhofer M (2010) Chiral recognition by enantioselective chromatography: mechanisms and modern chiral stationary phases. J Chromatogr A 1217:814–856
112. Scriba GKE (2011) Chiral recognition mechanisms in analytical separation sciences. Chromatographia 75:815–838
113. Scriba GKE (2013) Chiral recognition in separation science: an overview. In: Scriba GKE (ed) Chiral separations, methods and protocols, vol 970, 2nd edn, Methods in molecular biology. Humana, New York, pp 1–27
114. Berthod A (ed) (2010) Chiral recognition in separation methods. Springer, Heidelberg
115. Schneider HJ, Hacket F, Rüdiger V (1998) NMR studies of cyclodextrins and cyclodextrin complexes. Chem Rev 98:1755–1785
116. Dodziuk H, Kozinski W, Ejchart A (2004) NMR studies of chiral recognition by cyclodextrins. Chirality 16:90–105
117. Chankvetadze B (2004) Combined approach using capillary electrophoresis and NMR spectroscopy for an understanding of enantioselective recognition mechanisms by cyclodextrins. Chem Soc Rev 33:337–347
118. Morris KF, Froberg AL, Becker BA, Almeida VK, Tarus J, Larive CK (2005) Using NMR to develop insights into electrokinetic chromatography. Anal Chem 77:254A–263A
119. Uccello-Barretta G, Vanni L, Balzano F (2010) Nuclear magnetic resonance approaches to the rationalization of chromatographic enantiorecognition processes. J Chromatogr A 1217: 928–940
120. Lipkowitz KB (2001) Atomistic modeling of enantioselection in chromatography. J Chromatogr A 906:417–442
121. Del Rio A (2009) Exploring enantioselective molecular recognition mechanisms with chemoinformatic techniques. J Sep Sci 32:1566–1584
122. Fanali S (2000) Enantioselective determination by capillary electrophoresis with cyclodextrins as chiral selectors. J Chromatogr A 875:89–122
123. Fanali S (2009) Chiral separations by CE employing CDs. Electrophoresis 30:S203–S210
124. Chankvetadze B (2009) Separation of enantiomers with charged chiral selectors in CE. Electrophoresis 30:S211–S221
125. Scriba GKE (2008) Cyclodextrins in capillary electrophoresis – recent developments and applications. J Sep Sci 31:1991–2001
126. Scriba GKE, Altria K (2009) Using cyclodextrins to achieve chiral and non-chiral separations in capillary electrophoresis. LC GC Eur 22:420–430
127. Juvancz Z, Kendrovics RB, Ivanyi R (2008) The role of cyclodextrins in chiral capillary electrophoresis. Electrophoresis 29:1701–1712
128. Schmitt U, Branch SK, Holzgrabe U (2002) Chiral separations by cyclodextrin-modified capillary electrophoresis – determination of the enantiomeric excess. J Sep Sci 25:959–974

129. Gübitz G, Schmid MG (2010) Cyclodextrin-mediated chiral separations. In: Van Eeckhaut A, Michotte Y (eds) Chiral separations by capillary electrophoresis, vol 100, Chromatogr science series. CRC, Boca Raton, pp 47–85
130. Rekharsky MV, Inoue Y (1998) Complexation thermodynamics of cyclodextrins. Chem Rev 98:1875–1917
131. Servais AC, Rousseau A, Fillet M, Lomsadze K, Salgado A, Crommen J, Chankvetadze B (2010) Capillary electrophoretic and nuclear magnetic resonance studies on the opposite affinity pattern of propranolol enantiomers towards various cyclodextrins. J Sep Sci 33: 1617–1624
132. Chankvetadze B, Lomsadze K, Burjanadze N, Breitkreutz J, Pintore G, Chessa M, Bergander K, Blaschke K (2003) Comparative enantioseparations with native β-cyclodextrin, randomly acetylated β-cyclodextrin and heptakis-(2,3-di-O-acetyl)-β-cyclodextrin in capillary electrophoresis. Electrophoresis 24:1083–1091
133. Waibel B, Schreiber J, Meier C, Hammitzsch M, Baumann K, Scriba GKE, Holzgrabe U (2007) Comparison of cyclodextrin-dipeptide inclusion complexes in the absence and presence of urea by means of capillary electrophoresis, nuclear magnetic resonance and molecular modeling. Eur J Org Chem 2921–2930
134. Kahle C, Deubner R, Schollmayer C, Schreiber J, Baumann K, Holzgrabe U (2005) NMR spectroscopic and molecular modeling studies on cyclodextrin-dipeptide inclusion complexes. Eur J Org Chem 1578–1589
135. Wei Y, Wang S, Chao J, Wang S, Cong C, Shuang S, Paau MC, Choi MMF (2011) An evidence for the chiral discrimination of naproxen enantiomers: a combined experimental and theoretical study. J Phys Chem C 115:4033–4040
136. Berthod A (2009) Chiral recognition mechanisms with macrocyclic glycopeptides selectors. Chirality 21:167–175
137. Loll PJ, Kaplan J, Selinsky BS, Axelson PH (1999) Vancomycin binding to low-affinity ligands: delineating a minimum set of interactions necessary for high-affinity binding. J Med Chem 42:4714–4719
138. Loll PJ, Derhovanessian A, Shapovalov MV, Kaplan J, Yang L, Axelson PH (2009) Vancomycin forms ligand-mediated supramolecular complexes. J Mol Biol 385:200–211
139. Lehmann C, Bunkoczi G, Vertesy L, Sheldrick GM (2002) Structures of glycopeptide antibiotics with peptides that model bacterial cell-wall precursors. J Mol Biol 318:723–732
140. Fernandes C, Tiritan ME, Cass Q, Kairys V, Fernandes MX, Pinto M (2012) Enantioseparation and chiral recognition mechanism of new chiral derivatives of xanthones on macrocyclic antibiotic stationary phases. J Chromatogr A 1241:60–68
141. Desiderio C, Fanali S (1998) Chiral analysis by capillary electrophoresis using antibiotics as chiral selectors. J Chromatogr A 807:37–56
142. Prokhorova A, Shapovalova EN, Shpigun OA (2010) Chiral analysis of pharmaceuticals by capillary electrophoresis using antibiotics as chiral selectors. J Pharm Biomed Anal 53: 1170–1179
143. Kuhn R (1999) Enantiomeric separations by capillary electrophoresis using a crown ether as chiral selector. Electrophoresis 20:2605–2613
144. Elbashir AA, Aboul-Enein HY (2010) Application of crown ethers as buffer additives in capillary electrophoresis. Curr Pharm Anal 6:101–113
145. Nagata H, Nishi H, Kamagauchi M, Ishida T (2008) Guest-dependent conformation of 18-crown-6 tetracarboxylic acid: relation to chiral separation of racemic amino acids. Chirality 20:820–827
146. Bang E, Jung JW, Lee W, Lee DW, Lee W (2001) Chiral recognition of (18-crown-6)-tetracarboxylic acid as a chiral selector determined by NMR spectroscopy. J Chem Soc Perkin Trans 2:1685–1692
147. Gerbaux P, De Winter J, Cornil D, Ravicini K, Pesesse G, Cornil J, Flammang R (2008) Noncovalent interactions between ([18]crown-6)tetracarboxylic acid and amino acids. Chem Eur J 14:11039–11049
148. Nagata H, Nishi H, Kamagauchi M, Ishida T (2004) Structural scaffold of 18-crown-6 tetracarboxylic acid for optical resolution of chiral amino acid: X-ray crystal analyses and

energy calculations of complexes of D- and L-isomers of tyrosine, isoleucine, methionine and phenylglycine. Org Biomol Chem 2:3470–3475
149. Nagata H, Nishi H, Kamagauchi M, Ishida T (2006) Structural scaffold of 18-crown-6 tetracarboxylic acid for optical resolution of chiral amino acid: X-ray crystal analyses of complexes of D- and L-isomers of serine and glutamic acid. Chem Pharm Bull 54:452–457
150. Nagata H, Machida Y, Nishi H, Kamagauchi M, Minoura K, Ishida T (2009) Structural requirement for chiral recognition of amino acid by (18-crown-6)-tetracarboxylic acid: binding analysis in solution and solid states. Bull Chem Soc Jpn 82:219–229
151. Schmid MG, Gübitz G (2011) Enantioseparation by chromatographic and electromigration techniques using ligand-exchange as chiral separation principle. Anal Bioanal Chem 400: 2305–2316
152. Aizawa S, Yamamoto A, Kodama S (2006) Mechanism of enantioseparation of DL-pantothenic acid in ligand exchange capillary electrophoresis using a diol-borate system. Electrophoresis 27:880–886
153. Schmid MG (2012) Chiral metal-ion complexes for enantioseparation by capillary electrophoresis and capillary electrochromatography: a selective review. J Chromatogr A 1267: 10–16
154. Zhang H, Qi L, Mao L, Chen Y (2012) Chiral separation using capillary electromigration techniques based on ligand exchange principle. J Sep Sci 35:1236–1248
155. Chen Z, Uchiyama K, Hobo T (2000) Estimation of formation constants of ternary Cu(II) complexes with mixed amino acid enantiomers based on ligand exchange by capillary electrophoresis. Anal Sci 16:837–841
156. Maccarrone G, Contino A, Cucinotta V (2012) The study of solution equilibria in chiral capillary electrophoresis by the ligand-exchange mechanism. Trends Anal Chem 32:133–153
157. Cucinotta V, Giuffrida A, Maccarrone G, Messina M, Puglisi A, Rizzarelli E, Vecchio G (2005) Coordination properties of 3-functionalized β-cyclodextrins. Thermodynamic stereoselectivity of copper(II) complexes on the A,B-diamino derivative and its exploitation in LECE. Dalton Trans 2731–2736
158. Shtyrlin VG, Zyavkina YI, Gilyazetdinov EM, Burkharov MS, Krutikov AA, Garipov RR, Mukhtarov AS, Zakharov AV (2012) Complex formation, chemical exchange, species structure, and stereoselective effects in the copper(II)-L/DL-histidine systems. Dalton Trans 41:1216–1228
159. Mofaddel N, Adoubel AA, Morin CJ, Desbene PL, Dupas G (2010) Molecular modeling of complexes between two amino acids and copper(II): correlation with ligand exchange capillary electrophoresis. J Mol Struct 975:220–226
160. Dobashi A, Hamada M, Dobashi Y, Yamaguchi J (1995) Enantiomeric separation with sodium dodecanoyl-L-amino acidate micelles and poly(sodium (10-undecenoyl)-L-valinate) by electrokinetic chromatography. Anal Chem 67:3011–3017
161. Dey J, Ghosh A (2010) Chiral separations by micellar electrokinetic chromatography. In: Van Eeckhaut A, Michotte Y (eds) Chiral separations by capillary electrophoresis. CRC, Boca Raton, pp 195–234
162. Yarabe HH, Billot E, Warner IM (2000) Enantiomeric separations by use of polymeric surfactant electrokinetic chromatography. J Chromatogr A 875:179–206
163. Hebling CM, Thompson LE, Eckenroad KW, Manley GA, Fry RA, Mueller KT, Strein TG, Rovnyak D (2008) Sodium cholate aggregation and chiral recognition of the probe molecule (R,S)-1,1´-binaphthyl-2.2´-dihydrogenphosphate (BNDHP) observed by ^{1}H and ^{31}P NMR spectroscopy. Langmuir 24:13866–13874
164. Rugutt JK, Billot E, Warner IM (2000) NMR study of the interaction of monomeric and polymeric chiral surfactants with (R)- and (S)-1,1′-binaphthyl-2-2′-diyl hydrogen phosphate. Langmuir 16:3022–3029
165. Kingsbury SA, Ducommun CJ, Zahakaylo BM, Dickinson EH, Morris KF (2010) NMR characterization of (S)-1,1′-binaphthyl-2-2′-diyl hydrogen phosphate binding to chiral molecular micelles. Magn Reson Chem 48:184–191

166. Morris KF, Becker BA, Valle BC, Warner IM, Larive CK (2006) Use of NMR binding interaction mapping techniques to examine interactions of chiral molecules with molecular micelles. J Phys Chem B 110:17359–17369
167. Valle BC, Morris KF, Fletcher KA, Fernand V, Sword DM, Eldridge S, Larive CK, Warner IM (2007) Understanding chiral molecular micelle separations using steady-state fluorescence anisotropy, capillary electrophoresis, and NMR. Langmuir 23:425–435
168. Yarabe HH, Rugutt JK, McCarroll ME, Warner IM (2000) Capillary electrophoretic separation of binaphthyl enantiomers with two polymeric chiral surfactants: ^{1}H-nuclear magnetic resonance and fluorescence spectroscopy study. Electrophoresis 21:2025–2032
169. Kano K, Minami K, Horiguchi K, Ishimura T, Kodera M (1995) Ability of non-cyclic oligosaccharides to form molecular complexes and its use for chiral separation by capillary zone electrophoresis. J Chromatogr A 694:307–313
170. Nishi M, Izumoto S, Nakamura K, Nakai H, Sato T (1996) Dextran and dextrin as chiral selectors in capillary zone electrophoresis. Chromatographia 42:617–630
171. Chen J, Du Y, Zhu F, Chen B (2010) Glycogen: a novel branched polysaccharide chiral selector in CE. Electrophoresis 31:1044–1050
172. Chankvetadze B, Saito M, Yashima E, Okamoto Y (1998) Enantioseparation of atropisomeric 1,1′-binaphthyl-2,2′-diyl hydrogen phosphate in capillary electrophoresis by using di- and oligosaccharides as chiral selectors: di- and oligosaccharide chiral selectors in capillary electrophoresis. Chirality 10:134–139
173. Du X, Taga A, Suzuki S, Liu W, Honda S (2002) Effect of structure modification of chondroitin sulfate C on its enantioselectivity to basic drugs in capillary electrophoresis. J Chromatogr A 947:287–299
174. Nojavon S, Fakhar AR (2011) Chiral separation and quantitation of cetirizine and hydroxzine by maltodextrin-mediated CE in human plasma: effect of zwitterionic property of cetirizine on enantioseparation. Electrophoresis 32:764–771
175. Wei W, Guo B, Lin JM (2009) Helical- and ahelical-dependent chiral recognition mechanism is capillary electrophoresis using amylose as the selector. Electrophoresis 30:1380–1387
176. Sawada M, Tanaka T, Takai Y, Hanafusa T, Taniguchi T, Kawamura M, Uchiyama T (1991) The crystal structure of cycloinulohexaose produced from inulin by cycloinulo-oligosacchride fructanotransferase. Carbohydr Res 217:7–17
177. Immel S, Schmitt GE, Lichtenthaler FW (1998) Cyclofructans with six to ten β-(1→2)-linked fructofuranose units: geometries, electrostatic profiles, lipophilicity patterns, and potential for inclusion complexation. Carbohydr Res 313:91–105
178. Jiang C, Tong M, Breitbach ZS, Armstrong DW (2009) Synthesis and examination of sulfated cyclofructans as a novel class of chiral selectors in CE. Electrophoresis 30:3897–3909
179. Haginaka J (2010) Chiral separations using proteins and peptides as chiral selectors. In: Van Eeckhaut A, Michotte Y (eds) Chiral separations by capillary electrophoresis. CRC, Boca Raton, pp 139–161
180. Haginaka J (2011) Mechanistic aspects of chiral recognition on protein-based stationary phases. In: Grushka E (ed) Advances in chromatography, vol 49. CRC, Boca Raton, pp 37–69
181. Bica K, Gaertner P (2008) Applications of chiral ionic liquids. Eur J Org Chem 3235–3250
182. Francois Y, Varenne A, Juillerat E, Villemin D, Gareil P (2007) Evaluation of chiral ionic liquids as additive to cyclodextrins for enantiomeric separations by capillary electrophoresis. J Chromatogr A 1155:134–141
183. Tran CD, Mejac I (2008) Chiral ionic liquids for enantioseparations of pharmaceutical products by capillary electrophoresis. J Chromatogr A 1204:204–209
184. Rizvi SAA, Shamsi SA (2006) Synthesis, characterization, and application of chiral ionic liquids and their polymers in micellar electrokinetic chromatography. Anal Chem 78: 7061–7069
185. Liu Q, Wu K, Tang F, Yao L, Yang F, Nie Z, Yao S (2009) Amino acid ionic liquids as chiral ligands in ligand-exchange chiral separations. Chem Eur J 15:9889–9896

186. Bi W, Tian M, Row KH (2011) Chiral separation and determination of ofloxacin enantiomers by ionic liquid-assisted ligand-exchange chromatography. Analyst 136:379–387
187. De Rooy A, Li M, Bwambok DK, El-Zahab B, Challa S, Warner IM (2011) Ephedrinium-based protic chiral ionic liquids for enantiomeric recognition. Chirality 23:54–62
188. Kroupa DM, Brown CJ, Heckman LM, Hopkins TA (2012) Chiroptical study of chiral discrimination by amino acid based ionic liquids. J Phys Chem B 116:4952–4958
189. Ellington AD, Szostak JW (1990) In vitro selection of RNA molecules that bind specific ligands. Nature 346:818–822
190. Patel DJ, Suri AK, Jiang F, Jiang L, Fan P, Kumar RA, Nonin S (1997) Structure, recognition and adaptive binding in RNA aptamer complexes. J Mol Biol 272:645–664
191. Hermann T, Patel DJ (2000) Adaptive recognition by nucleic acid aptamers. Science 287: 820–825
192. Yang X, Bing T, Mei H, Fang C, Cao Z, Shangguan D (2011) Characterization and application of a DNA aptamer binding to L-tryptophan. Analyst 36:577–585
193. Bishop GR, Ren J, Polander BC, Jeanfreau BD, Trent JO, Chaires JB (2007) Energetic basis of molecular recognition in a DNA aptamer. Biophys Chem 126:165–175
194. Peyrin E (2009) Nucleic acid aptamer molecular recognition principles and application in liquid chromatography and capillary electrophoresis. J Sep Sci 32:1531–1536
195. Jung G, Hofstetter H, Feiertag S, Stoll D, Hofstetter O, Wiesmüller KH, Schurig V (1996) Cyclopeptide libraries as new chiral selectors in capillary electrophoresis. Angew Chem Int Ed Engl 35:2148–2150
196. Chiari M, Desperati V, Manera E, Longhi R (1998) Combinatorial synthesis of highly selective cyclohexapeptides for separation of amino acid enantiomers by capillary electrophoresis. Anal Chem 70:4967–4973
197. Ravelet C, Peyrin E (2006) Recent developments in the HPLC enantiomeric separation using chiral selectors identified by a combinatorial strategy. J Sep Sci 29:1322–1331
198. Evans CE, Stalcup AM (2003) Comprehensive strategy for chiral separations using sulfated cyclodextrins in capillary electrophoresis. Chirality 15:709–723
199. Jimidar IM, van Ael W, van Nyen P, Peeters M, Redlich D, de Smet M (2004) A screening strategy for the development of enantiomeric separation method in capillary electrophoresis. Electrophoresis 25:2772–2785
200. Ates H, Mangelings D, Vander Heyen Y (2008) Fast generic chiral separation strategies using electrophoretic and liquid chromatographic techniques. J Pharm Biomed Anal 48:288–294
201. Nhujak T, Sastravaha C, Palanuvej C, Petsom A (2005) Chiral separation in capillary electrophoresis using dual neutral cyclodextrins: theoretical models of electrophoretic mobility difference and separation selectivity. Electrophoresis 26:3814–3823
202. Matthijs N, Van Hemelryck S, Maftouh M, Luc Massart D, Vander Heyden Y (2004) Electrophoretic separation strategy for chiral pharmaceuticals using highly sulfated and neutral cyclodextrins based dual selector systems. Anal Chim Acta 525:247–263
203. Fillet M, Hubert P, Crommen J (2000) Enantiomeric separations of drugs using mixtures of charged and neutral cyclodextrins. J Chromatogr A 875:123–135
204. Jakubetz H, Juza M, Schurig V (1998) Dual chiral recognitions system involving cyclodextrin derivatives in capillary electrophoresis. Part 2. Enhancement of enantioselectivity. Electrophoresis 19:738–744
205. Mayer S, Schleimer M, Schurig V (1994) Dual chiral recognition system involving cyclodextrin derivatives in capillary electrophoresis. J Microcolumn Sep 6:42–48
206. Skanchy DJ, Xie GH, Tait RJ, Luna E, Demarest C, Stobaugh JF (1999) Application of sulfobutylether-β-cyclodextrin with specific degrees of substitution for the enantioseparation of pharmaceutical mixtures by capillary electrophoresis. Electrophoresis 20:2638–2649
207. Sänger-van de Griend CE, Gröningsson K (1996) Validation of a capillary electrophoresis method for the enantiomeric purity testing of ropivacaine, a new local anaesthetic compound. J Pharm Biomed Anal 14:295–304
208. Wongwan S, Hammitzsch-Wiedemann M, Scriba GKE (2009) Determination of related substances of levodopa including the R-enantiomer by CE. Electrophoresis 30:3891–3896
209. Kenndler E (2009) Organic solvents in CE. Electrophoresis 30:S101–S111

210. Lämmerhofer M (2005) Chiral separations by capillary electromigration techniques in non-aqueous media. I. Enantioselective nonaqueous capillary electrophoresis. J Chromatogr A 1068:3–30
211. Shamsi SA (2002) Chiral capillary electrophoresis-mass spectrometry: modes and applications. Electrophoresis 23:4036–4051
212. Somsen GW, Mol R, de Jong GJ (2010) On-line coupling of electrokinetic chromatography and mass spectrometry. J Chromatogr A 1217:3978–3991
213. Simo C, Garcia-Canas V, Cifuentes A (2010) Chiral CE-MS. Electrophoresis 31:1442–1456
214. Sheppard RL, Tong X, Cai J, Henion JD (1995) Chiral separation and detection of terbutaline and ephedrine by capillary electrophoresis coupled with ion spray mass spectrometry. Anal Chem 67:2054–2058
215. Hempel G, Blaschke G (1996) Enantioselective determination of zopiclone and its metabolites in urine by capillary electrophoresis. J Chromatogr B 675:139–146
216. Jimidar MI, van Ael W, de Smet M (2004) Optimization of enantiomeric separations in capillary electrophoresis by applying a design of experiments approach. J Capill Electrophor Microchip Technol 9:13–21
217. Hanrahan G, Montes R, Gomez FA (2008) Chemometric experimental design based optimization techniques in capillary electrophoresis: a critical review of modern applications. Anal Bioanal Chem 390:169–179
218. Hanrahan G, Gomez FA (eds) (2010) Chemometric methods in capillary electrophoresis. Wiley, Hoboken
219. Dejaegher S, Mangelings E, Vander Heyden Y (2013) In: Scriba GKE (ed) Chiral separations, methods and protocols, vol 970, 2nd edn, Methods in molecular biology. Humana, New York, pp 409–427
220. Sänger-van de Griend CE (2008) General considerations to improve performance of CE methods. In: Ahuja S, Jimidar IM (eds) Capillary electrophoresis methods for pharmaceutical analysis. Academic, London, pp 123–144
221. Hammitzsch M, Rao RN, Scriba GKE (2006) Development and validation of a robust capillary electrophoresis method for impurity profiling of etomidate including the determination of the chiral purity using a dual cyclodextrin system. Electrophoresis 27:4334–4344
222. Dey J, Ghosch A (2008) Chiral separations by micellar electrokinetic chromatography. In: Van Eekhaut A, Michotte Y (eds) Chiral separations by capillary electrophoresis. CRC, Boca Raton, pp 195–234
223. Billot FH, Billot EJ, Warner IM (2001) Comparison of monomeric and polymeric amino acid based surfactants for chiral separations. J Chromatogr A 922:329–338
224. Thibodeaux SJ, Billot EJ, Torres E, Valle BC, Warner IM (2003) Enantiomeric separations using polymeric L-glutamate surfactant derivatives: effect of increasing steric factors. Electrophoresis 24:1077–1082
225. Thibodeaux SJ, Billot EJ, Warner IM (2002) Enantiomeric separation using poly(L-valine) and poly(L-leucine) surfactants: investigation of steric factors near the chiral center. J Chromatogr A 966:179–186
226. Lin CE, Huang HC, Chen HW (2001) A capillary electrophoresis study on the influence of β-cyclodextrin on the critical micelle concentration of sodium dodecyl sulfate. J Chromatogr A 917:297–310
227. Bendazzoli C, Mileo E, Lucarini M, Olmo S, Cavrini C, Gotti R (2010) Capillary electrophoretic study on the interaction between sodium dodecyl sulfate and neutral cyclodextrins. Microchim Acta 171:23–31
228. Melani F, Giannini I, Pasquini B, Orlandini S, Pinzauti S, Furlanetto S (2011) Evaluation of the separation mechanism of electrokinetic chromatography with a microemulsion and cyclodextrins using NMR and molecular modeling. Electrophoresis 32:3062–3069
229. Shamsi SA (2001) Micellar electrokinetic chromatography-mass spectrometry using a polymerized chiral surfactant. Anal Chem 73:5103–5108

230. Hou J, Rizvi SAA, Zheng J, Shamsi SA (2006) Application of polymeric surfactants in micellar electrokinetic chromatography-electrospray ionization mass spectrometry of benzodiazepines and benoxazocine chiral drugs. Electrophoresis 27:1263–1275
231. Hou J, Zheng J, Rizvi SAA, Shamsi SA (2007) Simultaneous chiral separation and determination of ephedrine alkaloids by MEKC-ESI-MS using polymeric surfactants: method development. Electrophoresis 28:1352–1363
232. Rizvi SAA, Zheng J, Apkarian RP, Dublin SN, Shamsi SA (2007) Polymeric amino acid surfactants: a class of versatile chiral selectors for micellar electrokinetic chromatography (MEKC) and MEKC-MS. Anal Chem 79:879–898
233. Wang X, Hou J, Jann M, Hon YY, Shamsi SA (2013) Development of a chiral micellar electrokinetic chromatography-tandem mass spectrometry assay for simultaneous analysis of warfarin and hydroxywarfarin metabolites: application to the analysis of patients serum samples. J Chromatogr A 1271:207–216
234. Watari H (1991) Microemulsion capillary electrophoresis. Chem Lett 20:391–394
235. Cao Y, Ni X, Sheng J (2011) Comparison of microstructures of microemulsion and swollen micelle in electrokinetic chromatography. J Chromatogr A 1218:2598–2603
236. Mertzman MD, Foley JP (2004) Effect of oil substitution on chiral microemulsion electrokinetic chromatography. Electrophoresis 25:723–732
237. Pascoe R, Foley JP (2002) Rapid separation of pharmaceutical enantiomers using electrokinetic chromatography with a novel chiral microemulsion. Analyst 127:710–714
238. Mertzman MD, Foley JP (2005) Temperature effects on chiral microemulsion electrokinetic chromatography employing the chiral surfactant dodecylcarbonylvaline. J Chromatogr A 1073:181–189
239. Zheng ZX, Lin JM, Chan WH, Lee AWM, Huie CW (2004) Separation of enantiomers in microemulsion electrokinetic chromatography using chiral alcohols as cosurfactants. Electrophoresis 25:3263–3269
240. Aiken JH, Huie CW (1993) Use of a microemulsion system to incorporate a lipophilic chiral selector in electrokinetic capillary chromatography. Chromatographia 35:448–450
241. Hu SQ, Chen YL, Zhu HD, Shi HJ, Ayn N, Chen XG (2010) Effect of molecular structure of tartrates on chiral recognition of tartrate-boric acid complex chiral selectors in chiral microemulsion electrokinetic chromatography. J Chromatogr A 1217:5529–5535
242. Kahle KA, Foley JP (2006) Chiral microemulsion electrokinetic chromatography with two chiral components: improved separations via synergies between a chiral surfactant and a chiral cosurfactant. Electrophoresis 27:896–904
243. Kahle KA, Foley JP (2007) Two-chiral-component microemulsion electrokinetic chromatography – chiral surfactant and chiral oil: part 1. Dibutyl tartrate. Electrophoresis 28:1723–1734
244. Kahle KA, Foley JP (2007) Two-chiral-component microemulsion electrokinetic chromatography—chiral surfactant and chiral oil: part 2. Diethyl tartrate. Electrophoresis 28:2644–2657
245. Kahle KA, Foley JP (2007) Influence of microemulsion chirality on chromatographic figures of merit in EKC: results with novel three-chiral component microemulsions and comparison with one- and two-chiral-component microemulsions. Electrophoresis 28:3024–3040
246. Hu SQ, Lü WJ, Ma YH, Dong LJ, Chen XG (2013) Chiral separation of β-blockers by MEEKC using neutral microemulsion: analysis of separation mechanism and further elucidation of resolution equation. Electrophoresis 34:260–268
247. Chu BL, Guo BY, Wang Z, Lin JM (2008) Enantioseparation of esbiothrin by cyclodextrin-modified microemulsion and micellar electrokinetic chromatography. J Sep Sci 31: 3911–3920
248. Bitar Y, Holzgrabe U (2007) Enantioseparation of chiral tropa alkaloids by means of cyclodextrin-modified microemulsion electrokinetic chromatography. Electrophoresis 28: 2693–2700
249. Borst C, Holzgrabe U (2008) Enantioseparation of dopa and related compounds by cyclodextrin-modified microemulsion electrokinetic chromatography. J Chromatogr A 1204:191–196

250. Borst C, Holzgrabe U (2010) Comparison of chiral electrophoretic separation methods for phenylethylamines and application on impurity analysis. J Pharm Biomed Anal 53: 1201–1209
251. Wongwan S, Scriba GKE (2010) Impurity profiling of dexamphetamine sulfate by cyclodextrin-modified microemulsion electrokinetic chromatography. Electrophoresis 31: 3006–3011
252. Yu L, Chu K, Ye H, Liu X, Yu L, Xu X, Chen G (2012) Recent advances in microemulsion electrokinetic chromatography. Trends Anal Chem 34:140–151
253. Ryan R, Altria K, McEvoy E, Donegan S, Power J (2013) A review of developments in the methodology and application of microemulsion electrokinetic chromatography. Electrophoresis 34:159–177
254. Wen Y, Li J, Ma J, Chen L (2012) Recent advances in enrichment techniques for trace analysis in capillary electrophoresis. Electrophoresis 33:2933–2952
255. Mala Z, Gebauer P, Bocek P (2011) Contemporary sample stacking in analytical electrophoresis. Electrophoresis 32:116–126
256. Mikus P, Marakova K (2010) Chiral capillary electrophoresis with on-line sample preparation. Curr Pharm Anal 6:76–100
257. Garcia-Ruiz C, Marina ML (2006) Sensitive chiral analysis by capillary electrophoresis. Electrophoresis 27:195–212
258. Guidance for Industry, Analytical Procedures and Methods Validation, Chemistry Manufacturing and Controls Documentation, Draft Guidance, FDA (2000) http://www.fda.gov/downloads/Drugs/. . ./Guidances/ucm122858.pdf
259. Muijselaar PG (2008) Overview of current regulatory guidance. In: Ahuja S, Jimidar MI (eds) Capillary electrophoresis methods for pharmaceutical analysis, Separation science and technology. Academic, London, pp 145–169
260. Sänger-van de Griend CE (2012) Revival of capillary electrophoresis techniques in the pharmaceutical industry. LC GC N Am 30:954–971